Analysis of energy, exergy and Greenhouse Gas emissions for Variable Air Volume systems in an office building

Zhentao Wei

A Thesis

in

The Department

of

Building, Civil and Environmental Engineering

Presented in Partial Fulfillment of the Requirements
for the Degree of Master of Applied Science (Building Engineering) at
Concordia University
Montreal, Quebec, Canada

February 2006

Your file Votre référence
ISBN: 978-0-494-34607-5
Our file Notre référence
ISBN: 978-0-494-34607-5

ABSTRACT

Analysis of energy, exergy and Greenhouse Gas emissions for Variable Air Volume systems in an office building

Zhentao Wei

The concept of sustainability applied to the building industry requires that engineers consider the reduction of both energy use and the related environmental impacts during both design and commissioning phases. According to estimates of the end-use energy consumption and related greenhouse gas (GHG) emissions, issued by National Resources Canada, the commercial building sector contributed by about 14% to the total national end-use energy consumption and by 13% to the total national GHG emissions in 2003, while GHG emissions associated with space heating and cooling accounted for more than half of total emissions (NRCan 2005). Therefore, the increase of the energy efficiency of Heating, Ventilating and Air-Conditioning (HVAC) systems in commercial buildings and the reduction of their associated environmental impacts are extremely important.

Two types of Variable Air Volume (VAV) systems applied to an existing office building in Montreal are analyzed in this research. The first uses a constant temperature for the supply air from an air handling unit (AHU), while the second varies the temperature of the supply air in terms of the highest instantaneous cooling load of all zones. In order to estimate the energy performance of the two VAV systems, thermodynamic analysis based on both first and second laws of thermodynamics is applied, and mathematical models are developed to simulate the system operation. The Engineering Equation Solver (EES) environment is used to implement and solve the mathematical models. At the system

level, the annual system Coefficient of Performance (COP) of the first system is 0.99, while the COP of the second system is 1.24. However, the annual energy efficiency of both VAV systems drops by about 34% when the power plant and delivery systems are taken into consideration. The hourly maximum exergy efficiency of both VAV systems is less than 0.16, indicating that a large potential of the improvement of exergy efficiency exists for both VAV systems. The annual GHG emissions due to the off-site primary energy use by both VAV systems are 43 tons/yr and 33.5 tons/yr, respectively.

The study outlines that the most exergy destruction within both VAV systems is due to heat sources, i.e., electric boilers. Therefore, the largest improvement of exergy efficiency can be obtained by changing the heat source from an electric boiler to renewable energy sources such as solar or geothermal energy. Moreover, this change may also lead to the reduction of the GHG emissions due to the operations of HVAC systems.

ACKNOWLEDGEMENTS

I would like to thank many people who supported and encouraged me during my studies toward my Master's degree at Concordia University. If there were not their support and encouragement, the thesis would not have been finished.

I give a lot of thanks to my Master's supervisor Dr. Radu G. Zmeureanu. I have benefited from his guidance and enthusiasm over my study period. He provided insightful comments and suggestions that enriched the contents of the thesis. His questions kept me thinking of new approaches for my research. I also want to thank other professors in the department who also gave me a lot of help in my research. I benefited a lot from the courses provided by Dr. Fariborz Haghighat, Dr. Theodore Stathopoulos and Dr. Kamran Siddiqui.

In addition, during my life, my family always gives me love, support and encouragement. Thank you for everything you did for me.

Table of Contents

List of Figures

Page

List of Tables

Nomenclature

Symbol	Parameter	Units
A	floor area	[m^2]
c	specific heat	[kJ/kg·K]
t	simulation time	[h]
P	pressure	[kPa]
ΔH	pressure drops	[kPa]
T	temperature	[K] or [°C]
$\dot{m}$	mass flow rate	[kg/s]
$\dot{V}$	volumetric flow rate	[m^3/s]
v	specific volume	[m^3/kg]
ρ	density	[m^3/kg]
h	specific enthalpy	[kJ/kg]
s	specific entropy	[kJ/kg·K]
ω	specific humidity ratio	[kg/kg]
$\dot{E}$	energy flow rate	[kW]
$\dot{Q}$	heat transfer rate	[kJ/kg]
$\dot{\Phi}$	exergy flow rate	[kW]
ψ	specific exergy	[kJ/kg]

$\dot{I}$	irreversibility or exergy destruction rate	[kW]
$\dot{\sigma}$	entropy generation	[kW/K]
η	efficiency	--
PLR	part-load ratio	--
COP	coefficient of performance	--

Subscripts

a	air
@	at
c	chiller
cc	central cooling coil
cd	condenser
com	compressor
CT	cooling tower
CTW	cooling tower water
CTWP	cooling tower water pump
CW	chilled water
CWP	chilled water pump
DB	dry-bulb
ev	evaporator
e	out
f	saturated liquid
FL	full-load
FR	fresh air or outdoor air

g	saturated vapor
HW	hot water
HWP	hot water pump
i	in
lat	latent loads
min	minimum
max	maximum
MW	makeup water
o	the dead-state or reference state
RH	reheat coil
PL	part-load
sat	saturated state
SDA	supply dry air
sys	system
sen	sensible loads
t	total
w	water
I	the fist law or energy
II	the second law of exergy

Chapter 1 Introduction

Since the world energy crisis in the early 1970s, scientists have paid more attention to improve energy usage, exploit renewable energy resources and reduce the impacts of energy use on the environment. More and more evidence shows that the global climate changing is mainly caused by greenhouse gas (GHG) emissions, which are directly related to the combustion of fossil fuels. In recent decades, the concept of sustainability has entered in the engineering world, and it appears to be connected with every aspect of an engineer's profession. In the building industry, "building sustainability is a means to provide a safe, healthy, comfortable indoor environment while simultaneously limiting the impact on the Earth's natural resources" (ASHRAE 2002b). Sustainable development in the building industry is concerned with a quite wide range of issues including building materials, construction sites, integrated systems, energy consumption and indoor environment. The concept of green building design applied to the HVAC industry requires that design engineers regard not only the reduction of the energy use by HVAC systems but also the mitigation of the related environmental impacts. While every building seems like to be connected with sustainability, the environmental impacts of buildings continue to increase. As of 2003, commercial buildings in Canada account for 14% of the annual national end-use energy consumption and 13% of the annual national GHG emissions (NRCan 2005). In commercial building sector, the end-use energy consumption of air-conditioning systems accounts for more than 60% of the total end-use energy consumption, and the related GHG emissions account for more than 58% of the total GHG emissions (NRCan 2005). Therefore, the effectiveness of energy use for space

heating and cooling is increasingly important and essential for the application of sustainable development in the building industry.

Over the past 30 years, many advanced technologies have been developed and used in the HVAC industry. Accordingly, the efficiency of major energy consumed components of HVAC systems, such as chillers, boilers, fans, pumps, and heat exchangers, have been dramatically raised. Some optimal control strategies have been promoted to make the operations of HVAC systems more effective. Most studies based on the first law of thermodynamics analysis, also called energy analysis, to evaluate the energy performance of HVAC systems. Energy analysis is based on the quantity of energy alone but does not involve the quality of energy, which is realized as the most important aspect of energy. On the contrary, the second law of thermodynamics based analysis, also called exergy analysis, deals with the capacity of energy doing useful work and reveals the nature of energy consumption, which refers to energy degradation. It introduces an index of the energy degradation, entropy, and based on the index, exergy analysis can locate the most inefficient components or subsystems in an energy involved process. Therefore, exergy analysis is more meaningful and rational than energy analysis when applied to the system or process involving more than one type of energy sources. Since the 1970s, exergy analysis has been mainly developed in the cases of intensive energy use such as power generation plants. Only little literature about exergy analysis applied to the HVAC industry can be found, but most of them just focused on system components such as chillers or on subsystems such as the air-distribution system.

The goals of this research include developing the detailed component models of VAV systems and evaluating the performance of VAV systems by using the energy-exergy analysis and the GHG emissions at both system and power plant level.

The thesis contains six chapters. Chapter 2 presents literature review about the application of thermodynamic analysis to the HVAC field and the objectives of this research.

Chapter 3 demonstrates the development of the mathematical models of VAV systems and their components including chillers, boilers, and cooling towers using the energy and exergy analysis or the 1^{st} and 2^{nd} law analyses.

Chapter 4 devotes a case study of two VAV systems for an office building in Montreal, using the mathematical models developed in chapter 3.

Chapter 5 exhibits the evaluation of GHG emissions due to the off-site primary energy use required by HVAC systems.

Chapter 6 lists conclusions from this research and suggests a few avenues for future work.

Chapter 2 Literature Review

This chapter introduces the knowledge of the thermodynamic analysis applied to the HVAC field and the background information that gives the motivation of this research. Some energy and exergy related indices used in the research are introduced first. In addition, some publications about the first law and the second law analysis for evaluating the energy performance of HVAC systems are cited. Meanwhile, the significance of improving the energy performance of commercial buildings is examined; several types of HVAC systems commonly used in commercial buildings are introduced. The comparisons of those HVAC systems are listed as well. Finally, the importance of combining the first law analysis with the second law analysis for evaluating the performance of HVAC systems is presented.

2.1. Thermodynamic analysis for HVAC applications

HVAC systems are mostly defined as open systems or control volume systems. The studied fluids involved in this research are referred to the thermal transferring media, water and air. The air is treated as a mixture of dry air and water vapor satisfying the ideal gas equations.

Currently, more and more people are concerned about saving energy in all sectors of the world. This sparks the interest of utilizing thermodynamic analysis for all energy conversed processes. Thermodynamic analyses include the first and second laws analysis,

also called energy and exergy analysis. The first law analysis is based on the first law of thermodynamics, which is the conservation principle of energy. The second law analysis is based on the second law of thermodynamics, which indicates the directions of any energy involved process and introduces energy degradation related indices, entropy and exergy. Exergy refers to the capacity of energy doing useful work. It effectively defines the quality of different types of energy. Even though energy is conservative in quantity through any process, the quality of energy is degraded inevitably. Therefore, people should be concerned about both aspects of energy, quality and quantity, when talking about energy conservation. The following details the first law and second law analyses used in the HVAC field.

2.1.1. The first law analysis

The first law analysis applied to the HVAC field is based on the energy balance equations established for systems and components; thereby, energy related indices can be properly estimated, and the energy performance of components or systems can be evaluated. The energy related indices include energy inputs, outputs, and energy efficiency - also called the first law efficiency - in this research. In a HVAC system, energy consuming components include chillers, boilers, fans, pumps and heat exchangers. The following general equation is used to calculate the energy efficiency, η_I , of a system or components:

$$\eta_I = \frac{\dot{Q}_{useful}}{\dot{E}_{input}} \quad \text{or} \quad \eta_I = \frac{\dot{W}_{useful}}{\dot{E}_{input}} \tag{2-1}$$

where $\dot{Q}_{useful}$ or $\dot{W}_{useful}$ denotes the useful heat flow rate or the net work output, respectively;

$\dot{E}_{input}$ denotes the primary energy or the heat input to the system or components.

The performance of chillers

The nominal performance of a chiller is expressed with an indicator called Coefficient of Performance (COP) formulated as Equation 2-2. The COP is defined as the ratio of the nominal cooling capacity ($\dot{Q}_{ev}$) of a chiller over its electric input ($\dot{E}_{com}$).

$$COP_{chiller} = \frac{\dot{Q}_{ev}}{\dot{E}_{com}} \tag{2-2}$$

Efficiency of boilers

The nominal boiler energy efficiency is defined as the useful heat delivered by the boiler through the hot water, which is equal to heat gained by the water, ($\dot{Q}_{hw}$) divided by the heat provided by the primary energy ($\dot{E}_{electricity}$), for instance electricity in this research.

$$\eta_{I,boiler} = \frac{\dot{Q}_{hw}}{\dot{E}_{electricity}} \tag{2-3}$$

The performance of the whole HVAC system

The efficiency of the entire system is also call the COP of the system and can be expressed as Equation 2-4, where the numerator expresses the required thermal energy

including space thermal loads and its ventilation loads, and the denominator refers to the total on-site or off-site energy input to the system:

$$COP_{system} = \frac{\sum_{i=1}^{5}\left|\dot{Q}_i\right| + m_{out,air} \times \left|(h_{out} - h_{in})\right|}{\dot{E}_{total}} \tag{2-4}$$

where the notation "i" denotes the number of zones.

2.1.2. The second law analysis

In order to identify exergy, analysts have to define the dead-state or the reference state, where exergy content of any substance is zero. Traditionally, the atmospheric environment is treated as the dead-state (i. e., Wark 1995 and Cengel et al. 2002). As long as a system or a substance is in equilibrium with the dead-state, there is no potential work to be performed, or there is no exergy.

The formulas calculating the exergy interaction with different energy transfer or mass transfer can be developed by analyzing an imaginary control volume system, which only exchanges heat with its environment and reservoirs and gets the net work output. The schematic of such process is shown in Figure 2-1 (Wark 1995).

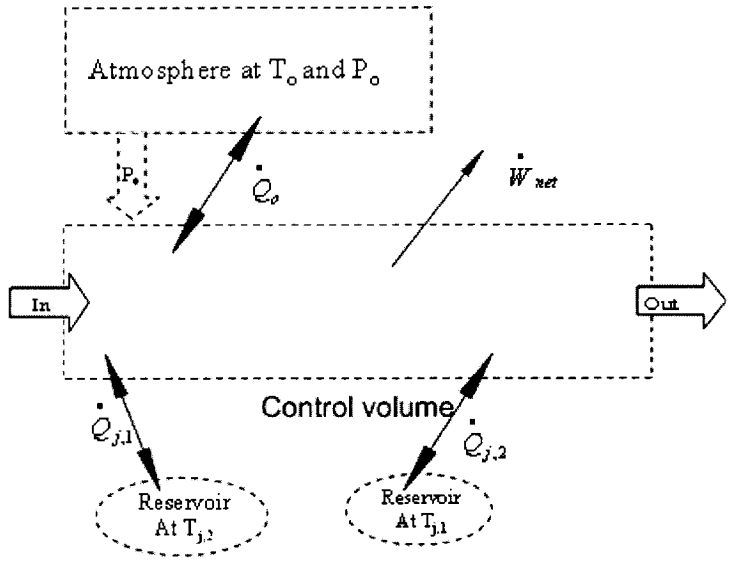

Figure 2-1: Schematic of a control volume

The energy balance equation of this process is expressed as follows:

$$\dot{Q}+\dot{W}_{net}+\dot{m}_{in}\times(h+Ke+Pe)_{in}-\dot{m}_{out}\times(h+Ke+Pe)_{out}=\frac{dE_{CV}}{dt} \tag{2-5}$$

where "*Ke*" denots kinetic energy, and "*Pe*" denotes potential energy;

"*W*" denotes work, and "*dE*" denotes internal energy increase.

By rewriting the term of heat transfer into $\dot{Q}_o$, $\dot{Q}_{j,1}$, and $\dot{Q}_{j,2}$, Equation 2-5 is rearranged as:

$$\dot{Q}_o+\sum\dot{Q}_j+\dot{W}_{net}+\dot{m}_{in}\times(h+Ke+Pe)_{in}-\dot{m}_{out}\times(h+Ke+Pe)_{out}=\frac{dE_{CV}}{dt} \tag{2-6}$$

The net useful work can be written as follows (Wark 1995):

$$\dot{W}_{net,u}=\dot{W}_{net}+P_o\times\left[\frac{d(vol)}{dt}\right] \tag{2-7}$$

The entropy balance equation for the system is written as follows:

$$\dot{\sigma}_{CV}=\frac{dS_{CV}}{dt}-\dot{m}_{in}\times s_{in}+\dot{m}_{out}\times s_{out}-\frac{\dot{Q}_o}{T_o}-\sum\frac{\dot{Q}_j}{T_j} \tag{2-8}$$

Combining Equations 2-6 to 2-8, and eliminating the term of heat exchange between the system and the environment, the net useful work could be returned as follows:

$$\dot{W}_{net,u} = \dot{m}_{out} \times (h + Ke + Pe - T_o s)_{out} - \dot{m}_{in} \times (h + Ke + Pe - T_o s)_{in} - \sum \dot{Q}_j \times \left(1 - \frac{T_o}{T_j}\right) + \frac{d(E + P_o V - T_o s)_{CV}}{dt} + T_o \times \dot{\sigma}_{tot} \quad (2\text{-}9)$$

From Equation 2-9, the exergy associated with mass, heat, and work interactions can be developed as follows:

- The exergy transfer associated with the working interaction is written as:

$$\dot{\Phi}_{work} = \dot{W} \quad (2\text{-}10)$$

- The exergy transfer associated with heat interaction is written as:

$$\dot{\Phi}_{heat} = \sum \dot{Q}_j \times \left(1 - \frac{T_o}{T_j}\right) \quad (2\text{-}11)$$

- The exergy transfer associated with mass exchange through the system's boundaries is written as:

$$\dot{\Phi}_{flow} = \dot{m}[(h - h_o) + Ke + Pe - T_o(s - s_o)] \quad (2\text{-}12)$$

The relation between entropy and exergy is expressed as follows (Wark 1995):

$$\dot{I} = T_o \times \dot{\sigma}_{tot} \quad (2\text{-}13)$$

Equation 2-12 can be further developed into the exergy content of a substance, neglecting its kinetic and potential energy on a mass basis, as follows:

$$\varphi_{flow} = (h - h_o) - T_o(s - s_o) \tag{2-14}$$

The exergy calculated by using Equation 2-14 is based on the restricted dead-state, which refers to be only in thermo-mechanical equilibrium with the dead state. The composition difference between the studied system and the dead state are not considered. In the application of HAVC studies, one of the main concerned substances, conditioned air that is treated as a mixture of dry air and water vapor, always changes its moisture content during the air-conditioning process. The moisture content of conditioned air may differ from that of the environment; accordingly, the chemical exergy should be also considered in HVAC applications, and the general formula applied to the chemical exergy can be express as (Wark 1995):

$$\varphi_{ch} = \sum_{i=1}^{n} y_i \times (\mu_{i,o} - \mu_{i,oo}) \tag{2-15}$$

where μ denotes the Gibbs free energy function expressed on a molar basis and y_i denotes the mole fraction of the i^{th} component; the subscript of "o" or "oo" refers to the system state or the dead-state, respectively.

Applied to an ideal gas that is the case of conditioned air in HVAC applications, Equation 2-15 can be further developed into the following:

$$\varphi_{ch} = R \times T_o \times \sum_{i=1}^{n} y_i \times \left(\ln \frac{y_i}{y_{i,oo}} \right) \tag{2-16}$$

Another important exergy involved in this research is the chemical exergy of fuels. The steady-flow fuel exergy of light hydrocarbon gases and their mixtures can be evaluated accurately when the composition is known (Wark 1995). For a large number of light hydrocarbons, the ratio of the chemical exergy to the lower heating value (LHV) is quite constant and can be estimated as follows (Brzustowski et al. 1986):

$$\frac{\varphi}{LHV} = 1.065 \tag{2-17}$$

where LHV denotes the lower heating value of the fuel.

The total exergy of a substance or a system is the summation of the thermal-mechanical and the chemical exergy. The total exergy of some substances used in this research, such as liquid water and moisture air, is introduced as follows:

Exergy of moisture air

Based on the assumptions of the ideal-gas behavior and constant heat capacity, Wepfer et al. (1979) developed the specific exergy of moisture air on a molar basis as follows:

$$\varphi_{tot} = (h - h_o) - T_o(s - s_o) + RT_o \times \left(1 + 1.608\omega \times \ln\frac{1 + 1.608\omega_o}{1 + 1.608\omega} + 1.608\omega \times \ln\frac{\omega}{\omega_o}\right) \tag{2-18}$$

$$y_v = \frac{1.608\omega}{1 + 1.608\omega} \quad \text{And} \quad y_a = \frac{1}{1 + 1.608\omega} \tag{2-19}$$

where y_v and y_a denote the molar content of water vapor and dry air in 1 mol moisture air;

ω denotes the humidity ratio of the moisture air.

Exergy of liquid water

The exergy of liquid water is estimated by the formula presented by Wark (1995):

$$\varphi_{tot} = (h_{f@T} - h_{f@T_o}) + v_{f@T} \times \left(P - P_{sat@T}\right) - T_o (s_{f@T} - s_{f@T_o}) - RT_o \times \ln \frac{y_{v,oo} \times P_o}{P_{g@T_o}} \quad (2\text{-}20)$$

where the subscript "f" and "g" represents the saturated water and the saturated gas, respectively;

$y_{v,oo}$ denotes the mole number of the water vapor in the reference or dead-state.

The second law analysis applied to HVAC systems

The indices related the second law analysis include the second law efficiency of systems or devices, exergy demand, exergy supply, exergy destruction and entropy generation. A general equation used to calculate exergy efficiency can be defined as follows (Wark 1995 and Cengel et al. 2002):

$$\eta_{II} = \frac{\dot{\Phi}_{useful/recovery}}{\dot{\Phi}_{input}} \quad (2\text{-}21)$$

where $\dot{\Phi}_{useful/recovery}$ denotes the useful or recovered exergy;

$\dot{\Phi}_{input}$ denotes the exergy input to the system or device;

In this research, the exergy-related calculations are performed for HVAC components such as the chiller, boiler, fan, pump, cooling tower and heat exchanger. The following lists the exergy input and recovery of each HVAC component.

- The exergy supply of an electric boiler is equal to the electricity input to the boiler, while the exergy recovery is defined as the exergy difference of circulated water between the inlet and outlet of the boiler.
- The exergy input of an electric chiller is equal to the electricity input to the chiller, while the exergy recovery is defined as the exergy difference of chilled water between the inlet and outlet of the evaporator.
- The exergy input of a cooling tower include the electricity input to the circulation fan of the cooling tower, the exergy content of makeup water and the exergy difference of the condenser water between the inlet and outlet of the cooling tower. The exergy recovery is defined as the exergy increase on air side that eventually depletes to the outdoor environment, so the exergy recovery is considered as part of the exergy destruction within the cooling tower in this research. Therefore, the exergy efficiency of the cooling tower is not estimated in this research.
- The exergy inputs to fans or pumps are equal to the electricity inputs to those devices while the exergy recovery from those devices is defined as the exergy differences of those transported fluids, moisture air or water, between the inlets and outlets of the devices.
- In this research, heat exchangers refer to heating or cooling coils used in air distribution systems and transferring heat between working fluids (hot water or chilled water) and conditioned air. All heat exchangers are treated as well insulated, so the heat loss to the environment is neglected. The exergy efficiency of the heat exchanger can be calculated as follows:

$$\eta_{II,heat/cooling,coil} = \frac{\dot{m}_{ca} \times \left|(\varphi_2 - \varphi_1)\right|_{ca}}{\dot{m}_{hw/cw} \times \left|(\varphi_1 - \varphi_2)\right|_{hw/cw}} \tag{2-22}$$

The irreversibility of heat transfer process in heat exchangers is expressed as follows:

$$\dot{I}_{heat,coil} = \dot{m}_{hw/cw} \times \left|(\varphi_1 - \varphi_2)\right|_{hw} - \dot{m}_{ca} \times \left|(\varphi_2 - \varphi_1)\right|_{ca} \tag{2-23}$$

- In the mixing chamber, the outdoor air mixes with the return air in given proportions that are controlled for the mixture by certain temperatures. The second law efficiency of the process can be defined as follows:

$$\eta_{II,mixing} = \frac{\left(\dot{m}_{ra} + \dot{m}_{fa}\right) \times \varphi_2}{\dot{m}_{ra} \times \varphi_{1,ra} + \dot{m}_{fa} \times \varphi_{1,fa}} \tag{2-24}$$

When evaluating the second law efficiency of an entire system, another kind of efficiency called the task exergy efficiency of a system (Franconi et al. 1999) is used. It differs from the definition of exergy efficiency applied to components, which is developed from the generation Equation 2-24. The task exergy efficiency of the system is expressed as follows:

$$\eta_{II} = \frac{\dot{\Phi}_{task}}{\dot{\Phi}_{total}} \tag{2-25}$$

where $\dot{\Phi}_{task}$ denotes the minimum required exergy to perform the task;

$\dot{\Phi}_{total}$ denotes the total exergy input to the system.

In Equation 2-25, the numerator is independent of the system configurations, and its value is only dependent upon the properties of indoor environment such as temperature, and humidity ratio, and the space sensible and latent thermal loads. Therefore, the task second law efficiency of the system makes the comparisons of the system efficiency between different systems commissioning the same task more comparable.

2.2. Energy performance of HVAC systems in commercial buildings

Since the energy crisis in the early 1970s, scientists have paid more attention to more effective use of energy resources, the exploitation of renewable energy resources and the reduction of the impacts of energy use on the environment. The combustion of fossil fuels and the release of corresponding greenhouse gas (GHG) emissions appear to have significant impacts on the global climate change. One key-point of the sustainable development concept applied to the building industry is of the development of safe, healthy, energy-efficient and comfortable buildings, and the reduction or mitigation of their impacts on natural resources and the environment. In the building sector, energy consumption in HVAC systems was in excess of one-half of the total energy consumed in the United States (Ardehali et al. 1997). Commercial buildings accounted for 12% of the total national energy consumption in the United States (Franconi 1999). In 2003, commercial buildings in Canada accounted for 14% of the annual national end-use energy consumption and 13% of the total annual GHG emissions (NRCan 2005). The energy consumption of the air-conditioning in commercial buildings accounted for more than 60% of the national energy consumption in commercial buildings, and the related

GHG emissions accounted for more than 58% of the national GHG emissions in the commercial building sector (NRCan 2005). Therefore, the effectiveness of energy use for space heating and cooling is essential for the successful implementation of sustainable development concept in the building industry.

Heating, Ventilating, and Air Conditioning (HVAC) systems provide thermal comfortable conditions in commercial buildings. Commonly, HVAC systems include the primary central plants and the secondary energy delivering systems, which can be a central air distribution system or a decentralized terminal system.

The primary central plants provide thermal heating or cooling needed by HVAC systems. In practice, heating or cooling sources can be: 1) purchasing district heating or cooling; and 2) on-site heating or cooling generated by equipment in the central plants. In addition to energy generation devices, other main equipment is energy delivering equipment that transports energy carrying media such as the conditioned air and water.

Based on the classification of the secondary energy transferring systems, HVAC systems are generalized into three principal types: 1) all-air systems, 2) air-water systems and 3) all-water systems. As the name implied, all-air systems are referred to as systems where space heating and cooling loads are all provided by the central conditioned air, while other two types of HVAC systems are referred to providing space heating and cooling partially or thoroughly by the central conditioned water. The following sections introduce each of those HVAC systems separately.

2.2.1. All-air system

An all-air system provides complete cooling, preheating, and humidification capacity by the conditioned air supplied by systems. No additional cooling or humidification is required at zones. Heating could be accomplished by the air stream, either in a central system or at a particular zone. All-air systems can be classified into two categories: single-duct and dual-duct systems, and then, according to the different terminal unit configurations, they can be further divided as follows:

- Single-duct, constant air volume for multiple-zones with reheating coils in each individual zone (CAV-RH);
- Single-duct, variable air volume for multiple-zones with reheating coils in each individual zone (VAV-RH);
- Dual-duct, constant volume for multiple-zones.

All-air systems have the following advantages:

- The location of a central mechanical room accommodating major equipment allows operations and maintenance to be performed in unoccupied areas. In addition, it allows the maximum ranges of the choices of filtration equipment, and vibration and noise controls;
- Systems provide the greatest potential for the use of outdoor air as free cooling instead of mechanical refrigeration for cooling;
- Air-to-air and other heat recovery equipment is possible for incorporation;
- By increasing the air change rate for conditioned spaces and using high quality

controls, it is possible for systems to maintain the temperature and humidity of conditioned spaces within little fluctuation or even constant.

All-air systems have the following disadvantages:

- Systems require an additional duct clearance, which could increase the height of buildings and, in turn, increase the initial construction costs of buildings;
- Air balancing, particularly for large systems, can be more difficult to be obained.

Single-duct constant air volume (CAV) systems with reheat coils for multiple-zones changes supplied air temperatures in response to a variety of space loads, while maintaining a constant airflow rate. The supply air from a central air handling unit (AHU) is conditioned to be a fixed cold air temperature, which is normally set at 13°C. However, the supply air temperatures can be set to be variable by a proper control to reduce both the amount of required reheat and its associated energy consumption. The schematic of an air distribution system for a CAV system is shown in Figure 2-2.

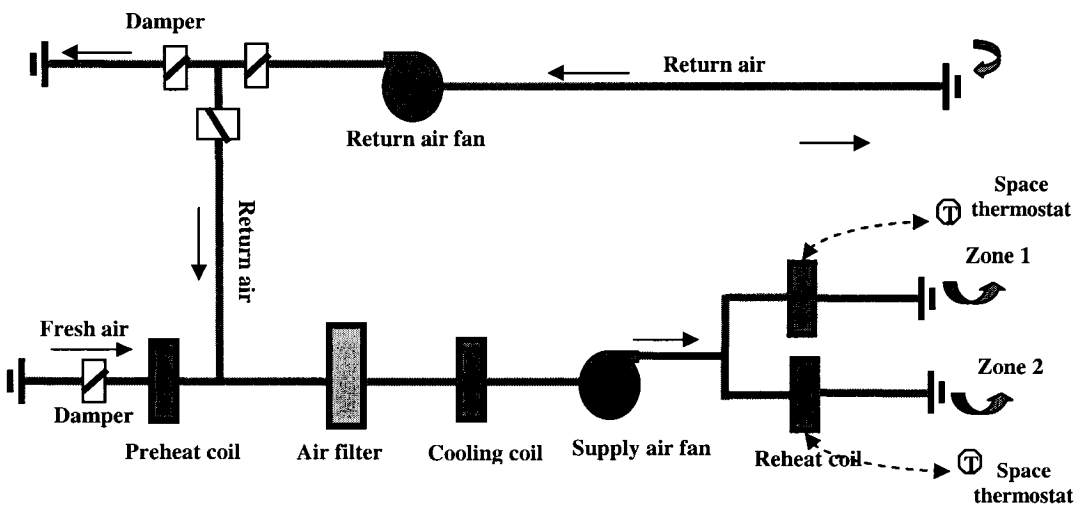

Figure 2-2: Schematic of a single-duct CAV system with reheat coils

Obviously, a single duct CAV system consumes more energy than a single duct VAV system due to its operation mechanism under part-load conditions, but a CAV system requires simpler controls; thereby, it decreases the initial and maintenance costs of the system.

Single-duct variable air volume (VAV) systems control individual zone temperatures by varying supply airflow rates rather than supply air temperatures. Traditionally, a VAV system for multiple-zone spaces supplies the conditioned air at a fixed temperature of 13°C for cooling. The airflow rate of supply air is firstly varied in response to various zone thermal loads. After the airflow rate of supply air hits its minimum value, the system then operates like a CAV system does in response to a further decline in zone thermal loads. The schematic of a VAV system for multiple-zone spaces is shown in Figure 2-3.

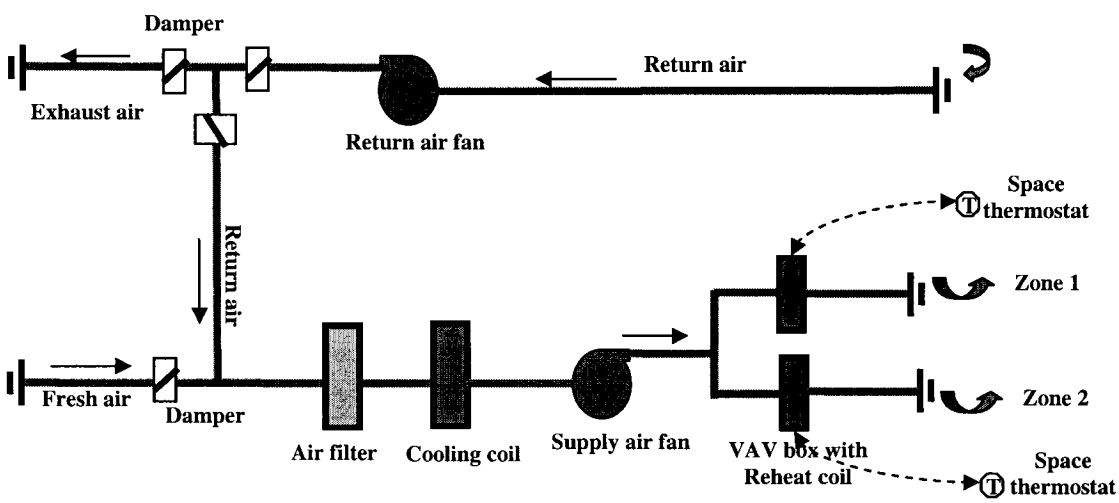

Figure 2-3: Schematic of a single-duct VAV system with reheat coil VAV boxes

Apparently, compared with a CAV system, a VAV system diminishes the unnecessary thermal mixing and lessens the energy use for air transportation at part-load conditions (ASHRAE 1996). The large energy savings associated with a VAV system arise from its operations in perimeter zones, where space thermal loads are significantly affected by outdoor conditions. However, in a central zone, where thermal loads are relatively constant, the potential of the energy reduction of a VAV system is not obvious. Humidity control is a potential problem with a VAV system at part-load conditions (ASHRAE 1996). If humidity is crucial, as in research labs or some industrial process workplaces, HVAC systems may have to be limited to CAV systems.

VAV terminal devices are available in many configurations including reheat, fan-powered, and induction.

Dual-duct constant air volume systems condition air in a central AHU and distribute it to the conditioned spaces through two parallel mains or ducts. One carries cold air, and the other carries warm air. The general schematic of a dual duct constant air volume system is shown in Figure 2-4.

In each conditioned space, a mixing box blends the two air flows in proper proportion to meet various space loads. Dual-duct all-air systems can be designed as constant volume or variable air volume systems.

As shown in Figure 2-4, the dual-duct CAV system is similar in effect to a single duct constant volume system with reheat coils.

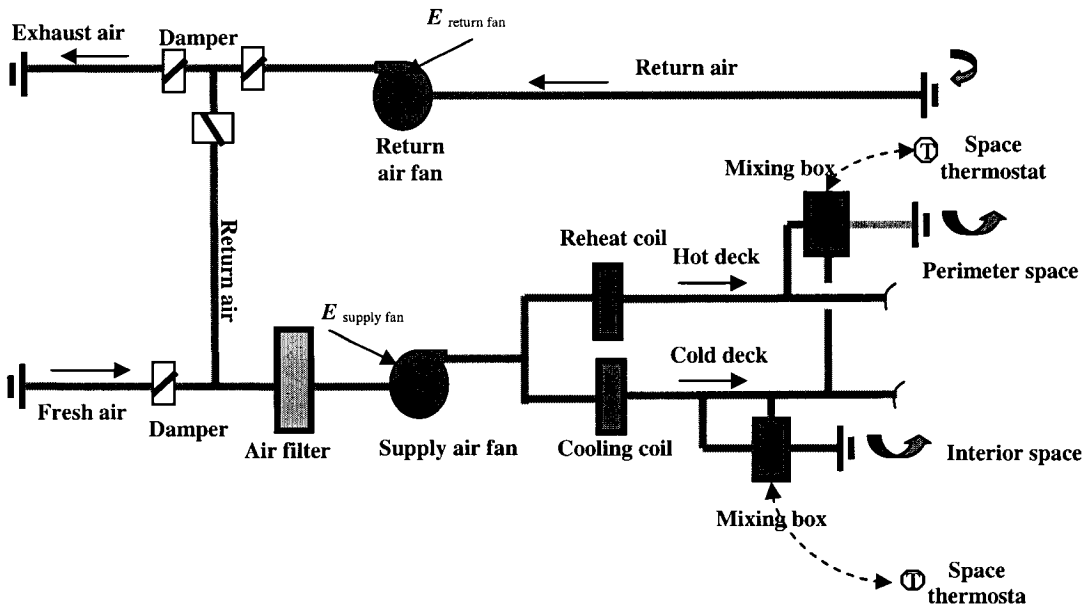

Figure 2-4: Schematic of a dual-duct constant air volume system

The only difference is to replace individual reheat coils applied to a single duct CAV-RH system with the central reheat coil applied to the dual-duct CAV system. Comparing with a single duct system, a dual-duct system requires more complicated controls, and thus, it is more complex than a single duct system. The initial capital investments and maintenance costs are all higher than those of a single duct system. A dual-duct system is generally more energy-intensive than a single duct system, but it is easy to control indoor conditions.

2.2.2. Air-water system

As the name implied, air-water systems provide heating or cooling through distributed air

and water. According to the different configurations of terminals, air-water systems include fan-coil unit systems and induction systems etc. Normally, main heating or cooling is provided by the conditioned water through individual terminals, and the central distributed conditioned air is only used for ventilation requirements; thus, one of the main advantages is to require less vertical installation spaces for the system. One of main disadvantages is of no accurate indoor set-point to be obtained.

2.2.3. All-water system

All-water systems for heating and cooling use both hot and chilled water for space conditioning. The principle types of all-water systems include: 1) Baseboard radiation; 2) Wall, ceiling, or floor panels; 3) Fan-coil units; 4) Bare pipe (racked on wall or slab). The main advantages include easy installation, less vertical installation space and that they are applicable for lower temperature heating and higher temperature cooling. One of the main disadvantages is that ventilation is significantly affected by factors such as weather conditions and the stack effect because there is no central mechanical ventilation system in use.

In the previously introduced three types of HVAC systems, all-air systems are always chosen for large office buildings. One of the main reasons is due to the physical characteristics of large office buildings. Large office buildings normally have large open floor areas, and partitions are different from floor to floor. The space of each floor can be typically separated into five zones: four perimeter zones and a central zone, according to the characteristics of space thermal loads. Thermal loads of perimeter zones are effected

significantly by weather conditions while those of the central zone are always cooling loads and are independent from outdoor conditions. Therefore, the HVAC system applied to large office buildings is normally required to be capable of simultaneously heating or cooling individual thermal zones.

Currently, the international trends of new construction show that VAV systems are the dominant type of HVAC systems applied to large commercial buildings. However, some surveys revealed that CAV systems still hold a large share in existing commercial buildings especially in developing countries. Even in the United States, data from the California utility surveys showed that the most common HAVC systems in existing large office buildings are CAV systems (Franconi 1999). VAV systems only accounted for about 20% of the total installed systems, while all-water systems only accounted for about 6% (Franconi 1999). Even though CAV systems still possess a large share in the existing commercial building stock, the advanced energy performance of VAV systems have been proved by numerous researchers (e.g., Ardehali et al. 1996, Ardehali et al. 1997 and Franconi 1999). For instance, Ardehali et al. (1996) noted that the variable air volume with reheat (VAV-RH) is the most energy efficient system used for commercial office buildings. After comparing with constant air volume with reheat systems (CAV-RH), they outlined that the VAV-RH system can achieve a reduction of 42% in annual operating costs. Franconi (1999) came to the similar conclusion about the energy performance between CAV and VAV systems. Since a variable air volume (VAV) system has been used as an alternative to other all-air systems for large commercial office buildings, the further improvements of the energy performance of VAV systems can

bring the potential of energy savings on the operation of large office buildings; thus, the studies on the energy performance of VAV systems can be one of the main issues concerned with improving the energy performance of large office buildings.

In summary, based on the consideration of the world trends of HVAC systems installed in modern large office buildings and some achievements already obtained in the energy performance of HVAC systems applied to large office buildings, this research is focused on the energy performance of VAV systems in large office buildings.

2.3. Potential energy savings in HVAC systems

In the world, more buildings become air conditioned due to the increasing expectation of thermal comfort. Air-conditioning market trends suggest that the use of air conditioning in the future should increase, which leads to the increase of international energy demand. Therefore, the studies of the evaluation of the energy performance of air-conditioning systems are important and urgent. In past several decades, a number of studies have been done in this field.

Reddy et al. (1994) revealed that HVAC systems in large office buildings provide thermal energy in excess of the summation of building heating and cooling loads. The excessive portion is due to the fact that a single HVAC system serving a multiple-zone space that contains different zones with different instantaneous thermal loads has to either reheat cold air or mix cold air with hot air. The phenomenon is called thermal mixing. They also indicated that a HVAC system serving a multi-zone building cannot totally

eliminate thermal mixing. Thermal mixing should be diminished as much as possible in order to reduce the energy use of a HVAC system. For instance, the utilization of discriminatory central supply air temperatures rather than a fixed one, in the case of a multi-zone VAV system, can effectively reduces the total energy usage for overcooling and reheating. On the other hand, the increase of the supply air temperatures of an air handling unit can result in raising the temperatures of chilled water as well. By doing so, the chiller can work under a higher COP of part-load conditions. Accordingly, the reduction of the energy consumption of a chiller can be achieved.

In order to characterize the penalty of thermal mixing existing in a multi-zone HVAC system and rate the energy performance of a multi-zone HVAC system on an absolute scale, Reddy et al. (1994) presented the concept of Energy Delivery Efficiency (EDF). They noted that EDF considers neither primary system conversion efficiencies nor effects such as transport losses. The concept is limited to the thermal efficiency of the air-side sub-system and allows the analyst to decide whether the HVAC system is performing adequately or whether fine-tuning or drastic improvement is warranted.

Another important role in the overall energy consumption of HVAC systems is the energy consumption of transporting working fluids (e.g., air and water), which is proportional to the volumetric flow rate of the related fluid. For instance, Ardehali et al. (1996) pointed out that the annual energy consumption of supply air fan in the case of CAV-RH is about twice compared with that for VAV-RH in office buildings.

Some energy saving strategies for all-air systems include the use of economizers on both the water-side and the air-side. For example, Ardehali et al. (1996) mentioned that the use of an air-side enthalpy economizer can significantly improve the energy performance of HVAC systems. Olsena and Chen (2003) utilized the EnergyPlus program to evaluate the potential energy savings of several different systems for a recently built building outside London, UK. They concluded that systems maximizing free cooling from outside air had the best energy performance. The annual energy costs of a VAV system operating with free cooling was about 20% less than those of the existing HVAC system operating with a fixed minimum outdoor airflow rate and being incapable of taking advantage of free cooling. They also pointed out a hybrid HVAC system, which referred to a VAV system with the night cooling strategy plus a natural ventilation system, were the best HVAC system.

Other operating strategies for HVAC systems, such as night purge, fan optimum start and stop, condenser water reset, and chilled water reset, have been studied. However, Ardehali et al. (1997) noted that the effects of using those operating strategies were not absolute but mostly dependent on many factors, such as building construction, local utility energy policy, and local weather conditions.

The application of the second law analysis of thermodynamics in thermal systems is not a new approach. However, only a few published papers discussed the application of the second law to the analysis of the performance of HVAC systems in commercial buildings. Currently, energy analysis programs such as DOE-2, TRNSYS and EnergyPlus are only

based on the first law analysis. Therefore, this research addresses the building simulation using another dimension, which normally neglected.

Wepfer et al. (1979) developed formulas to calculate the exergy of different fluids in HVAC applications such as liquid water, moist air and water vapor. They examined the exergy efficiency of some typical air-conditioning processes, by utilizing the outdoor environment state as the dead or reference state. Since then, most research on the exergy analysis of HVAC systems has focused only on components or subsystems such as heat pumps or air distribution systems. For example, Tsaros et al. (1987) analyzed a residential heat pump and presented the exergy flow diagram to identify the exergy consumption and transportation between each component of the equipment. Franconi et al. (1999) compared the exergy performance of two types of air distribution systems, the Constant Air Volume (CAV) and the Variable Air Volume (VAV). They outlined that the negative exergy load may occur in some building zones that require cooling and have the indoor air temperature higher than the outdoor temperature, or in some zones that require heating and have the indoor air temperature lower than the outdoor temperature. Bridges et al. (2001) analyzed the performance of domestic refrigerators and air conditioners by using the exergy analysis, and located the most inefficient sub-components.

Only a few papers presented the exergy analysis of HVAC systems at the system level. For instance, Ren et al. (2002) utilized the exergy analysis to evaluate the performance of evaporative cooling. They applied a novel selection of the dead state to the exergy analysis of HVAC systems; they used the outdoor temperature with 100% relative

humidity as the dead state. The use of this dead state was regarded as avoiding the underestimation of the exergy efficiency of HVAC systems. Asada and Takeda (2002) used experimental data to evaluate a ceiling radiant cooling system using well water as the cooling source. They concluded that the well water pump consumed a major portion of exergy in this cooling system and also estimated the impact of outdoor shading on indoor thermal environment. Alpuche et al. (2004) studied three packaged single zone air-conditioning units, serving a rural health center in Mexico, by using the PowerDOE program. The annual exergy efficiency of the three systems was 1.8-6.3%.

At the same time, many studies have been performed using renewable energy sources for the operations of HVAC systems. Solar energy as a renewable energy is more and more widely used for ecological buildings. Badescu (2002) studied a heat pump heating system with PV panels, using both energy and exergy analyses. He concluded that solar energy can properly drive the compressor during the heating mode if an appropriate electrical storage system is provided. The exergy analysis revealed that the compression and condensation are the two most inefficient processes during the operations of heat pumps.

Ground source heat pumps (GSHPs) provide high levels of comfort, offer significant reduction of electricity energy use and demand, have very low levels of maintenance requirements and are environmentally attractive (Hepasli et al. 2004). Based on the energy and exergy analysis of a ground source heat pump serving a class room in Turkey, and using field measured data, they concluded that the most inefficient part is the compressor. One recommended improvement is to bring the condensing and evaporating

temperature closer together. Ozgener et al. (2005) studied a geothermal district heating system in Turkey and indicated that exergy losses are mainly due to pumps, heat exchangers, thermal water injection, and hot water distribution pipeline. The exergy efficiency of the entire district heating system is 46%, which is significantly grater than that of a GSHP system, of around 3% presented by Hepasli et al. (2004). However, the energy efficiency of the former is 41.9% (Ozgener et al. 2005) while the COP of the GSHP is around 1.7 (Hepasli et al. 2004). From the comparison of energy efficiency, engineers may conclude that the GSHP system are more advanced than the geothermal district heating system; however, the exergy analysis indicates an opposite story.

Only a few published papers have discussed the energy efficiency of a whole air-conditioning system. For instance, Dunn et al. (2005) found good agreement between the measured system efficiency of air-conditioning systems in office buildings and the simulation results from the TAS and DOE-2 programs. The seasonal energy efficiency of VAV systems in office buildings was estimated as 0.81 (TAS) and 1.19 (DOE-2). They outlined that the various chilled ceiling configurations and the DX (Direct expansion) air-conditioning system offer significant energy efficiency advantages over others centralized systems, such as CAV, VAV, and fan coil or induction air-water systems.

2.4. Summary

In summary, commercial buildings have the significant potential of reducing the energy usage in HVAC systems and lowering the greenhouse gas emissions due to their operations. Based on literature review, the following conclusions can be drawn:

- VAV systems are currently the most effective HVAC systems used in large modern office buildings.
- The first law analysis alone sometimes cannot reflect the energy performance of a HVAC system. The second law analysis is very useful tool, but its developments in HVAC applications currently are very limited.
- The renewable energy sources for heating and cooling should be exploited and adopted in the operation of HAVC systems.

2.5. Objectives of this research

This research focuses on simulating the energy performance of VAV systems in a large office building. The first and second laws analyses are both used to evaluate the on-site and off-site energy performance of VAV systems. GHG emissions related to the energy use of VAV systems are evaluated.

Chapter 3 Mathematical Models of VAV Systems

This chapter describes the mathematical models of the VAV systems that are developed to perform a detailed thermodynamic analysis for both VAV systems including the air distribution systems and the heating and cooling plants. The simulation models are specifically used to 1) Evaluate the operations of the systems; 2) Track the system energy flows; and 3) Calculate the energy and exergy related indices for the systems and components.

In this chapter, the entire VAV system will be broken down into several subsystems: the air distribution system, the hot-water circuit and the chilled water circuit including the heat rejection cycle. Though the thermodynamic analysis is limited to VAV systems, the approach can be extended to all types of HVAC systems.

3.1. Approaches

A HVAC system is composed of a series of subsystems including an air distribution system, a hot water system and a chilled water system that includes cooling towers. Each subsystem is composed of a set of components interconnected through their inputs and outputs. The mathematical model of the entire VAV system includes three parallel subsystem models, which are the models of the air distribution system, the hot-water system and the chilled water system including the condenser water system. The models are composed of systems of equations in terms of mass, energy and exergy balance for

each component of the VAV system. All equations are written in an English-like language in the Engineer Equation Solver (EES) environment (Klein 2004) and then solved by the EES program, which employs Newton's methods to solve the systems of non-linear algebraic equations. The following flow chart illustrates the frame of the model of the VAV system. The simulation is based on a quasi steady-state model using one-hour time step.

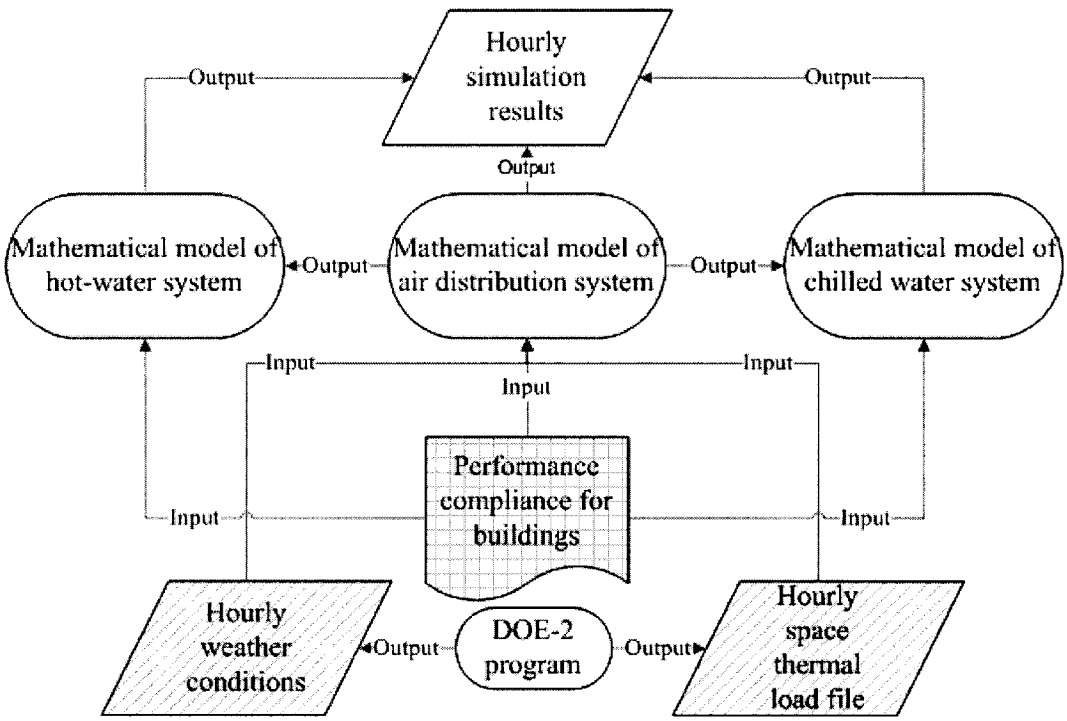

Figure 3-1: Frame of the model of the VAV system

Design parameters of the VAV system, such as design supply air temperatures and ventilation and circulation requirement, in accordance with the performance compliance for buildings (NRCC 1998) are input to the three subsystem models. Two variables, which are the hourly weather conditions and space thermal loads, are generated by any simulation program (e.g., DOE-2) and input to the air distribution model; in addition, some of the output of the air distribution model is then input to the two other models.

Eventually, the output of the three models consists of the simulation results. Since the accuracy of two input variables, hourly weather conditions and spaces thermal loads, can significantly affect the reliability of simulation results, uncertainty about the estimation of outdoor weather conditions, space thermal loads and efficiency of equipment etc. is the main limitation of the mathematical models of the VAV systems.

3.2. System model assumptions

This research focuses on variable air volume (VAV) systems. The systems have central heating coils and zone VAV boxes with reheat coils. Exhaust air flows directly outside without passing any heat recovery equipment. The free cooling control strategy also called the air-side economizer control is used for both VAV systems. The minimum amount of outdoor air of 0.4 $L/s \cdot m^2$ complies with Canadian regulations (NRCC 1998). The VAV systems operate from 8:00 am to 11:00 pm, from Monday to Friday, with a total operation time of 4176 hours per year.

Each VAV systems is further divided into an air distribution system, hot-water system and chilled water system including a cooling tower. The general layout of each subsystem is shown in the corresponding section. The VAV systems serve a five-floor office building, located in Montreal, and each floor contains five zones: one central zone and four perimeter zones.

Zone temperature set-points are 20°C for heating and 23°C for cooling. Zone loads are estimated by Zmeureanu et al. (1995) and input to the EES program (Klein 2004). The weather data for the simulation are also input from the DOE-2 program (DOE 1982).

The mixing processes, such as outdoor air mixing with the return air in the mixing chamber and the supply air from diffusers mixing with the room air, are well stirred; thus, the properties of mixtures are uniform and the stratification effect is ignored. Equipment, water piping, and ductwork are well insulated, and the heat exchange or air leaks from or to the environment is ignored. Even though in practice, VAV systems might take time to get a stable indoor air state when space thermal loads change from one hour to another, the time delay of VAV system response to the change of space thermal loads is ignored in the simulation process.

With respect to the mathematical models, the major limitations, except of the uncertainty introduced before, are the following:

1. Simulation is performed in a quasi-steady state mode; hence, the transient phenomena in fans, coils and controllers are not included;
2. Models of major equipment, such as boilers and chillers, are based on available publications; hence, additional work has to be performed to generate some new performance models for the equipment.

3.3. Mathematical model for the air distribution system

Figure 3-2 pictures a general flow chart of an air distribution system containing five VAV boxes with reheat coils.

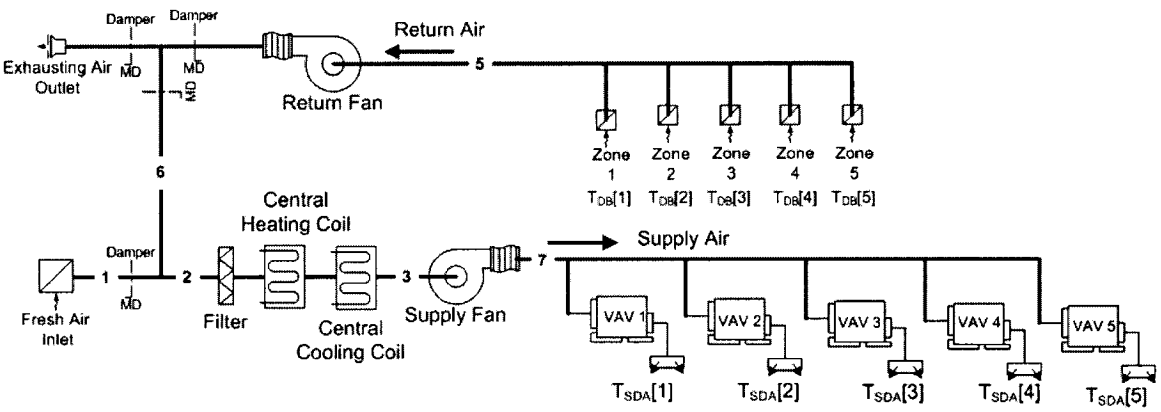

Figure 3-2: Diagram of a VAV system with reheat coils for multiple zones

The return and outdoor air flows are mixed and treated in the central air-handling unit, and then sent to individual zones through VAV boxes. VAV systems vary supply airflow rates in such a way to maintain individual temperature set points under various zone load conditions, but systems has to maintain supply airflow rates to be higher than or equal to a minimum supply airflow rate that is set to satisfy both ventilation and circulation requirements in compliance with Canadian regulations (NRCC 1998) and the characteristics of individual VAV boxes (the turndown airflow rate of individual VAV boxes). Generally, the temperature set point for the supply air directly following the central AHU is 13°C (NRCC 1998) for a multi-zone VAV system. VAV system no. 1 is designed according to this set point. In order to diminish overcooling that could occur in VAV system no. 1, VAV system no. 2 uses a discriminatory control, which resets the central supply air temperature in such a way to satisfy the zone having the highest cooling load.

At design conditions, the zone supply air temperatures for both VAV systems are set at 43°C (NRCC 1998) for heating, and 13°C (NRCC 1998) for cooling. The airflow rate for the ventilation or the circulation requirement is 0.4 l/s·m^2 or 2.0 l/s·m^2, respectively. The circulation requirement is only set up for cooling (NRCC 1998). The turndown airflow rate of VAV boxes is 30% of the design airflow rate.

3.3.1. Calculation of the air characteristics of each zone

The hourly air characteristics of each zone, calculated in this section, include the supply air temperature, the airflow rate, the indoor air humidity increase due to the latent loads, the indoor air temperature, and the reheating loads.

VAV system no. 1

Using the sign convention on space thermal loads employed by most energy analysis programs, the cooling load is considered as positive and the heating load is considered as negative. The latent load is considered to be positive. The mass flow rate of the supply air is calculated as follows:

$$\dot{m}_j = \frac{\dot{Q}_{sen,j}}{C_{pa} * \Delta T} \qquad (3\text{-}1)$$

where $\dot{m}_j$ denotes the mass flow rate (kg/s) of the supply air to the jth zone;

$\dot{Q}_{sen,j}$ denotes the sensible load (kW) of the jth zone;

ΔT denotes the temperature difference (K) between the supply and return air of the j^{th} zone; ΔT is equal to 10K for cooling (NRCC 1998) and -23K for heating (NRCC 1998);

C_{pa} denote the specific heat of air, 1.006 (kJ/kg·K).

Then, the volumetric flow rate of the supply air can be estimated by Equation 3-2.

$$\dot{V}_{i,j} = \nu * \dot{m}_j \tag{3-2}$$

where $\dot{V}_{i,j}$ denotes the volumetric flow rate (m^3/s) of the supply air in the j^{th} zone, at the i^{th} hour;

ν denotes the specific volume of the supply air (m^3/kg); the mean value of the specific volume of moisture air at the states (43°C, $\omega = 0.007609$ kg/kg) and (43°C, $\omega = 0$ kg/kg) is accounted for the heating mode; the mean value of the specific volume of moisture air at the states (13°C, $\omega = 0.007609$ kg/kg) and (13°C, $\omega = 0$ kg/kg) is accounted for the cooling mode.

0.007609kg/kg is the maximum humidity content that the supply air can reach with respect to the temperature of 11.49°C and the relative humidity of 90%. The value of $0.8182 m^3/kg$ or $0.904 m^3/kg$ is returned as the specific air volume for the cooling or the heating mode, respectively. Therefore, the volumetric supply airflow rate for each zone can be calculated as:

$$\dot{V}_{i,j} = 0.8182 * \frac{\dot{Q}_{sen,j}}{C_{pa} * 10} \text{ for the cooling mode} \tag{3-3}$$

$$\dot{V}_{i,j} = 0.904 * \frac{\dot{Q}_{sen,j}}{C_{pa} * (-23)} \text{ for the heating mode} \quad (3\text{-}4)$$

The design volumetric airflow rate of each VAV box is determined by the following equations:

$$\dot{V}_{\max,j} = \underset{i=1}{\overset{4176}{MAX}} (\dot{V}_{i,j}) \quad (3\text{-}5)$$

where $\dot{V}_{\max,j}$ denotes the design volumetric airflow rate of the j^{th} VAV box.

The minimum volumetric airflow rate of each zone can be then determined as follows:

- For the heating mode

$$\dot{V}_{\min,j} = MAX\left(\dot{V}_{\max,j} * 0.3, \frac{A_j * 0.4}{1000}\right) \quad (3\text{-}6)$$

where A_j denotes the floor area (m^2) of the j^{th} zone;

0.4 ($l/s \cdot m^2$) is the minimum airflow rate based on the ventilation requirement for the office building (NRCC 1998).

- For the cooling mode

$$\dot{V}_{\min,j} = MAX\left(\dot{V}_{\max,j} * 0.3, \frac{A_j * 1.2}{1000}\right) \quad (3\text{-}7)$$

where A_j denotes the floor area (m^2) of the j^{th} zone;

1.2 ($l/s \cdot m^2$) is the minimum airflow rate based on the circulating requirement for office buildings (NRCC 1998).

The VAV system can operate under two conditions - variable supply airflow rates or variable supply air temperature - for either the heating or the cooling mode. In the cooling mode, when the thermal loads of a zone shift from the design load to a partial load, the VAV system first cuts its supply airflow rate while maintaining a constant supply air temperature at the design supply air temperature of 13°C. However, after the supply airflow rate reaches its minimum value, the VAV system increases the supply air temperature if the space thermal loads further decrease. The conditions of variable supply air temperatures for the heating or the cooling mode is described as follows:

- for the heating mode

$$\dot{V}_{\min,j} = v * \frac{\left|\dot{Q}_{sen,j}\right|}{1.006 * \Delta T'} \tag{3-8}$$

$$v = f(20 + \Delta T') \tag{3-9}$$

where $f(20+\Delta T')$ denotes a built-in function of the EES program used to calculate the specific volume of air at the temperature of $20+\Delta T'$;

Equations 3-8 and 3-9 can return the temperature differences between the supply air and the indoor air, $\Delta T'$.

The mass flow rate and temperatures of supply air and the thermal loads of reheat coils can be calculated as follows:

$$\dot{m}_{i,j} = \frac{\dot{V}_{\min,j}}{v} \tag{3-10}$$

$$T_{SA} = 20 + \Delta T' \tag{3-11}$$

$$\dot{Q}_{RH} = 1.006 * \dot{m}_{i,j} * (T_{SA} - 13) \tag{3-12}$$

where the subscript of *SA* or *RH* denotes supply air or reheat, respectively.

- For the cooling mode

$$\dot{V}_{\min,j} = \nu * \frac{\dot{Q}_{sen,j}}{1.006 * \Delta T'} \tag{3-13}$$

$$\nu = f(23 - \Delta T') \tag{3-14}$$

Equations 3-13 and 3-14 can return the temperature differences between the supply air and the indoor air, $\Delta T'$.

The mass flow rate and temperatures of supply air and the thermal loads of reheat coils can be calculated as follows:

$$\dot{m}_{i,j} = \frac{\dot{V}_{\min,j}}{\nu} \tag{3-15}$$

$$T_{SA} = 23 - \Delta T' \tag{3-16}$$

$$\dot{Q}_{RH} = 1.006 * \dot{m}_{i,j} * (T_{SA} - 13) \tag{3-17}$$

Some control conditions are designed in the simulation models to determine the operations of individual VAV boxes. The first determination of either heating or cooling is based on the sign of thermal loads in the input file: 1) the cooling mode when the sensible load of the zone has a positive value and 2) the heating mode when the sensible load of the zone has a negative value. Subsequently, another determination of either variable airflow rates or variable supply air temperatures is verified as follows:

- In the heating mode

$\dot{m}_j * 0.904 \geq \dot{V}_{\min,j}$ for variable supply airflow rates (3-18)

$\dot{m}_j * 0.904 < \dot{V}_{\min,j}$ for variable supply air temperatures (3-19)

- In the case of cooling mode

$$\dot{m}_j * 0.8182 \geq \dot{V}_{\min,j} \text{ for variable supply airflow rates} \tag{3-20}$$

$$\dot{m}_j * 0.8182 < \dot{V}_{\min,j} \text{ for variable supply air temperatures} \tag{3-21}$$

The temperatures and mass flow rates of the supply air, the humidity increase in the supply air, and the reheat loads of individual VAV boxes are simulated as the follows:

- For the cooling mode under variable air flow rates:

$$\dot{m}_{SDA,j} = \frac{\dot{Q}_{sen,j}}{1.006 * 10} \tag{3-22}$$

$$T_{SA,j} = 13\,^{\circ}\mathrm{C} \tag{3-23}$$

$$\dot{Q}_{RH,j} = \dot{m}_{SDA,j} * 1.006 * (T_{SA,j} - 13) \tag{3-24}$$

$$\Delta\omega_j = \frac{\dot{Q}_{lat,j}}{\dot{m}_{SDA,j} * (2501 + 1.805 * 23)} \tag{3-25}$$

- For the cooling mode under variable supply air temperatures:

$$\dot{V}_{\min,j} = \nu_j * \frac{\dot{Q}_{sen,j}}{1.006 * \Delta T_j'} \tag{3-26}$$

$$\nu_j = f(23 - \Delta T_j') \tag{3-27}$$

$$\dot{m}_{SDA,j} = \frac{\dot{V}_{\min,j}}{\nu_j} \tag{3-28}$$

$$T_{SA,j} = 23 - \Delta T'_j \tag{3-29}$$

$$\dot{Q}_{RH,j} = 1.006 * \dot{m}_{SDA,j} * (T_{SA,j} - 13) \tag{3-30}$$

$$\Delta\omega_j = \frac{\dot{Q}_{lat,j}}{\dot{m}_{SDA,j}\left(2501 + 1.805 * T_{SA,j}\right)} \tag{3-31}$$

- For the heating modes under variable airflow rates:

$$\dot{m}_{SDA,j} = \frac{\dot{Q}_{sen,j}}{1.006 * (-23)} \tag{3-32}$$

$$T_{SA,j} = 43\,^{\circ}\mathrm{C} \tag{3-33}$$

$$\dot{Q}_{RH,j} = \dot{m}_{SDA,j} * 1.006 * (T_{SA,j} - 13) \tag{3-34}$$

$$\Delta\omega_j = \frac{\dot{Q}_{lat,j}}{\dot{m}_{SDA,j} * \left(2501 + 1.805 * 43\right)} \tag{3-35}$$

- For the heating mode under variable supply air temperatures:

$$\dot{V}_{mim,j} = \nu_j * \frac{\left|\dot{Q}_{sen,j}\right|}{1.006 * \Delta T'_j} \tag{3-36}$$

$$\nu_j = f(20 + \Delta T'_j) \tag{3-37}$$

$$\dot{m}_{SDA,j} = \frac{\dot{V}_{\min,j}}{\nu_j} \tag{3-38}$$

$$T_{SA,j} = 20 + \Delta T'_j \tag{3-39}$$

$$\dot{Q}_{RH,j} = 1.006 * \dot{m}_{SDA,j} * (T_{SA,j} - 13) \tag{3-40}$$

$$\Delta\omega_j = \frac{\dot{Q}_{lat,j}}{\dot{m}_{SDA,j} * \left(2501 + 1.805 * T_{SA,j}\right)} \tag{3-41}$$

VAV system no. 2

In order to model the operations of VAV system no. 2, two new parameters, which are the cooling air temperature and its dew-point humidity content of air, need to be developed from the simulation of VAV system no. 1. The definitions of the two parameters and the formulas used to calculate them are listed as follows:

- The cooling air temperature, which is the central supply air temperature used in the case of VAV system no. 2, is determined as the minimum supply air temperature required by all zones minus the temperature increase due to the effect of the supply air fan. Indeed, it is the supply air temperature after the cooling coil in the case of VAV system no. 2 and can be calculated as:

$$T_{CA} = \underset{j=1}{\overset{5}{MIN}}\left(T_{SA,j}\right) - \Delta T_{\sup ply,fan} \tag{3-42}$$

where $\Delta T_{\sup ply,fan}$ denotes the air temperature increase (°C) due to the effect of the supply air fan (see Equation 3-45).

- The dew-point humidity content of air refers to the maximum theoretical humidity content that the supply air can be obtained after the central cooling coil in the case of VAV system no. 2. It is used to determine whether the central cooling coil operates in a dehumidification mode or not. It is calculated in terms of the cooling air temperature and the relative humidity of 90% as follows:

$$\omega_{dew,point} = f\left(airH_2O, T = T_{CA}, P = 101[kPa], R = 0.9\right) \tag{3-43}$$

where T_{CA} denotes the cooling air temperature (°C);

P denotes the operation pressure (kPa) that is equal to the atmospheric pressure;

R denotes the relative humidity of the cooling coil dew-point.

The hourly temperature, the mass flow rate and the hourly humidity increase of the supply air for each zone can be estimated by using the same Equations introduced in the case of VAV system no. 1. The hourly reheat loads of individual zones are calculated as follows:

$$\dot{Q}_{RH,j} = 1.006 * \dot{m}_{SDA,j} * (T_{SA,j} - T_{CA}) \tag{3-46}$$

3.3.2. Calculation of the characteristics of the air distribution system

In this section, the model of estimating the hourly air properties at each state shown in Figure 3-2 is introduced. In Figure 3-2, the return air from each zone blends in the return mains to reach a uniform state represented by state no. 5. The state of return air after the return air fan is state no. 6 that also represents both the state of exhausted air and return air to be mixed with outdoor air. The state of outdoor air denotes state no. 1 while state no. 2 stands for the state of the air leaving the mixing chamber in the AHU. The state of supply air after the cooling coil is symbolized as state no. 3. State no. 7 represents the state of the air leaving the supply air fan. At state no. 7, the air temperature is called the

central supply air temperature after the AHU. It is a constant temperature of 13°C in the case of VAV system no. 1 but variable temperatures in the case of VAV system no. 2.

The air temperature increase through a fan due to the fan motor effect can be calculated as follows:

$$\Delta T_{fan} = \frac{\Delta P_t}{1.2 * 1005 * \eta_{1,combined,fan}} \tag{3-45}$$

where ΔP_t denotes the total pressure increase in the air through the fan;

$\eta_{1,combined,fan}$ denotes the total efficiency of the fan; the values of these variables are taken as follows (NRCC 1998):

$\Delta P_{t,return} = 250Pa$ and $\eta_{1,combined,return,fan} = 0.3$;

$\Delta P_{t,\text{sup }ply} = 1000Pa$ and $\eta_{1,combined,\text{sup }ply,fan} = 0.55$.

Based on Equation 3-45 and the variables applied to the supply and return air fans, the temperature increase in the air through the fans is:

$\Delta T_{return,fan} = 0.70°C$ or $\Delta T_{\text{sup }ply,fan} = 1.51°C$

Since the air temperature increases by 1.51°C through the supply fan, the air temperature at state no. 3 is equal to 11.49°C for VAV system no. 1.

The simulation of VAV system no. 1

Figure 3-3 is a flow chart including all possible cases of air mixing processes that could be operated in the case of VAV system no. 1 in terms of different control conditions.

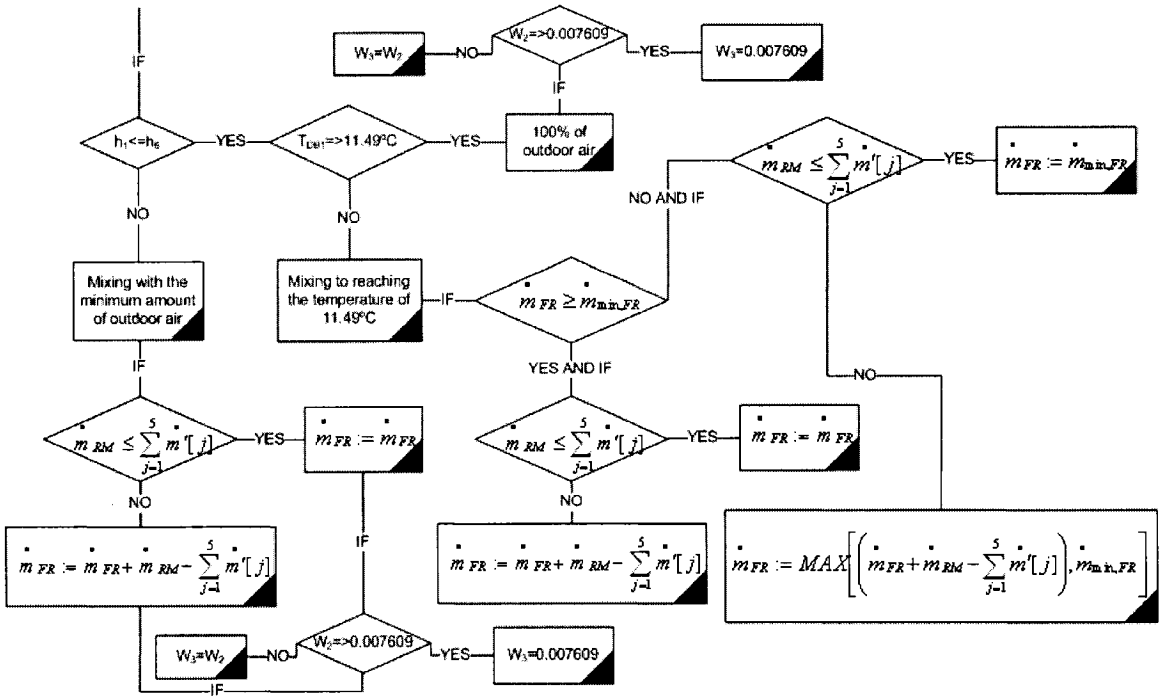

Figure 3-3: Algorithm of air mixing processes in the case of VAV system no. 1

When the simulation time changes forward from one hour to another, the VAV system may experience several cycles to obtain a stable indoor air state if it is called one cycle of the VAV system that air circulates through the whole air-distribution system once. For each cycle, the VAV system can operate along with one flow line according to certain conditions. In general, there are three types of mixing processes based on different control conditions in the operation flow chart (Figure 3-3): 1) mixing with the minimum amount of outdoor air; 2) mixing to reach the isothermal of 11.49°C; 3) no mixing or utilizing 100% outdoor air. Figures 3-4 and 3-5 show specifically the flow charts of the first two mixing processes. An enthalpy-based air side economizer control (free cooling)

is utilized in order to reduce the energy use for mechanical cooling. At the beginning of each cycle, the enthalpy of the return air (state no. 6) at the previous cycle compares with that of the outdoor air (state no. 1) at the present cycle to determine which mixing process the VAV system should take. Rhombi represent the control conditions while rectangles represent the destinations in the flow charts. The following sections introduce the three types of air mixing processes:

Mixing with the minimum amount of outdoor air

When the enthalpy of outdoor air is greater than that return air, the minimum amount of outdoor air is used to be mixed with return air. The portion of air in the mixture excluding the outdoor air is called the recirculated air. The amount of the outdoor air and the recirculated air in the mixture is first determined as follows:

$$\dot{m}_{FR} = \sum_{j=1}^{5} \frac{A_j * 0.4}{1000 * v_{outair}} \tag{3-46}$$

where A_j and v_{outair} denote the floor area of each zone and the specific volume of the outdoor air at this time;

$$\dot{m}_{RM} = \sum_{j=1}^{5} \dot{m}_{SDA,j} - \dot{m}_{FR} \tag{3-47}$$

where $\dot{m}_{SDA,j}$ denotes the amount of the supply air of each zone at this time (kg/s);

$\dot{m}_{RM}$ denotes the amount of the recirculated air in the mixture at this time (kg/s);

Figure 3-4 shows the algorithm in the case of mixing with the minimum amount of outdoor air, and $\sum_{j=1}^{5} \dot{m}'[j]$ denotes the total amount of the return air from each floor at the previous cycle, which is the summation of the return air from each zone at the previous cycle. Since the mass flow rate of the return air from each zone is accounted for being equal to that of the supply air to each zone at each cycle, $\sum_{j=1}^{5} \dot{m}'[j]$ is also equal to the summation of zone supply air at the previous cycle.

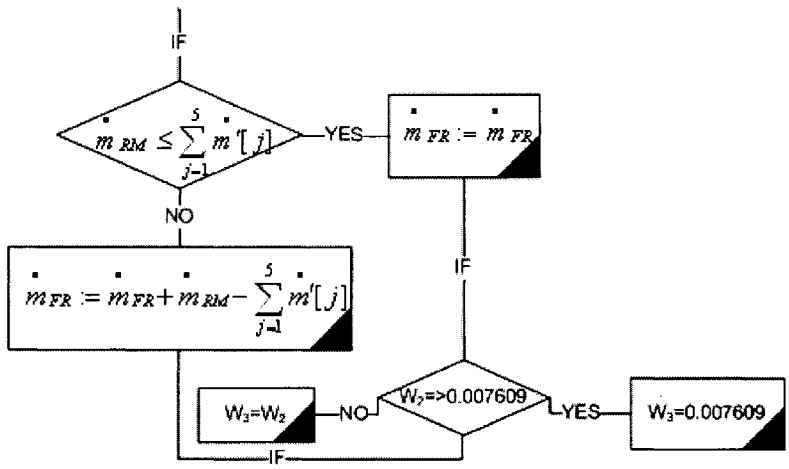

Figure 3-4: Algorithm of mixing with the minimum amount of outdoor air in the case of VAV system no. 1

In Figure 3-4, the first control condition is whether the amount of the recirculated air calculated by Equation 3-47 is equal or lower than the total amount of the return air at the previous cycle; in fact, this condition is used to determine whether the recirculated air in the mixture could be thoroughly provided by the return air or not. If the condition is satisfied (the recirculated air in the mixture can be totally provided by the return air), the quantity of the outdoor air and recirculated air in the mixture keeps the values calculated

by using Equations 3-46 and 3-47; otherwise, they should be rearranged by using Equations 3-48 and 3-49.

$$\dot{m}_{FR} := \dot{m}_{FR} + \dot{m}_{RM} - \sum_{j=1}^{5} \dot{m}'[j] \tag{3-48}$$

$$\dot{m}_{RM} = \sum_{j=1}^{5} \dot{m}'[j] \tag{3-49}$$

where the symbol ":=" stands for assignment instead of equal sign;

$\sum_{j=1}^{5} \dot{m}'[j]$ denotes the flow arte of the total return air from all zones at the previous cycle (kg/s).

The humidity content ω_2 and the dry-bulb temperature T_{DB2} of the mixture are calculated by using the follow equations:

$$\omega_2 = \frac{\dot{m}_{FR} * \omega_1 + \dot{m}_{RM} * \omega_6}{\dot{m}_{FR} + \dot{m}_{RM}} \tag{3-50}$$

$$T_{DB2} = \frac{\dot{m}_{FR} * T_{DB1} + \dot{m}_{RM} * T_{DB6}}{\dot{m}_{FR} + \dot{m}_{RM}} \tag{3-51}$$

The second control condition in Figure 3-4 compares the humidity content of the mixture air with the highest humidity content that the supply air can reach in the case of VAV system no. 1. The highest humidity content of the central supply air in VAV system no. 1 is 0.007609kg/kg, with respect to the dry-bulb temperature of the air after the cooling coil (11.49°C) and the machine dew-point applied to the cooling coil (90% relative humidity). If the condition is satisfied, the cooling coil would operate on the mode of

dehumidification, so the air properties at state no. 3 can be determined by Equation 3-52; otherwise, the cooling coil would work under a dry condition, so the air properties at state no. 3 can be estimated by Equation 3-53.

$\omega_3 = 0.007609$ kg/kg and $T_{DB3} = 11.49$°C for the wet cooling coil (3-52)

$\omega_3 = \omega_2$ and $T_{DB3} = 11.49$°C for the dry cooling coil (3-53)

Mixing to reach the isotherm of 11.49°C

Figure 3-5 shows algorithm in the case of mixing to reach the fixed supply air temperature of 11.49°C.

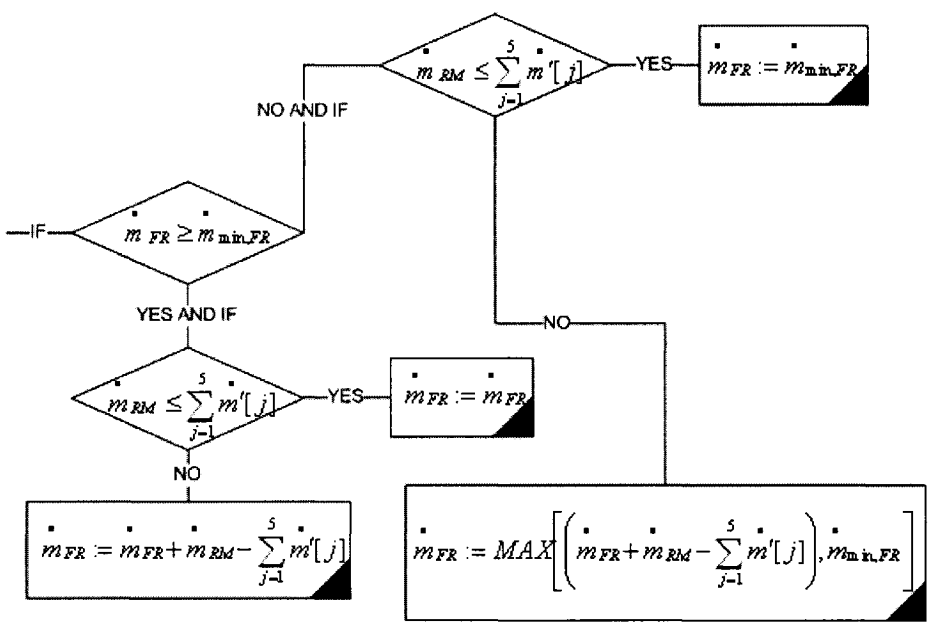

Figure 3-5: Algorithm of the mixing process to reach the isotherm of 11.49°C in the case of VAV system no. 1

This situation occurs when the enthalpy of outdoor air (state no. 1) at the present cycle is lower than that of the return air (state no. 6) at the previous cycle, and the temperature of outdoor air (state no. 1) at the present cycle is also lower than 11.49°C. The system

should be controlled with the certain proportion of outdoor air in order to most probably obtain the mixed air at the temperature of 11.49°C. Based on the control strategy – most probably obtaining a mixture of 11.49°C, the mass flow rate of outdoor air and recirculated air in the binary mixture is first calculated as follows:

$$\frac{\dot{m}_{RM}}{\dot{m}_{FR}} = \frac{11.49 - T_{DB1}}{T_{DB6} - 11.49} \tag{3-54}$$

$$\dot{m}_{FR} + \dot{m}_{RM} = \sum_{j=1}^{5} \dot{m}_{SDA,j} \tag{3-55}$$

where $\dot{m}_{FR}$ denotes the mass flow rate of the outdoor air in the mixture;

$\dot{m}_{RM}$ denotes the mass flow rate of the remaining air in the mixture;

$\sum_{j=1}^{5} \dot{m}_{SDA,j}$ denotes the mass flow rate of the central supply air at the present cycle.

The first control condition in Figure 3-5 is whether the outdoor airflow rate calculated from Equations 3-54 and 3-55 is higher than or equal to the minimum outdoor airflow rate determined by Equation 3-46. The second control condition compares the airflow rate of the recirculated air in the mixture calculated from Equations 3-54 and 3-55 with the airflow rate of the return air from all zones at the previous cycle. In Figure 3-5, $\sum_{j=1}^{5} \dot{m}'[j]$ denotes the summation of the return airflow rate from all zones at the previous cycle. There are four final destinations in Figure 3-5, and they are introduced separately as follows:

The first destination occurs when the first control condition is satisfied but the second one is not matched. Indeed, the situation happens when the outdoor temperatures are not quite lower than 11.49°C but the indoor thermal load varies significantly from one hour to another so that the flow rate of the return air from all zones at the previous cycle is lower than that of the recirculated air needed in the mixture. The deficit of airflow rate, therefore, should be supplemented by increasing the airflow rate of outdoor air. Therefore, the proportion of the outdoor air and the recirculated air for the mixing process can be recalculated by Equations 3-56 and 3-57:

$$\dot{m}_{FR} := \dot{m}_{FR} + \dot{m}_{RM} - \sum_{j=1}^{5} \dot{m}'[j] \tag{3-56}$$

$$\dot{m}_{RM} := \sum_{j=1}^{5} \dot{m}'[j] \tag{3-57}$$

where the symbol ":=" stands for the assignment instead of the equal sign

The second destination occurs when both the first and second conditions are not matched. In this situation, the flow rate of the outdoor air is not satisfied with the ventilation requirements, and the flow rate of the recirculated air is greater than that of the total return air at the previous cycle. The deficits in outdoor air and return air should be complemented by the flow rate of outdoor air. The flow rate of the outdoor air and the recirculated air in the mixture has to be estimated as follows:

$$\dot{m}_{FR} := MAX\left[\left(\dot{m}_{FR} + \dot{m}_{RM} - \sum_{j=1}^{5} \dot{m}'[j]\right), \dot{m}_{\min, FR}\right] \tag{3-58}$$

$$\dot{m}_{RM} := \sum_{j=1}^{5} \dot{m}'[j] \tag{3-59}$$

The third destination encounters when the first condition is not satisfied but the second one is matched, so the minimum flow rate of the outdoor air is set to that of the outdoor air in the mixture and the flow rate of the remainder in the mixture excluding the outdoor air is set to that of the recirculated air. The flow rate of the outdoor air and the recirculated air in the mixture is calculated by Formulas 3-60 and 3-61:

$$\dot{m}_{FR} := \sum_{j=1}^{5} \frac{A_j * 0.4}{1000 * v_{outair}} \tag{3-60}$$

$$\dot{m}_{RM} := \sum_{j=1}^{5} \dot{m}[j] - \dot{m}_{FR} \tag{3-61}$$

For all three destinations listed before, the respective air properties at state no. 2 are calculated as follows:

$$\omega_2 = \frac{\dot{m}_{FR} * \omega_1 + \dot{m}_{RM} * \omega_6}{\dot{m}_{FR} + \dot{m}_{RM}} \tag{3-62}$$

$$T_{DB2} = \frac{\dot{m}_{FR} * T_{DB1} + \dot{m}_{RM} * T_{DB6}}{\dot{m}_{FR} + \dot{m}_{RM}} \tag{3-63}$$

where the mass flow rates of the outdoor air and the remaining air account for the values calculated by the Equations applied to each of destinations.

The forth destination in Figure 3-5 occurs when the first and the second control conditions are all satisfied. The airflow rates of the recirculated and the outdoor air keep the values returned by Equations 3-54 and 3-55, and the respective air properties at state no. 2 are calculated as follows:

$$\omega_2 = \frac{\omega_1 + \omega_6 * \left(\frac{11.49 - T_{DB1}}{T_{DB6} - 11.49} \right)}{1 + \left(\frac{11.49 - T_{DB1}}{T_{DB6} - 11.49} \right)} \tag{3-64}$$

$$T_{DB2} = 11.49\,^{\circ}\mathrm{C} \tag{3-65}$$

When the mixing process is controlled in such a way to most probably obtain the temperature of 11.49°C for the mixture, mechanical cooling is not needed any more; however, the central heating coil still has to heat the mixed air from states no. 2 to no. 3 if the temperature of the mixture before the central heating coil is lower than 11.49°C. Therefore, air properties at state no. 3 in VAV system no. 1 are estimated as the following:

$$\omega_3 = \omega_2 \text{ and } T_{DB3} = 11.49\ ^{\circ}\mathrm{C} \tag{3-66}$$

Operation with 100% outdoor air

When the enthalpy of the outdoor air (state no. 1) at the present cycle is less than that of the return air (state no. 6) at the previous cycle, and the dry-bulb temperatures of the outdoor air are greater than 11.49°C (Figure 3-3), VAV system no. 1 operates with 100% outdoor air, so air properties at state no. 2 are the properties of the outdoor air; the control condition in this situation determines the central cooling coil working modes – either the dry mode or the dehumidification mode.

If the humidity content of the outdoor air is greater than or equal to 0.007609kg/kg, air properties at state no. 3 are determined as follows:

$$\omega_3 = 0.007609\,\text{kg/kg and } T_{DB3} = 11.49\,^{\circ}\text{C} \tag{3-67}$$

If the humidity content of the outdoor air is less than 0.007609kg/kg, the air properties at state no. 3 are determined as follows:

$$\omega_3 = \omega_2 \text{ and } T_{DB3} = 11.49\,^{\circ}\text{C} \tag{3-68}$$

Air properties at the rest states of the air distribution system are calculated as follows:

$$h'_5 = \frac{\sum_{j=1}^{5}\left(\dot{m}'[j] * h'[j]\right)}{\sum_{j=1}^{5}\dot{m}'[j]} \tag{3-69}$$

$$\omega'_5 = \frac{\sum_{j=1}^{5}\left(\dot{m}'[j] * \omega'[j]\right)}{\sum_{j=1}^{5}\dot{m}'[j]} \tag{3-70}$$

$$T'_{DB5} = f\left(airH_2O, h = h'_5, P = 101[kPa], \omega = \omega'_5\right) \tag{3-71}$$

where the symbol of "′" denotes the previous cycle;

"j" denotes the number of zones;

$f\left(airH_2O, h = h'_5, P = 101[kPa], \omega = \omega'_5\right)$ denotes psychrometric function with variables of enthalpy, humidity content, and atmospheric pressure as arguments, coded in the EES program (Klein 2004);

$$T_{DB6} = T'_{DB5} + 0.69\,^{\circ}\text{C} \tag{3-72}$$

$$\omega_6 = \omega'_5 \tag{3-73}$$

$$h_6 = f\left(airH_2O, T = T_{DB6}, P = 101[kPa], \omega = \omega_6\right) \tag{3-74}$$

$$T_{DB7} = 13\,^{\circ}\text{C} \tag{3-75}$$

$$\omega_7 = \omega_3 \tag{3-76}$$

The indoor air conditions of each zone are:

$$T_{DB}[j] = 20\,^{\circ}\mathrm{C} \text{ for heating or } T_{DB}[j] = 23\,^{\circ}\mathrm{C} \text{ for cooing} \tag{3-77}$$

$$\omega[j] = \omega_7 + \Delta\omega[j] \tag{3-78}$$

where $\Delta\omega[j]$ is calculated in section 3.3.1;

$$h[j] = f\left(airH_2O, T = T_{DB}[j], P = 101[kPa], \omega = \omega[j]\right) \tag{3-79}$$

The properties of air at state no. 5 at the present cycle can be calculated as

$$h_5 = \frac{\sum_{j=1}^{5}\left(\dot{m}[j] * h[j]\right)}{\sum_{j=1}^{5}\dot{m}[j]} \tag{3-80}$$

$$\omega_5 = \frac{\sum_{j=1}^{5}\left(\dot{m}[j] * \omega[j]\right)}{\sum_{j=1}^{5}\dot{m}[j]} \tag{3-81}$$

$$T_{DB5} = f\left(airH_2O, h = h_5, P = 101[kPa], \omega = \omega_5\right) \tag{3-82}$$

Time step in the simulation is set to one hour. During each hour, the airflow rates of the VAV system remain constantly, and the air properties at each state of the air-distribution system are also stable. However, when the simulation time changes forward from one hour to another, the VAV system may take several cycles to obtain another stable indoor air condition again. Only when the stable indoor air properties are obtained, are the respective characteristics of the air distribution system used for the simulation at the new

hour. The criterion of judging whether the VAV system in a stable state or not is that both the difference of the dry-bulb temperature and that of the humidity content of the return air at state no. 5 between the previous and the present cycles are in tolerance set in the EES program. In other words, when the simulation hour changes from one hour to another, the calculation iterates until the differences between T_{DB5} and T'_{DB5}, and ω_5 and ω'_5 are in tolerance. The final results are accounted for the analysis at the new hour.

The operation simulation of VAV system no. 2

Figure 3-6 illustrates the algorithm for the simulation of VAV system no. 2.

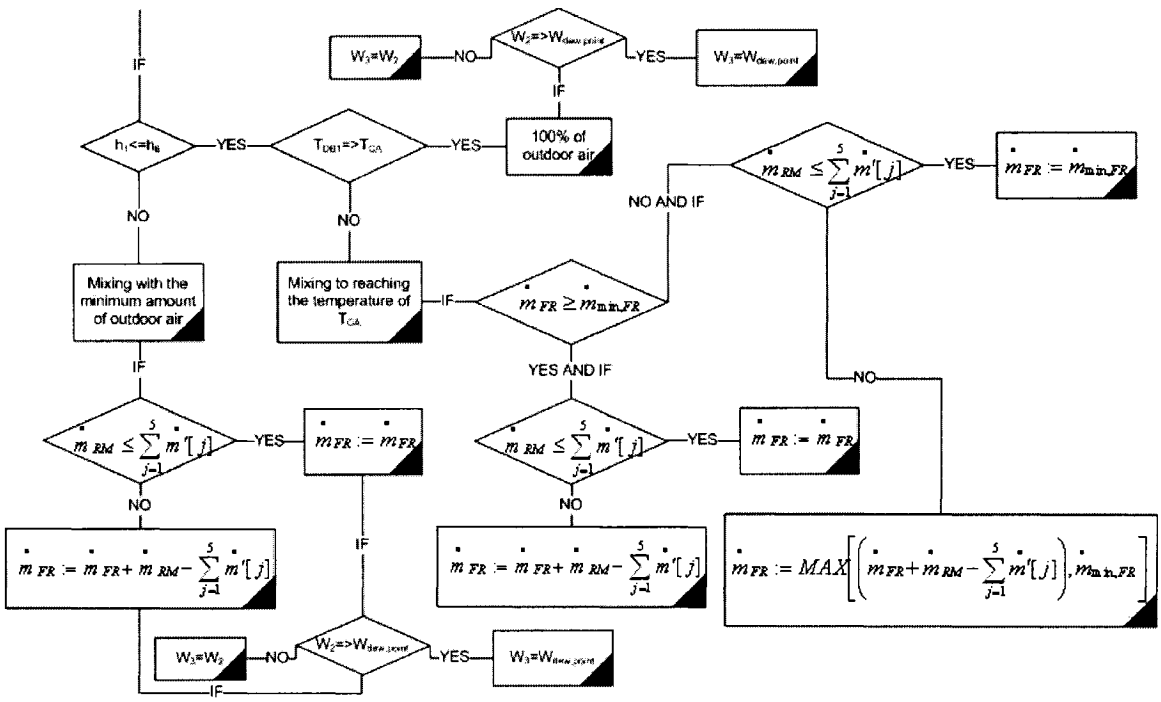

Figure 3-6: Algorithm of air mixing processes in the case of VAV system no. 2

Since the only difference between the two VAV systems is the methods of setting the central supply air temperature, the operation flows and control conditions for both VAV systems are similar. The differences include replacing the temperature of 11.49°C and the

humidity content of 0.007609kg/kg in the case of VAV system no. 1 with the cooling air temperature, T_{CA}, and the dew-point humidity content of air, $\omega_{dew,point}$, (calculated by Equations 3-44 and 3-45) in the case of VAV system no. 2. The formulas used in simulating the operation of VAV system no. 1 can be also utilized to simulate the operation of VAV system no. 2 after replacing 11.49°C with T_{CA}, and 0.007609kg/kg with $\omega_{dew,point}$.

3.3.3. Energy and exergy analyses for the air distribution system

The air distribution system consists of supply and return air fans, a central cooling coil, a central heating coil, a mixing chamber, an exhaust plenum and five reheat coils. Both energy and exergy analyses would cover all these components. The selection of the dead state or reference state related to the exergy analysis will be introduced first.

3.3.3.1. Properties of the dead state

From the thermodynamic point of view, the dead state refers to the state where the exergy of any substance is equal to zero. In recent decades, exergy analysis or availability analysis have been widely applied to the air-conditioning field. In general, there are four types of the selections of the dead state. Some analysts chose an arbitrary state as the dead state, for example, a state with a fix dry-bulb temperature of 21°C and 50% relative humidity. Wepfer et al. (1979) utilized the outdoor environment state as the dead state to apply exergy analysis to some typical HVAC processes. Bejan (1988) outlined the sensitivity of the numerical results of exergy related indices to the selections of the dead

state. Krakow (1991) proposed a selection of the dead state – the use of the effective reservoir temperature and specific humidity to define the dead state – that is specified in the application of exergy analysis for heat pumps, refrigerators or heat engines and examined two exergy related indices, exergy destruction and exergy efficiency, by using the different selections of the dead state temperature. He pointed out that the differences were less than 1-2% between using the effective reservoir temperature and the environment temperature but quite large (5-10% for exergy destruction and 15-35% for exergy efficiency) between the uses of the effective reservoir temperature and a fixed arbitrary temperature (e.g., 21.1°C) for the selection of the dead state. Ren et al. (2002) mentioned a novel selection of the dead state, which utilized the outdoor environment temperature and 100% relative humidity to define the dead state for the applications of HVAC systems. He regarded the new selection of the dead state as an effective way to avoid the underestimation of exergy efficiency for HVAC systems.

In air-conditioning applications, the composition of air except for water vapor is relatively constant, and the air can be treated as a mixture of ideal gases, dry air and water vapor. The content of dry air is considered constant during the air conditioning processes, but the moisture content may vary in the processes. Since the water vapor can still diffuse into the air as long as the air does not reach its saturated state at a given temperature and pressure, the available work can be obtained through a semi-permeable membrane. Accordingly, only the saturated air at the outdoor ambient temperature and pressure contains zero exergy. For this reason, the restricted dead state in this research is

defined as the state where the temperature and pressure are equal to the outdoor dry-bulb air temperature and pressure while the relative humidity ratio is 100%.

3.3.3.2. Supply and return air fans

Using fan laws (ASHRAE 2004), the electric demand of a fan at the full-load conditions is computed from the pressure the fan provides and the overall efficiency of the fan. The air volumetric flow rate of fans can be computed by using the following formulas:

$$\dot{V}_{RSF} = \underset{i=1}{\overset{4176}{MAX}} (\dot{V}_{SF}) \tag{3-83}$$

$$\dot{V}_{RRF} = \underset{i=1}{\overset{4176}{MAX}} (\dot{V}_{RF}) \tag{3-84}$$

$$\dot{V}_{SF} = \sum_{j=1}^{5} \dot{m}[j] * volume(airH_2O, T = T_{DB3}, \omega = \omega_3) \tag{3-85}$$

$$\dot{V}_{RF} = \sum_{j=1}^{5} \dot{m}[j] * volume(airH_2O, T = T_{DB5}, \omega = \omega_5) \tag{3-86}$$

where $\dot{V}_{RSF}$ and $\dot{V}_{RRF}$ denote the design airflow rate of the supply fan and the return fan, respectively (m^3/s);

$\dot{V}_{SF}$ and $\dot{V}_{RF}$ denote the hourly airflow rate of the supply and return air fans, respectively (m^3/s);

$volume(airH_2O, T = T_{DB3}, \omega = \omega_3)$ denotes a psychrometric function for specific volume calculated in terms of temperature and humidity ratio (m^3/kg), within the EES program;

$\sum_{j=1}^{5} \dot{m}[j]$ denotes the summation of hourly air mass flow rate of each zone (kg/s).

In the absence of the detailed design data, the total pressure the fans provide and the overall efficiency of the fans in the research are extracted from (NRCC 1998):

$\Delta P_{t,\text{sup } ply} = 1000kPa$ and $\Delta P_{t,return} = 250kPa$;

$\eta_{1,combined,\text{sup } ply,fan} = 0.55$ and $\eta_{1,combined,return,fan} = 0.3$.

The electric demand of fans at the design condition can be determined by using the following formulas:

$$\dot{E}_{RSF} = \frac{\dot{V}_{RSF} * \Delta P_{t,\text{sup } ply}}{\eta_{1,combined,\text{sup } ply,fan}} \tag{3-87}$$

$$\dot{E}_{RRF} = \frac{\dot{V}_{RRF} * \Delta P_{t,return}}{\eta_{1,combined,return,fan}} \tag{3-88}$$

The electric demand of the fans at part-load conditions is computed by using fan power coefficients of variable speed fans (BLAST VOL.2):

$$\dot{E}_{\text{sup } ply,fan} = \dot{E}_{RSF} * FFLP_{SF} \tag{3-89}$$

$$\dot{E}_{return,fan} = \dot{E}_{RRF} * FFLP_{RF} \tag{3-90}$$

where $FFLP$ denotes the fraction of full-load power and is calculated as following:

$$FFLP_{SF} = 0.00153 + 0.005208 * PL_{SF} + 1.1086 * PL_{SF}^{\ 2} - 0.11635563 * PL_{SF}^{\ 3} \tag{3-91}$$

$$FFLP_{RF} = 0.00153 + 0.005208 * PL_{RF} + 1.1086 * PL_{RF}^{\ 2} - 0.11635563 * PL_{RF}^{\ 3} \tag{3-92}$$

where PL denotes the part-load ratio of fans:

$$PL_{SF} = \frac{\dot{V}_{\sup ply}}{\dot{V}_{RSF}} \tag{3-93}$$

$$PL_{RF} = \frac{\dot{V}_{return}}{\dot{V}_{RRF}} \tag{3-94}$$

Energy balance:

$$\dot{E}_{\sup ply/return,fan} + \dot{m}_{air} \times h_i = \dot{m}_{air} \times h_e \tag{3-95}$$

where $\dot{E}_{fan}$ denotes the electric input to the fan (kW);

h denotes the enthalpy of air (kJ/kg);

the subscript i or e denote the inlet or outlet of fans, respectively.

The air enthalpy at the fan outlet is calculated as:

$$h_e = h_i + \frac{\dot{E}_{\sup ply/return,fan}}{\sum_{j=1}^{5} \dot{m}[j]} \tag{3-96}$$

where h_i accounts for h_3 for the supply fan or h_5 for the return fan.

Exergy balance of a fan:

The following Equations apply to both supply and return fans

$$\dot{\Phi}_{\sup ply,.F} - \dot{\Phi}_{recover,.F} - \dot{I}_{.F} = 0 \tag{3-97}$$

$$\dot{\Phi}_{\sup ply,.F} = \dot{E}_{fan} \tag{3-98}$$

$$\dot{\Phi}_{recover,.F} = \sum_{j=1}^{5} \dot{m}[j] * \left[h_{e,fan} - h_{i,fan} - T_0 * \left(s_{e,fan} - s_{i,fan}\right)\right] \tag{3-99}$$

where $\dot{\Phi}$ denotes the exergy flow rate through a fan (kW);

$\dot{I}_{.F}$ denotes the irreversibility or exergy destruction due to the return fan (kW);

the subscript of *i* or *e* represent the inlet or outlet of a fan, respectively.

Irreversibility due to the operation of a fan

$$\dot{I}_{.F} = \dot{\Phi}_{\text{sup}\,ply,.F} - \dot{\Phi}_{recover,.F} \tag{3-100}$$

Entropy generation due to a fan

Entropy generation due to a fan is calculated from the irreversibility of the fan as:

$$\dot{\sigma}_F = \frac{\dot{I}_F}{T_o} \tag{3-101}$$

where T_o denotes the absolute temperature of the dead state (K);

$\dot{\sigma}_F$ denotes the entropy generation of a fan (kW/K).

Second-law of efficiency of a fan

$$\eta_{II,F} = \frac{\dot{\Phi}_{recover,F}}{\dot{\Phi}_{\text{sup}\,ply,F}} \tag{3-102}$$

where $\eta_{II,F}$ denotes the exergy efficiency of a fan;

3.3.3.3. Exergy of the air distribution system at each point

$$\psi_1 = (h_1 - h_o) - T_o * (s_1 - s_o) + 0.287 * T_o * \left[\begin{array}{l} (1+1.608\omega_1) * \ln \dfrac{1+1.608\omega_o}{1+1.608\omega_1} \\ +1.608\omega_1 * \ln \dfrac{\omega_1}{\omega_o} \end{array} \right] \quad (3\text{-}103)$$

$$\psi_5 = (h_5 - h_o) - T_o * (s_5 - s_o) + 0.287 * T_o * \left[\begin{array}{l} (1+1.608\omega_5) * \ln \dfrac{1+1.608\omega_o}{1+1.608\omega_5} \\ +1.608\omega_5 * \ln \dfrac{\omega_5}{\omega_o} \end{array} \right] \quad (3\text{-}104)$$

$$\psi_6 = (h_6 - h_o) - T_o * (s_6 - s_o) + 0.287 * T_o * \left[\begin{array}{l} (1+1.608\omega_6) * \ln \dfrac{1+1.608\omega_o}{1+1.608\omega_6} \\ +1.608\omega_6 * \ln \dfrac{\omega_6}{\omega_o} \end{array} \right] \quad (3\text{-}105)$$

$$\psi_7 = (h_7 - h_o) - T_o * (s_7 - s_o) + 0.287 * T_o * \left[\begin{array}{l} (1+1.608\omega_7) * \ln \dfrac{1+1.608\omega_o}{1+1.608\omega_7} \\ +1.608\omega_7 * \ln \dfrac{\omega_7}{\omega_o} \end{array} \right] \quad (3\text{-}106)$$

where ψ denotes the specific exergy of air (kW/kg);

the subscript "o" denotes the dead state.

3.3.3.4. Exergy analysis of the exhausting process

The efficiency of the exhausting process is calculated only when return air is used to be mixed with outdoor air ($\dot{m}_{RM} \neq 0$), otherwise, the efficiency of this process is defined as zero.

Exergy balance:

$$\dot{\Phi}_{supply,exhaust} - \dot{\Phi}_{recover,exhaust} - \dot{I}_{exhaust} = 0 \tag{3-107}$$

$$\dot{\Phi}_{supply,exhaut} = \sum_{j=1}^{5} \dot{m}[j] * \psi_6 \tag{3-108}$$

where $\dot{m}[j]$ denotes the mass flow rate of the air to each zone (kg/s);

ψ_6 denotes the specific exergy of the conditioned air at state no. 6 of the VAV system (kW/kg);

$$\dot{\Phi}_{recover,exhaust} = \dot{m}_{RM} * \psi_6 \tag{3-109}$$

Entropy generation of the exhausting process

$$\dot{\sigma}_{exhaust} = \frac{\dot{I}_{exhaust}}{T_o} \tag{3-110}$$

Second-law efficiency of the exhausting process

$$\eta_{II,exhaust} = \frac{\dot{\Phi}_{recover,exhaust}}{\dot{\Phi}_{supply,exhaust}} \tag{3-111}$$

3.3.3.5. Exergy analysis of the mixing process

The exergy analysis would only be done when there is a mixing process ($\dot{m}_{RM} \neq 0$).

Exergy balance:

$$\dot{\Phi}_{\text{sup ply},mixing} - \dot{\Phi}_{recover,mixing} - \dot{I}_{mixing} = 0 \tag{3-112}$$

$$\dot{\Phi}_{\text{sup ply},mixing} = \dot{m}_{FR} * \psi_1 + \dot{m}_{RM} * \psi_6 \tag{3-113}$$

where $\dot{m}_{FR}$ denotes the mass flow rate of outdoor air (kg/s);

$$\dot{\Phi}_{recover,exhaust} = \sum_{j=1}^{5} \dot{m}[j] * \psi_2 \tag{3-114}$$

Entropy generation of the mixing process

$$\dot{\sigma}_{mixing} = \frac{\dot{I}_{mixing}}{T_o} \tag{3-115}$$

Second-law efficiency of the mixing process

$$\eta_{II,mixing} = \frac{\dot{\Phi}_{recover,mixing}}{\dot{\Phi}_{\text{sup ply},mixing}} \tag{3-116}$$

3.3.3.6. Exergy analysis of the central cooling coil with by-pass line

The system includes a central cooling coil and its by-pass line, and three working fluids: chilled water, condensate water and conditioned air. During each hour, all working fluids have steady flow rates and the temperature of condensation from the cooling coil in this research is assumed at 11°C. The exergy analysis is only executed when the chiller works ($\dot{Q}_{ev} \neq 0$). Heat interaction with the ambient is negligible.

Exergy balance:

$$\dot{\Phi}_{supply,CC} - \dot{\Phi}_{recover,CC} - \dot{I}_{CC} = 0 \tag{3-117}$$

where $\dot{I}$ denotes the irreversibility or exergy destruction of the system (kW) and includes the portion of energy contented by the condensate of the cooling coil, which is estimated by Equations 3-122 and 3-123;

the subscripts *"CC"* and *"cond"* denote the central cooling coil and the condensate from the cooling coil;

$$\dot{\Phi}_{supply,CC} = \dot{m}_{CWP} * \Delta\psi_{water,CC} \tag{3-118}$$

where $\dot{m}_{CWP}$ denotes the design mass flow rate of the chilled water (kg/s);

$\Delta\psi_{water,CC}$ denotes the exergy change of the chilled water through the central cooling coil (kW/kg);

$$\dot{\Phi}_{recover,CC} = \sum_{j=1}^{5} \dot{m}[j] * \Delta\psi_{air,CC} \tag{3-119}$$

where $\Delta\psi_{air,CC}$ denotes the exergy recovered by the conditioned air through the central cooling coil (kW/kg);

$$\Delta\psi_{air,CC} = (h_3 - h_2) - T_o * (s_3 - s_2) + 0.287 * T_o * \left[\begin{array}{l} (1+1.608\omega_3) * \ln\dfrac{1+1.608\omega_2}{1+1.608\omega_3} \\ +1.608\omega_3 * \ln\dfrac{\omega_3}{\omega_2} \end{array} \right] \tag{3-120}$$

$$\Delta\psi_{water,CH} = (h_{t_{CW,i}} - h_{t_{CW,e}}) - T_o * (s_{t_{CHW,i}} - s_{t_{CW,e}}) \tag{3-121}$$

$$\dot{\Phi}_{cond} = \sum_{j=1}^{5} \dot{m}[j] * (\omega_2 - \omega_3) * \psi_{coil,codensed} \tag{3-122}$$

$$\psi_{coil,condensed} = \upsilon_{f@11} * \left(P_0 - P_{sat@11}\right) + h_{f@11} - h_{f@t_0} - T_o * \left(s_{f@11} - s_{f@t_0}\right)$$
$$- 0.416 * T_o * \left[\ln\left(\frac{P_0}{P_{g@t_0}}\right) + \ln\left(\frac{1.6078 * \omega_0}{1 + 1.6078 * \omega_0}\right)\right] \quad (3\text{-}123)$$

where $P_{g@t_0}$ denotes the pressure of the saturated water vapor at environment temperature (kPa);

$\upsilon_{f@11}$ denotes the specific volume (m^3/s) of the saturated liquid water at 11°C.

Irreversibility due to the central cooling coil

$$\dot{I}_{CC} = \dot{\Phi}_{supply,CC} - \dot{\Phi}_{recover,CC} \quad (3\text{-}124)$$

Entropy generation due to the central cooling coils

$$\dot{\sigma}_{CC} = \frac{\dot{I}_{CC}}{T_o} \quad (3\text{-}125)$$

Second-law efficiencies of the central cooling coil

$$\eta_{II,CC} = \frac{\dot{\Phi}_{recover,CC}}{\dot{\Phi}_{supply,CC}} \quad (3\text{-}126)$$

3.3.3.7. Exergy analysis of the central heating coil

The central heating coil works only when the air temperature at state no. 2 is lower than 11.49°C in the case of VAV system no. 1, and lower than T_{CA} in the case of VAV system no. 2. The exergy analysis is used only when the thermal loads of the central heating coil

is not equal to zero ($\dot{Q}_{CH} \neq 0$). The heat exchange between hot water and conditioned air is considered to have an efficiency of 100%.

Exergy balance:

$$\dot{\Phi}_{supply,CH} - \dot{\Phi}_{recover,CH} - \dot{I}_{CH} = 0 \tag{3-127}$$

$$\dot{\Phi}_{supply,CH} = \dot{m}_{CHW} * \Delta\psi_{water,CH} \tag{3-128}$$

where $\dot{m}_{CHW}$ denotes the mass flow rate of the hot water passing through the central heating coil (kg/s);

$\Delta\psi_{water,CH}$ denotes the specific exergy provided by the hot water (kW/kg), calculated by Equation 3-131;

$$\Delta\psi_{water,CH} = (h_{t_{CH,win}} - h_{t_{CH,wout}}) - T_o * (s_{t_{CH,win}} - s_{t_{CH,wout}}) \tag{3-129}$$

$$\dot{\Phi}_{recover,CH} = \sum_{j=1}^{5} \dot{m}[j] * \Delta\psi_{air,CH} \tag{3-130}$$

where $\Delta\psi_{air,CH}$ denotes the exergy recovered by the conditioned air (kW/kg):

$$\Delta\psi_{air,CH} = (h_3 - h_2) - T_o * (s_3 - s_2) + 0.287 * T_o * \left[\begin{array}{l} (1+1.608\omega_3) * \ln\dfrac{1+1.608\omega_2}{1+1.608\omega_3} \\ +1.608\omega_3 * \ln\dfrac{\omega_3}{\omega_2} \end{array} \right] \tag{3-131}$$

Entropy generation of the central heating coil

$$\dot{\sigma}_{CH} = \frac{\dot{I}_{CH}}{T_o} \tag{3-132}$$

Second-law efficiency of the central heat coil

$$\eta_{II,CH} = \frac{\dot{\Phi}_{recover,CH}}{\dot{\Phi}_{supply,CH}} \tag{3-133}$$

3.3.3.8. Exergy analysis of the reheat coils

The exergy analysis of reheat coils is performed when the thermal loads of reheat coils are not equal to zero ($\dot{Q}_{RH}[j] \neq 0$), where j indicates the zone.

Exergy balance:

$$\dot{\Phi}_{supply,RH}[j] - \dot{\Phi}_{recover,RH}[j] - \dot{I}_{RH}[j] = 0 \tag{3-134}$$

where the subscript *RH* denotes the reheat coil;

$$\dot{\Phi}_{supply,RH}[j] = \dot{m}_{RHW}[j] * \Delta\psi_{water,RH}[j] \tag{3-135}$$

where $\dot{m}_{RHW}[j]$ denotes the mass flow rate of the hot water through the j[th] reheat coil (kg/s);

$\Delta\psi_{water,RH}[j]$ denotes the specific exergy provided by the hot water of the j[th] reheat coil (kW/kg);

$$\Delta\psi_{water,RH}[j] = (h_{t_{RH,win}[j]} - h_{t_{RH,wout}[j]}) - T_o * (s_{t_{RH,win}[j]} - s_{t_{RH,wout}[j]}) \tag{3-136}$$

$$\dot{\Phi}_{recover,CH} = \dot{m}[j] * \Delta\psi_{air,RH}[j] \tag{3-137}$$

where $\Delta\psi_{air,RH}[j]$ denotes the exergy recovered of the j[th] reheat coil by the conditioned air (kW/kg);

$$\Delta\psi_{air,RH}[j] = (h[j] - h_7) - T_o * (s[j] - s_7) \tag{3-138}$$

where $h[j]$ and $s[j]$ denote the specific enthalpy and entropy of the supply air of j^{th} zone.

Entropy generation of reheat coils

$$\dot{\sigma}_{RH}[j] = \frac{\dot{I}_{RH}[j]}{T_o} \tag{3-139}$$

Second-law efficiency of reheat coils

$$\eta_{II,RH}[j] = \frac{\dot{\Phi}_{recover,RH}[j]}{\dot{\Phi}_{supply,RH}[j]} \tag{3-140}$$

3.4. Mathematical model of the central heating plant

The general layout of the hot-water loop for both VAV systems is shown in Figure 3-7.

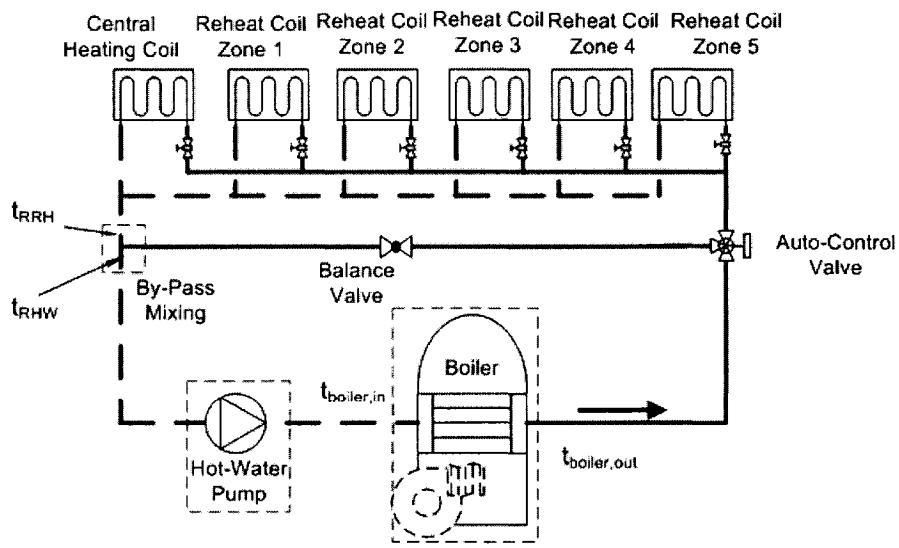

Figure 3-7: Schematic of the Hot-Water Loop for the VAV System

The main components of the hot-water loop include: a boiler, a hot-water circulating pump, a by-pass mixing pipe, and heating coils. All components are considered to be well insulated. The hot-water circuit is designed to be a constant water flow rate. The water temperature at the exit of the boiler is set at 65°C. An auto-control valve adjusts the proportion of the hot water through the by-pass line corresponding to part-load conditions. The analysis of heat/reheat coils is already manifested in the previous sections. The detailed analysis of the boiler, the hot-water pump, and the by-pass mixing process are presented in the following section.

3.4.1. Boiler

The nominal capacity of the electric boiler is calculated as the maximum hourly heating loads required by all heating and reheating coils.

Energy balance

At full-load conditions, the electric input to the boiler is calculated by the following formula:

$$\dot{E}_{electricity} = \frac{\dot{Q}_{rated,boiler}}{\eta_{I,boiler}} \tag{3-141}$$

where $\eta_{I,boiler}$ denotes the energy efficiency of the boiler, assumed to be equal to 80% at design conditions (NRCC 1998).

At part-load conditions, the electric input to the boiler is calculated according to the following formula (NRCC 1998):

$$\dot{E}_{electricity} = \frac{\dot{Q}_{rated,boiler}}{\eta_{1,boiler}} \times \left(0.082597 + 0.996764 \times PLR_B - 0.079361 \times PLR_B{}^2\right) \quad (3\text{-}142)$$

where $\dot{Q}_{rated,boiler}$ denotes the nominal capacity of the boiler (kW);

PLR_B denotes the part-load ratio of the boiler at off-peak conditions, calculated as:

$$PLR_B = \frac{\dot{Q}_{boiler}}{\dot{Q}_{rated,boiler}} \quad (3\text{-}143)$$

where $\dot{Q}_{boiler}$ denotes the hourly heat flow rate delivered by the boiler (kW).

Exergy balance

$$\dot{\Phi}_{supply,boiler} - \dot{\Phi}_{recover,boiler} - \dot{I}_{boiler} = 0 \quad (3\text{-}144)$$

$$\dot{\Phi}_{supply,boiler} = \dot{E}_{electricity} \quad (3\text{-}145)$$

$$\dot{\Phi}_{recover,boiler} = \dot{m}_{HWP} \times \Delta\psi_{HW} \quad (3\text{-}146)$$

$$\dot{I}_{boiler} = \dot{\Phi}_{supply,boiler} - \dot{\Phi}_{recover,boiler} \quad (3\text{-}147)$$

where $\dot{m}_{HWP}$ denotes the mass flow rate of hot-water through the hot-water pump (kg/s);

$\Delta\psi_{HW}$ denotes the hot-water specific exergy difference between inlet and outlet of the boiler (kJ/kg);

$$\Delta\psi_{HW} = h_{@t_{boiler,e}} - h_{@t_{boiler,i}} - T_0 \times \left(s_{@t_{boiler,e}} - s_{@t_{boiler,i}}\right) \quad (3\text{-}148)$$

where s and h denote entropy and enthalpy of hot-water, respectively.

Entropy generation

$$\dot{\sigma}_{boiler} = \frac{\dot{I}_{boiler}}{T_o} \tag{3-149}$$

Second-law efficiency of the boiler

$$\eta_{II,boiler} = \frac{\dot{\Phi}_{recover,boiler}}{\dot{\Phi}_{supply,boiler}} \tag{3-150}$$

3.4.2. Hot-water circulating pump

The pump is used to circulate hot-water through the piping system, the boiler and heating and reheating coils. The power input to the hot water pump is calculated by using the pump laws from (ASHRAE 2004).

Energy balance:

$$\dot{E}_{HW,pump} = \dot{m}_{HWP} \times \left(h_{e,HW,pump} - h_{i,HW,pump}\right) \tag{3-151}$$

where $\dot{m}_{HWP}$ denotes the hot-water mass flow rate through the hot-water pump (kg/s);

$\dot{E}_{HW,pump}$ denotes the electric input of the hot-water pump (kW);

h denotes the specific enthalpy of the hot-water (kJ/kg);

The subscripts i and e denote hot-water flowing into and out the pump, respectively.

The electric input to the pump can be calculated as follows:

$$\dot{E}_{hw,pump} = \frac{\dot{V}_{HWP} \times \Delta H_{t,HW}}{\eta_{1,combined,HW,pump}} \quad (3\text{-}152)$$

where $\dot{V}_{HWP}$ denotes the design volumetric flow rate of the hot-water pump (m^3/s);

$\Delta H_{t,HW}$ denotes the total pressure drop of the hot-water circuit at designed water flow-rate (kPa), assumed to be 250 kPa in the research;

$\eta_{1,combined,HW,pump}$ denotes the overall energy efficiency of the hot-water pump, accounted for 60% (NRCC 1998).

The volumetric flow rate of hot-water can be calculated as following:

$$\dot{V}_{HWP} = \frac{\dot{Q}_{rated,boiler}}{C_{p,W} * \Delta T_{HW} * \rho_{water}} \quad (3\text{-}153)$$

where $C_{p,W}$ denotes the specific heat of water (4.19kJ/kg.K);

ΔT_{HW} denotes the design water temperature difference of the hot-water loop (K), assumed to be16 K (NRCC 1998);

ρ_{water} denotes the water density (kg/m^3).

The design mass flow rate of the hot-water pump is calculated as follows:

$$\dot{m}_{HWP} = \dot{V}_{HWP} * \rho_{water} \quad (3\text{-}154)$$

Exergy balance:

$$\dot{\Phi}_{supply,HW,pump} - \dot{\Phi}_{recover,HW,pump} - \dot{I}_{HW,pump} = 0 \quad (3\text{-}155)$$

$$\dot{\Phi}_{supply,HW,pump} = \dot{E}_{HW,pump} \quad (3\text{-}156)$$

$$\dot{\Phi}_{recover,HW,pump} = \dot{m}_{HWP} * \left[h_{e,HW,pump} - h_{i,HW,pump} - T_0 * \left(s_{e,HW,pump} - s_{i,HW,pump}\right)\right] \quad (3\text{-}157)$$

$$\dot{I}_{HW,pump} = \dot{\Phi}_{supply,HW,pump} - \dot{\Phi}_{recover,HW,pump} \tag{3-158}$$

Entropy generation:

$$\dot{\sigma}_{HW,pump} = \frac{\dot{I}_{HW,pump}}{T_o} \tag{3-159}$$

Second-law efficiency of the hot-water pump:

$$\eta_{II,HW,pump} = \frac{\dot{\Phi}_{recover,HW,pump}}{\dot{\Phi}_{supply,HW,pump}} \tag{3-160}$$

3.4.3. By-pass mixing process

The entire hot-water loop is at a constant flow rate; however, each branch of heating coils is at variable flow rates. At part-load conditions, the additional water flows through by-pass piping line and mixes with the water returning from heating coils.

Exergy balance:

$$\dot{\Phi}_{supply,MHW} - \dot{\Phi}_{recover,MHW} - \dot{I}_{MHW} = 0 \tag{3-161}$$

where the subscript of *MHW* denotes the mixed hot-water;

$$\begin{aligned}\psi_{water@bypass} = {} & v_{f@t_{boiler,e}} * \left(P_0 - P_{sat@t_{boiler,e}}\right) + h_{f@t_{boiler,e}} - h_{f@t_0} - T_0 * \\ & \left(s_{f@t_{boiler,e}} - s_{f@t_0}\right) - 0.461 * T_0 \\ & * \left\{ \ln\left(\frac{P_0}{P_{g@t_0}}\right) + \ln\left[1.6078 * \left(\frac{\omega_0}{1+1.6078*\omega_0}\right)\right]\right\}\end{aligned} \tag{3-162}$$

where $\psi_{water@bypass}$ denotes the specific exergy of the hot-water through the by-pass line (kJ/kg);

$v_{f@t_{boiler,e}}$ denotes the specific volume of the hot-water at the exit temperature of the boiler (m^3/kg);

$P_{sat@t_{boiler,e}}$ denotes the saturated pressure of water at the exit temperature of the boiler (kPa);

subscripts *o, f,* and *g* denote the dead state, saturated liquid state, and saturated vapor state, respectively;

$$\psi_{water@RHW} = v_{f@t_{RHW}} * \left(P_0 - P_{sat@t_{RHW}}\right) + h_{f@t_{RHW}} - h_{f@t_0} - T_0 * \left(s_{f@t_{RHW}} - s_{f@t_0}\right) - 0.461 * T_0 * \left\{\ln\left(\frac{P_0}{P_{g@t_0}}\right) + \ln\left[1.6078 * \left(\frac{\omega_0}{1+1.6078*\omega_0}\right)\right]\right\} \quad (3\text{-}163)$$

where the subscript *RHW* indicates the returning hot-water flow after the mixing process;

$$\psi_{water@RH} = v_{f@t_{RRH}} * \left(P_0 - P_{sat@t_{RRH}}\right) + h_{f@t_{RRH}} - h_{f@t_0} - T_0 * \left(s_{f@t_{RRH}} - s_{f@t_0}\right) - 0.461 * T_0 * \left\{\ln\left(\frac{P_0}{P_{g@t_0}}\right) + \ln\left[1.6078 * \left(\frac{\omega_0}{1+1.6078*\omega_0}\right)\right]\right\} \quad (3\text{-}164)$$

where the subscripts of *RH* and *RRH* indicate returning from heat and reheat coils, respectively;

$$\dot{\Phi}_{supply,MHW} = \left(\dot{m}_{CHW} + \sum_{j=1}^{5} \dot{m}_{RHW}[j]\right) * \psi_{water@RH} + \left(\dot{m}_{HWP} - \dot{m}_{CHW} - \sum_{j=1}^{5} \dot{m}_{RHW}[j]\right) * \psi_{water@bypass} \quad (3\text{-}165)$$

where subscripts *CHW, RHW,* and *HWP* indicate water streams from the central heat coil, reheat coil, and hot-water pump, respectively;

$$\dot{\Phi}_{recover,MHW} = \dot{m}_{HWP} * \psi_{water@RHW} \tag{3-166}$$

$$T_{RHW} = T_{boiler,out} - \Delta T_{HWO} \tag{3-167}$$

$$T_{RRH} = T_{boiler,out} - \Delta T_{HW} \tag{3-168}$$

where ΔT_{HWO} denotes the operating temperature difference between the supply and return water from or to the boiler (K), calculated by Equation 3-169;

ΔT_{HW} denotes the temperature difference between the supply and return water from or to the boiler at design conditions, it is assumed to be constant at 16K (NRCC 1998);

$$\Delta T_{HWO} = \frac{\dot{Q}_{boiler}}{C_{p,w} * \dot{m}_{HWP}} \tag{3-169}$$

where $\dot{Q}_{boiler}$ denotes the hourly heating loads of the system (kW).

Entropy generation:

$$\dot{\sigma}_{MHW} = \frac{\dot{I}_{MHW}}{T_o} \tag{3-170}$$

Second-law efficiency:

$$\eta_{II,MHW} = \frac{\dot{\Phi}_{recover,MHW}}{\dot{\Phi}_{supply,MHW}} \tag{3-171}$$

3.5. Mathematical model of central cooling plant

The central cooling plant consists of a chiller, two pumps and a cooling tower (Figure 3-8). The chiller prepares the chilled water that satisfies the cooling loads of the whole HVAC system. Both the chilled water circuit and the cooling tower water loop are of the constant water flow rates. The exit temperature of the chilled water at the evaporator is 7°C (NRCC 1998), and the inlet temperature of the water at the condenser is 29°C (NRCC 1998). Under off-load conditions the water that passes through the by-pass line is mixed with the water from the cooling tower or the central cooling coil. The mathematical model of each component is developed according to mass, energy, and exergy balance equations. The flow chart of the chilled water and cooling tower water loop is shown in Figure 3-8.

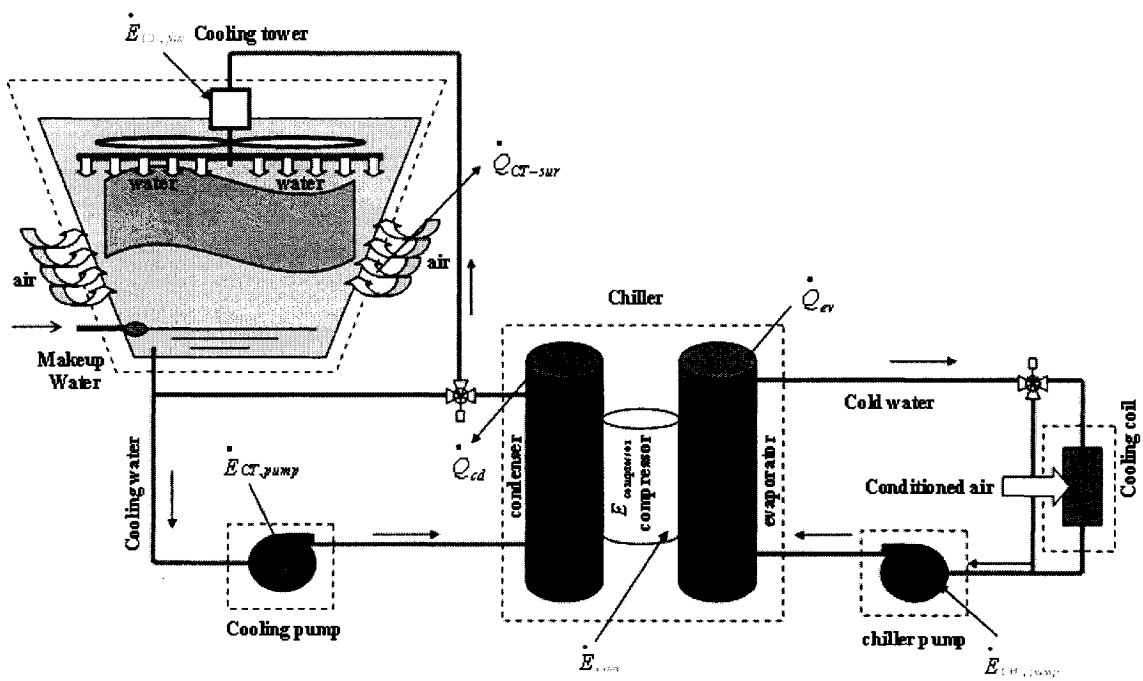

Figure 3-8: Schematic of the central cooling plant for the VAV system

3.5.1. Vapor compression chiller

The chiller consists of a compressor, a condenser, an evaporator, and a throttling valve. The primary energy input is electricity and the useful output is the heat absorbed by refrigerants from chilled water at the evaporator. The energy efficiency of the chiller is expressed with the Coefficient of Performance ($COP_{chiller}$), which is defined as the useful output over the total primary input to the chiller. The COP is a function of the temperature of chilled water and the temperature of water returning from a cooling tower to the condenser. The expression of the COP at full-load and part-load conditions is obtained from literature (Solati et al. 2003).

Energy balance:

$$\dot{Q}_{cd} = \dot{E}_{com} + \dot{Q}_{ev} \tag{3-172}$$

where subscripts *cd, ev, and com* denote condenser, evaporator, and compressor, respectively;

$\dot{E}_{com}$ denotes the electric demand of the compressor (kW);

$$\begin{aligned} COP_{FL} = {} & 8.02711 + 0.00268889 \times T_{CT,out}^2 - 0.25483 \times T_{CT,out} \\ & + 0.000367989 \times T_{EV,out}^2 + 0.203902 \times T_{EV,out} + 0.203902 \times T_{EV,out} \\ & - 0.00396354 \times T_{EV,out} \times T_{CT,out} \end{aligned} \tag{3-173}$$

$$\begin{aligned} COP_{PL} = {} & 7.81922 + 0.00530412 \times T_{CT,out}^2 - 0.455848 \times T_{CT,out} \\ & - 0.00926693 \times T_{EV,out}^2 - 0.0045712 \times T_{EV,out} \times T_{CT,out} \\ & + 0.450384 \times T_{EV,out} - 7.96205 \times PLR_C{}^2 + 11.8861 \times PLR_C \end{aligned} \tag{3-174}$$

$$\dot{E}_{com} = \frac{\dot{Q}_{ev}}{COP_{chiller}} \tag{3-175}$$

$COP_{chiller} = COP_{PL}$ at part-load ($PLR_C \neq 1$) operation (3-176)

or $COP_{chiller} = COP_{FL}$ at full-load ($PLR_C = 1$) operation (3-177)

where subscripts *FL, PL, CT, and EV* denote full-load and part-load conditions, cooling tower, and evaporator, respectively;

$\dot{Q}_{ev}$ denotes the heat flow rate from the chilled water to the refrigerants in the evaporator (kW).

Full-load conditions correspond to the design conditions of the chiller working under the rated capacity, otherwise, part-load conditions are considered.

$$PLR_c = \frac{\dot{Q}_{ev}}{\dot{Q}_{rate,ev}} \quad (3\text{-}180)$$

where $\dot{Q}_{rated,ev}$ denotes the nominal capacity of the chiller (kW);

PLR_c denotes the part-load ratio of the chiller at off-peak conditions.

Exergy balance:

The chiller exchanges heat with two different water streams through two heat exchangers. One of the water streams is the chilled water that exchanges heat with the refrigerants in the evaporator, and another is the condenser water that exchanges heat with the refrigerants in the condenser. Exergy interaction within the chiller includes electric input to the compressor and the exergy exchanges of those two water streams with refrigerants. The exergy balance equations describing these processes are given:

$$\dot{\Phi}_{supply,chiller} - \dot{\Phi}_{recover,chiller} - \dot{I}_{chiller} = 0 \quad (3\text{-}179)$$

where $\dot{\Phi}_{recover,chiller}$, the term denotes the exergy increase of chilled water in the evaporator (KW);

$\dot{I}_{chiller}$ denotes the irreversibility or exergy destruction of the chiller (kW), including the exergy increase of the condenser water through the condenser;

$$\dot{\Phi}_{supply,chiller} = \dot{E}_{com} \tag{3-180}$$

$$\dot{\Phi}_{recover,chiller} = \dot{m}_{CWP} * \Delta\psi_{CW} \tag{3-181}$$

$$\Delta\psi_{CW} = h_{t_{EV,e}} - h_{t_{EV,i}} - T_o * \left(s_{t_{EV,e}} - s_{t_{EV,i}}\right) \tag{3-182}$$

$$\dot{I}_{chiller} = \dot{\Phi}_{supply,chiller} - \dot{\Phi}_{recover,chiller} \tag{3-183}$$

Entropy generation

$$\dot{\sigma}_{chiller} = \frac{\dot{I}_{chiller}}{T_o} \tag{3-184}$$

Second-law efficiency

$$\eta_{II,chiller} = \frac{\dot{\Phi}_{recover,chiller}}{\dot{\Phi}_{supply,chiller}} \tag{3-185}$$

3.5.2. Circulating pumps for the chilled water and condensed water

Energy balance:

$$\dot{E}_{CW,pump} = \dot{m}_{CW,pump} \times \left(h_e - h_i\right) \tag{3-186}$$

$$\dot{E}_{CT,pump} = \dot{m}_{CT,pump} \times (h_e - h_i) \tag{3-187}$$

where $\dot{E}_{pump}$ denotes the electric input to the pumps (kW);

Subscripts *CT,* and *CW* denote cooling tower and chilled water, respectively;

h denotes the specific enthalpy of the hot-water (kJ/kg).

The power input to the circulating pump (ASHRAE 2004) is calculated as:

$$\dot{E}_{pump} = \frac{\dot{V}_w \times \Delta H_t}{\eta_{pump}} \tag{3-188}$$

where $\dot{V}_w$ denotes the volumetric flow rate of water on the respective water loop (m^3/s);

ΔH_t denotes the head of the respective pump (kPa), assumed about 182 and 250 kPa for the cooling tower water pump and the chilled water pump, respectively;

η_{pump} denotes the overall efficiency of the pump, which is assumed to be 60% (NRCC 1998) for the chilled water pump and 70% for the cooling tower pump;

$$\dot{m}_w = \dot{V}_w \times \rho_{water} \tag{3-189}$$

where ρ_{water} denotes the density of the water at temperature of 7°C and standard atmospheric pressure of P=101 kPa;

$\dot{m}_w$ denotes the mass flow rate of the respective water loop (kg/s).

Exergy balance:

$$\dot{\Phi}_{supply,pump} - \dot{\Phi}_{recover,pump} - \dot{I}_{pump} = 0 \tag{3-190}$$

$$\dot{\Phi}_{supply,pump} = \dot{E}_{pump} \tag{3-191}$$

$$\dot{\Phi}_{recover,pump} = \dot{m}_w * [h_e - h_i - T_0 * (s_e - s_i)] \quad (3\text{-}192)$$

$$\dot{I}_{pump} = \dot{\Phi}_{supply,pump} - \dot{\Phi}_{recover,pump} \quad (3\text{-}193)$$

Entropy generation:

$$\dot{\sigma}_{pump} = \frac{\dot{I}_{pump}}{T_o} \quad (3\text{-}194)$$

Second-law of efficiencies:

$$\eta_{II,pump} = \frac{\dot{\Phi}_{recover,pump}}{\dot{\Phi}_{supply,pump}} \quad (3\text{-}195)$$

3.5.3. Cooling tower (with the by-pass mixing pipeline)

The subsystem consists of a cooling tower and the mixing bypass pipeline of cooling tower water loop. Energy interaction between the system and its surroundings include the electric input to the cooling tower fan, the heat and mass exchange occurring between cooling tower water and atmospheric air. The heat rejected from the condenser of the chiller is released from cooling tower water to the environment. According to the literature (ASHRAE HVAC system and equipment 2004), the quantity of make-up water could be estimated as 1% of the flow rate of cooling tower water. In this research, 1% of design cooling tower water flow rate is considered as the makeup water flow rate and the temperature of makeup water is 15°C during the simulation hours. The cooling tower fan utilizes a cyclic control, and its electric demand is a function of a part-load ratio and is

derived from (NRCC 1998). The following Equations are used to calculate the electric demand of the cooling tower fan:

$$\dot{Q}_{CT} = \dot{Q}_{cd} \tag{3-196}$$

$$PR_{CT} = \frac{\dot{Q}_{CT}}{\dot{Q}_{rated,chiller} * \left(1 + \frac{1}{COP_{FL}}\right)} \tag{3-197}$$

$$\dot{E}_{CT} = 0.015 * \dot{Q}_{rated,chiller} * \left(1 + \frac{1}{COP_{FL}}\right) * PR_{CT} \tag{3-198}$$

where $\dot{Q}_{CT}$ denotes the heat rejected from the cooling tower (kW);

PR_{CT} denotes the part-load ration of the cooling tower;

$\dot{E}_{CT}$ denotes the electric demand of the cooling tower fan (kW).

Exergy balance

Exergy interaction takes place due to the heat transfer, the mass transfer, and the mixing process. The exergy supplied to the cooling tower includes the electrical input to the fan, the exergy decrease of the water stream, and the portion of exergy flowing into the system with the makeup water. The effect is the exergy increase in the air stream, which is included as a part of exergy losses of the cooling tower. Therefore, the exergy balance of the cooling tower is written as follows:

$$\dot{\Phi}_{\text{sup ply},CT} - \dot{I}_{CT} = 0 \tag{3-199}$$

$$\dot{\Phi}_{\text{sup ply},CT} = \dot{E}_{CT,fan} + \dot{m}_{MW} * \psi_{MW} + \dot{m}_{CTWP} * \left[h_{i,CT} - h_{e,CT} - T_o * \left(s_{i,CT} - s_{e,CT}\right)\right] \tag{3-200}$$

where subscripts *MW* and *CTWP* denote the makeup water and cooling tower water through the circulating pump.

The entropy generation:

$$\dot{\sigma}_{CT} = \frac{\dot{I}_{CT}}{T_o} \tag{3-201}$$

3.6. Calculations of water flow rate in piping system

In the VAV systems, the water circulating systems are of the constant flow rates, and pumps serving these systems are of the constant flow rates. The bypass auto-control valves are used to control the water flow rates of the central cooling coil, heating and reheating coils and the cooling tower under part-load conditions. These devices are, therefore, of variable water flow rates. The water temperature differences between inlets and outlets of these devices are constant. The design supply water temperature for the hot water system, the chilled water system and the cooling tower water system are taken from (NRCC 1998):

$T_{EV,out} = 7\,^{\circ}\mathrm{C}$, $T_{CT,out} = 29\,^{\circ}\mathrm{C}$, and $T_{boiler,out} = 65\,^{\circ}\mathrm{C}$

The design water temperature differences between inlets and outlets of the central cooling, heating and reheating coils and the cooling tower are taken from (NRCC 1998):

$\Delta T_{HW} = 16\,^{\circ}\mathrm{C}$, $\Delta T_{CTW} = 6\,^{\circ}\mathrm{C}$, and $\Delta T_{CW} = 5\,^{\circ}\mathrm{C}$

where subscripts *"HW"*, *"CTW"*, and *"CW"* refer to the hot water system, the cooling tower system and the chilled water system, respectively.

The design water flow rates of all water loops are calculated by using following equations

$$\dot{m}_{CWP} = \frac{Q_{rated,ev}}{C_{P,W}\Delta t_{CW}} \text{ for the chilled water system;} \quad (3\text{-}202)$$

$$\dot{m}_{CTWP} = \frac{Q_{rated,ev} * \left(1 + \frac{1}{COP_{FL}}\right)}{C_{P,W}\Delta t_{CW}} \text{ for the cooling tower water system;} \quad (3\text{-}203)$$

$$\dot{m}_{HWP} = \frac{Q_{rated,boiler}}{C_{P,W}\Delta t_{HW}} \text{ for the hot water system;} \quad (3\text{-}204)$$

where $\dot{m}$ denotes the mass flow rate (kg/s);

Subscripts *CWP, CTWP*, and *HWP* denote the chilled water, cooling tower water, and hot-water through each circulating pump.

Since the constant flow rate systems are designed for variable thermal loads, the temperature differences between supply and return water for the systems vary at part-load conditions, and they are calculated as follows:

$$\Delta T_{HWO} = \frac{\dot{Q}_{boiler}}{C_{P,W} * \dot{m}_{HWP}} \quad (3\text{-}205)$$

$$\Delta T_{CWO} = \frac{\dot{Q}_{ev}}{C_{P,W} * \dot{m}_{CWP}} \quad (3\text{-}206)$$

$$\Delta T_{CTWO} = \frac{\dot{Q}_{CT}}{C_{P,W} * \dot{m}_{CTWP}} \quad (3\text{-}207)$$

3.7. Energy and exergy analyses of the entire VAV system

The purpose of energy and exergy analysis applied to the VAV systems is to obtain indices such as the energy use, entropy generation, and exergy consumption of the entire system. Figure 3-9 shows the energy interaction within the VAV systems. Energy analysis and exergy analysis at the system level and at the power plant level are introduced separately in the following section.

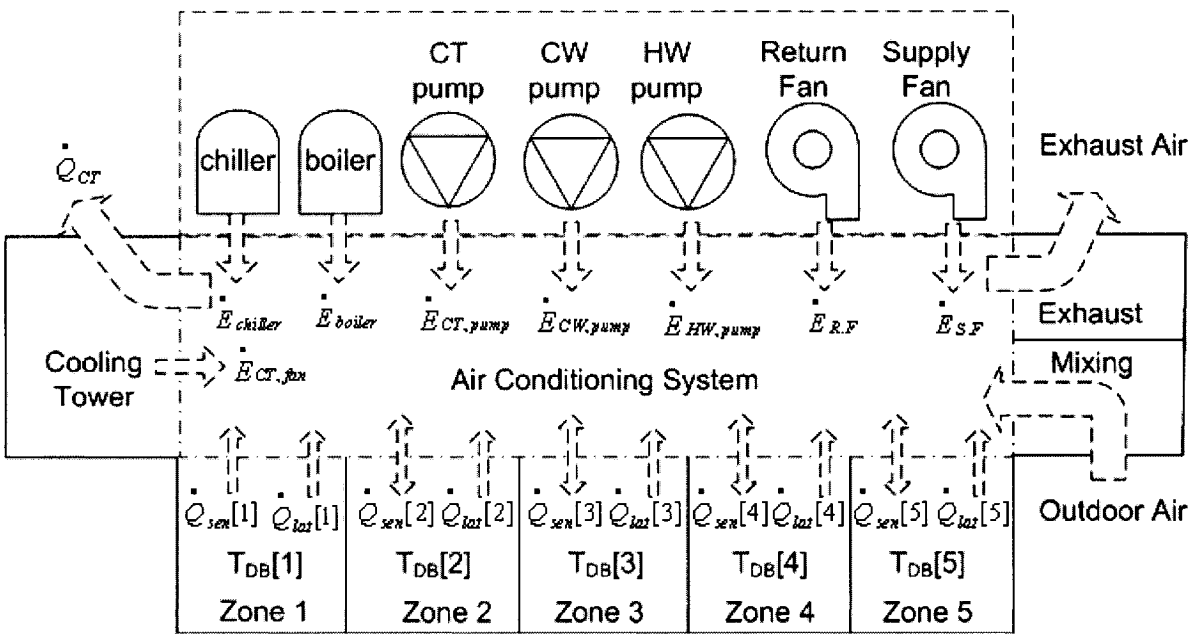

Figure 3-9: Diagram of energy interactions within the VAV system

3.7.1. Energy analysis

As shown in the Figure 3-9, two types of energy interactions, for example, thermal and electric energy, occur in the VAV systems. The electric energy supplied to the VAV systems is used to drive equipment in the VAV systems, such as fans, pumps, chillers and boilers. The useful energy produced by the VAV systems is defined as the summation of the thermal heating and cooling loads of zones plus the ventilation loads for conditioning

outdoor air to indoor air states. The task energy efficiency of the VAV systems, also called the Coefficient of Performance of the systems (COP_{sys}), is calculated as follows:

$$COP_{sys} = \frac{\sum_{t=1}^{4176} \left| \dot{Q}_{sys} \right|}{\sum_{t=1}^{4176} \dot{E}_{total}} \tag{3-208}$$

where $\dot{Q}_{sys}$ represents the hourly heating and cooling loads of the system (kW);

$\dot{E}_{total}$ represents the total hourly electric demand of the system (kW);

$$\dot{Q}_{sys} = \sum_{j=1}^{5} \left(\left| \dot{Q}_{sen}[j] \right| + \left| \dot{Q}_{lat}[j] \right| \right) + \dot{m}_{\min outair} * \left| h_5 - h_1 \right| \tag{3-209}$$

where $\sum_{j=1}^{5} \left(\left| \dot{Q}_{sen}[j] \right| + \left| \dot{Q}_{lat}[j] \right| \right)$ denotes the total thermal loads of all zones (kW);

$\dot{m}_{\min outair} * \left| h_5 - h_1 \right|$ represents the ventilation loads of all zones (kW);

$$\dot{m}_{\min outair} = 0.4 * \frac{\sum_{j=1}^{5} A[j]}{1000 * v} \tag{3-210}$$

where $\sum_{j=1}^{5} A[j]$ stands for the total of floor area of all zones served by the air conditioning system (m^2);

v is the specific volume of outdoor air (m^3/kg);

0.4 is the specific minimum ventilation flow rate of office buildings (l/s), rregulated by (NRCC 1998).

The total on-site electric demand is calculated as follows:

$$\dot{E}_{total} = \dot{E}_{\sup ply,fan} + \dot{E}_{return,fan} + \dot{E}_{CW,pump} + \dot{E}_{HW,pump} + \dot{E}_{CT,pump} + \dot{E}_{com} + \dot{E}_{CT,fan} + \dot{E}_{boiler} \tag{3-211}$$

By considering the energy losses due to transmission lines and the efficiency of power plants, the primary energy demand for the off-site generation of electricity that is required by the HVAC system is calculated with the following formula (Wu 2004):

$$\dot{E}_{power,plant} = \frac{\dot{E}_{total}}{\eta_{power,delivery}} * \left(\frac{0.967}{0.8} + \frac{0.011}{0.3} + \frac{0.011}{0.33} + \frac{0.011}{0.431} \right) \tag{3-212}$$

where $\eta_{power,delivery}$ denotes the efficiency of transmission lines, assumed to be equal to 0.86;

0.967 is the contribution of the electricity generated by hydro power plants, and 0.011 is the contribution of the electricity generated by nuclear power plants, gas fired power plants or oil fired power plants in Quebec (Baouendi 2003);

0.8 is the overall efficiency of hydro-power plants (Ileri et al. 1998);

0.3 is the overall efficiency of nuclear power plants (Rosen 2001);

0.33 is the overall efficiency of oil-fired plants (Kannan 2004);

0.431 is the overall efficiency of natural gas fired power plants (AIE 1998).

The Coefficient of Performance of the overall system, including the VAV system and the power generation and delivery system, is calculated as:

$$COP_{total} = \frac{\dot{Q}_{sys}}{\dot{E}_{power,plant}} \tag{3-213}$$

3.7.2. Exergy analysis

The exergy efficiency of the VAV systems is defined as the ratio of the demand exergy over the input exergy. The input exergy is the total exergy with the on-site energy for calculating the efficiency at the system level, or the total exergy with the off-site primary energy use for the estimation of the combined system, which includes the VAV system and the power generation and delivery system. The exergy input to the VAV system is the sum of the total electric exergy and the thermal exergy due to the outdoor air and the makeup water induced to the VAV system:

$$\dot{\Phi}_{\text{sup ply,sys}} = \dot{E}_{total} + \dot{m}_{MW} * \psi_{MW} + \dot{m}_{FR} * \psi_1 \tag{3-214}$$

where ψ_{MW} denotes the specific exergy of the makeup water of the cooling tower (kJ/kg);

$\dot{m}_{MW}$ denotes the mass flow rate of makeup water of the cooling tower (kg/s);

$$\psi_{MW} = h_{i,MW} - h_{@t_0} - T_0 * (s_{i,MW} - s_{@t_0}) - 0.416 * T_0 * \left[\ln\left(\frac{P_0}{P_{g@t_0}}\right) + \ln\left(\frac{1.6078 * \omega_0}{1 + 1.6078 * \omega_0}\right) \right] \tag{3-215}$$

where $h_{i,MW}$ and $s_{i,MW}$ denote the specific enthalpy and entropy of makeup water, assuming the temperature of the makeup water is constant at 15°C;

$P_{g@t_0}$ denotes the saturated pressure of water at oudoor temperature (kPa);

$h_{@t_0}$ denotes the specific enthalpy of the saturated liquid water at the outdoor temperature (kJ/kg).

The exergy demand of the system is defined as the task exergy needed by the building system, which includes the exergy associated to the thermal energy form or to zones plus

the exergy difference between the indoor and outdoor air. The positive task exergy refers to the exergy needed to be provided by the HVAC system to the building spaces while the negative task exergy refers to the exergy needed to be removed by the HVAC system from the building spaces. The task exergy of the VAV system is expressed as follows:

$$\dot{\Phi}_{demand,sys} = \sum_{j=1}^{5} \left[\left(\frac{T_o}{T_{DB}[j] + 273.15} - 1 \right) * \dot{Q}_{sen}[j] - 1.6078 * R_a * T_o * \ln\left(\frac{(1 + 1.6078\omega_o) * \omega}{(1 + 1.6078\omega) * \omega_o} \right) * \frac{\dot{Q}_{lat}[j]}{2501 + 1.87 * T_{DB}[j]} \right] + \dot{m}_{\min outair} * (\psi_5 - \psi_1) \quad (3\text{-}216)$$

where $\left(\frac{T_o}{T_{DB}[j] + 273.15} - 1 \right) * \dot{Q}_{sen}[j]$ denotes the exergy (kW) due to the sensible load of zones (Franconi et al. 1999);

$-1.6078 * R_a * T_o * \ln\left(\frac{(1 + 1.6078\omega_o) * \omega}{(1 + 1.6078\omega) * \omega_o} \right) * \frac{\dot{Q}_{lat}[j]}{2501 + 1.87 * T_{DB}[j]}$ denotes the exergy (kW) due to the latent load of zones (Ren et al. 2002);

$\dot{m}_{\min outair} * (\psi_5 - \psi_1)$ denotes the exergy (kW) due to ventilation requirement.

The exergy lost or irreversibility is calculated as:

$$\dot{I}_{sys} = \dot{\Phi}_{supply,sys} - \dot{\Phi}_{demand,sys} \quad (3\text{-}217)$$

The entropy generation is calculated as:

$$\dot{\sigma}_{sys} = \frac{\dot{I}_{sys}}{T_o} \quad (3\text{-}218)$$

The exergy efficiency of the VAV system is calculated as:

$$\eta_{II,sys} = \left| \frac{\dot{\Phi}_{demand,sys}}{\dot{\Phi}_{\text{sup }ply,sys}} \right| \tag{3-219}$$

The total exergy input to the combined system is calculated as follows:

$$\dot{\Phi}_{\text{sup }ply,sys} = \dot{\Phi}_{power,plants} + \dot{m}_{MW} * \psi_{MW} + \dot{m}_{FR} * \psi_1 \tag{3-220}$$

$$\dot{\Phi}_{power,plants} = \frac{\dot{E}_{total}}{0.86} * \left[\left(\frac{0.967}{0.8} + \frac{0.011}{0.3} \right) + \left(\frac{0.011}{0.431} + \frac{0.011}{0.33} \right) * \left(1 - \frac{T_o}{T_{flame}} \right) \right] \tag{3-221}$$

where T_{flame} denotes the flame temperature (K), estimated as 2200 K for gas and oil fired power plants;

0.86 denotes the efficiency of transmission lines (Zhang 1995);

0.967 is the contribution of the electricity generated by hydro power plants, and 0.011 is the contribution of the electricity generated by nuclear power plants, gas fired power plants or oil fired power plants in Quebec (Baouendi 2003);

0.8 is the overall efficiency of hydro-power plants (Ileri et al. 1998);

0.3 is the overall efficiency of nuclear power plants (Rosen 2001);

0.33 is the overall efficiency of oil-fired plants (Kannan et al. 2004);

0.431 is the overall efficiency of natural gas fired power plants (AIE 1998).

The total exergy flowing out of power generation plants is calculated as:

$$\dot{\Phi}_{power,delivery} = \frac{\dot{E}_{total}}{0.86} \tag{3-222}$$

The main components of the combined system are the power generation plants, transmission and power delivery grids, and the VAV system, so the exergy destruction on each component is calculated as:

$$\dot{I}_{power,plants,destruction} = \dot{\Phi}_{power,plants} - \dot{\Phi}_{power,delivery} \tag{3-225}$$

$$\dot{I}_{power,delivery} = \dot{\Phi}_{power,delivery} - \dot{\Phi}_{\sup ply,sys} \tag{3-226}$$

The exergy efficiency of the combined system is calculated as:

$$\eta_{II,total} = \left| \frac{\dot{\Phi}_{demand,sys}}{\dot{\Phi}_{power,plants}} \right| \tag{3-227}$$

Chapter 4 Case Study

This chapter presents the analysis of simulation results of two VAV systems serving the same office building but using different operation control strategies during the whole year. The characteristics of the office building are first introduced; then, the configurations of these VAV systems are manifested; finally, the simulation results analyzed by the first and second laws of thermodynamics are presented. The simulation is performed by implementing the mathematical models demonstrated in chapter 3 with the Engineering Equation Solver (EES) program (Klein 2004), and computing the energy and exergy related indices of the HVAC systems. The computer codes developed with the EES program are shown in the Appendices.

The analysis reveals that a large potential of energy reduction exists in the office building and addresses a more powerful evaluation approach, the second law analysis, for evaluating the energy performance of HVAC systems. Some suggestions about how to improve the energy performance of HVAC systems are also discussed, such as the selection of a more appropriate heating source and the reduction of friction losses occurred in HVAC systems.

4.1. Building prototype

The architectural characteristics of the office building are extracted from the literature (Zmeureanu et al. 1995). The building was constructed in Montreal in 1972, and has a total floor area of 10,410 m^2 spreading over a seven-floor office tower, an underground

garage and a ground floor with a bank, a restaurant, and office spaces. The air conditioning system for the office tower in this building is a central Variable Air Volume (VAV) system, providing cooling in the summer and ventilation year round, and operates from 8:00 am to 11:00 pm, Monday to Friday. The air conditioning system is equipped with a supply air fan of 38,000 L/s, and a return air fan of 35,000 L/s. The design electric demand of those fans is 93 kW and 56 kW, respectively. Cooling is provided by a direct expansion cooling coil with four compressors, each of nominal capacity of 90 kW. Electric baseboard heaters provide heating for most of the building with a total capacity of 118 W/m^2 of floor area. The indoor temperature set points are 20-21°C for heating and 23-24°C for cooling. Electricity is the only energy source for the building. The bank and restaurant utilize two separate roof top units. The garage is provided heating in the winter and ventilation year round.

Only a five-floor office tower, with a total floor area of 5,000 m^2, in the building is simulated in this research. The office spaces on each floor are divided into four zones: a central zone, named as zone no. 1, and four perimeter zones, called zone no. 2 to no. 5. Since the central zone needs cooling even in the winter, cooling is needed year round. Two types of VAV systems are designed in such a way to satisfy the hourly heating and cooling loads, which are calculated by the DOE-2 program and input to the EES program.

4.2. System configuration

The only difference between the two VAV systems is that VAV system no. 1 uses a conventional control strategy with a constant temperature of the supply air directly

following the central air handling unit (AHU) while VAV system no. 2 adopts a so-called discriminatory control approach that varies the supply air temperatures in terms of the minimum supply air temperature required among all zones. The design characteristics of both VAV systems are listed in Table 4-1.

Table 4-1: Design characteristics of both VAV systems

	Heating mode	Cooling mode
Design supply air temperature	43°C	13°C
Indoor design temperature	20°C	23°C
Supply temperature of hot/chilled water	65°C	7°C
Temperature of water leaving cooling tower	--	29°C
Design water temperature difference	16°C	5°C
Cooling tower water temperature difference	--	6°C
Head of circulating pump	250 kPa	
Head of circulating pump for cooling tower	--	180 kPa
Overall efficiency of circulating pump	60%	
Overall efficiency of cooling tower pump	--	70%
Head of supply air fan	1000 Pa	
Head of return air fan	250 Pa	
Overall efficiency of supply air fan	55%	
Overall efficiency of return air fan	30%	
Design efficiency of boiler	80%	--

Both VAV systems, serving the office building in Montreal, Canada, are simulated for one year period, excluding weekends, for a total of 4176 hours.

4.2.1. Design data of VAV System no. 1

VAV system no. 1 uses a constant supply air temperature of 13°C, which is referred to as the allowable lowest supply air temperature applied to comfortable HVAC systems in cooling (NRCC 1998, ASHRAE 1996, and ASHRAE 2002).

The HVAC equipment is sized according to the preliminary simulation results of VAV system no. 1. The nominal capacity of the chiller and boiler satisfies the hourly thermal loads of the cooling coil and heating coils, respectively. The nominal capacity of individual VAV boxes for each zone is equal to the maximum supply airflow rate of each zone. The nominal capacity of fans is equal to the maximum airflow rate of the air distribution system, which is calculated from the summation of airflow rates for five floors. The nominal capacity of the cooling tower is determined to satisfy the maximum amount of the heat rejected from the chiller. The nominal capacity of pumps is determined in terms of water flow rates for the operations of the chiller or boiler.

The nominal capacities of the main equipment for VAV system no. 1 are listed in Tables 4-2, 4-3, and 4-4.

Table 4-2: Nominal capacity of main equipment of VAV systems – part 1

Systems	Design Air Flow Rate of VAV Boxes					Central Heating Coil
	Zone1	Zone2	Zone3	Zone4	Zone5	
	[m^3/s]	[m^3/s]	[m^3/s]	[m^3/s]	[m^3/s]	[kW]
VAV1	0.9223	0.8248	0.8071	0.8977	0.5425	10.98
VAV2	0.9223	0.8248	0.8071	0.8977	0.5425	91.65

Table 4-3: Nominal capacity of main equipment of VAV systems – part 2

Systems	Reheat Coil Capacity of VAV Boxes					Capacity of CT
	Zone1	Zone2	Zone3	Zone4	Zone5	
	[kW]	[kW]	[kW]	[kW]	[kW]	[kW]
VAV1	9.494	10.95	9.088	10.33	8.854	419.95
VAV2	9.473	9.028	7.258	8.206	7.145	419.95

Table 4-4: Nominal capacity of main equipment of VAV systems – part 3

Systems	Chiller	Boiler	Fans		Pumps		
			Supply	Return	Heating	Cooling	Condensing
	[kW]	[kW]	[m^3/s]	[m^3/s]	[m^3/h]	[m^3/h]	[m^3/h]
VAV1	327.45	247.2	16.935	17.62	13.3	56.4	47.9
VAV2	327.45	247.2	16.935	17.62	13.3	56.4	47.9

4.2.2. Design data of VAV System No. 2

The simulation of the operations of VAV system no. 1 shows that even on the hottest day, the minimum supply air temperature of all zones can be higher than 13°C for several hours. Hence, the use of the constant temperature for the supply air directly following the AHU in the case of VAV system no. 1 can cause overcooling for the air in AHU and, in turn, need extra reheating from reheat coils. The overcooling should be avoided as much as possible in order to improve the energy performance of VAV system no. 1. VAV system no. 2 is designed to adopt a variable supply air temperature in terms of the highest instantaneous cooling load.

The nominal capacity of the main equipment is listed in Tables 4-2, 4-3, and 4-4. The difference of the capacity of equipment between the two systems is only noticed on the capacity of the central heating coil and zone reheating coils.

4.3. The first law analysis of VAV systems

The monthly space heating or cooling loads are compared with the thermal loads imposed on the boiler or the chiller for both VAV systems in Figures 4-1 and 4-2. The heating and cooling loads for ventilation air are not included.

The monthly heating loads of boilers of both VAV systems are higher than the monthly building heating loads due to thermal mixing and ventilation loads. The monthly cooling loads of chillers of both VAV systems are sometimes lower than the building cooling loads due to the use of free cooling obtained by an air-side economizer control. Since VAV system no. 2 reduces thermal mixing due to the use of the discriminatory control, the thermal loads of the boiler and the chiller of VAV system no. 2 are all lower than those of VAV system no. 1 (Figure 4-2).

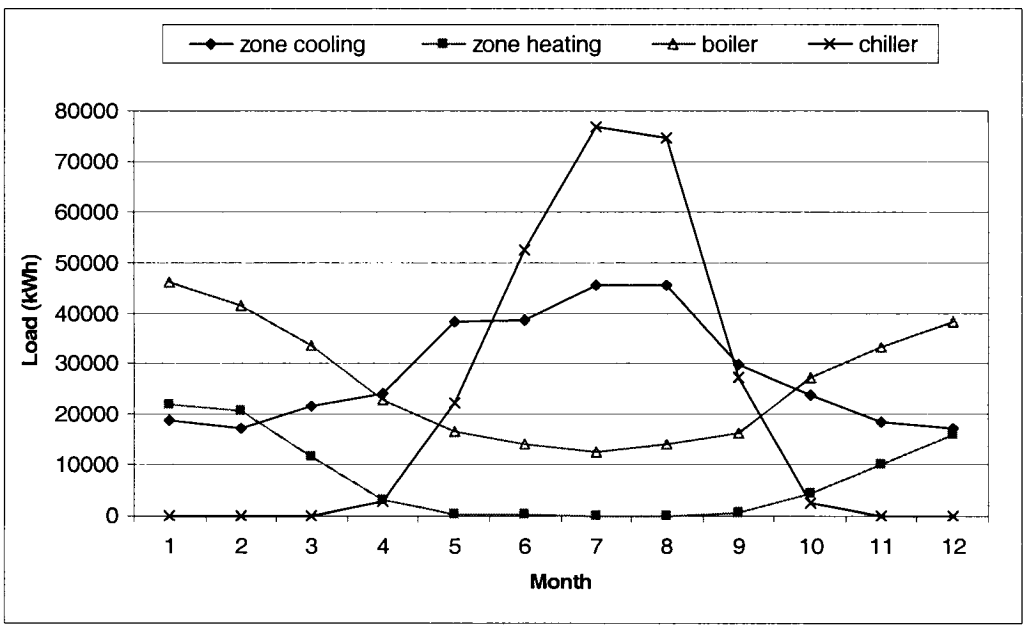

Figure 4-1: Monthly space heating and cooling loads vs. boiler and chiller loads for VAV system no. 1

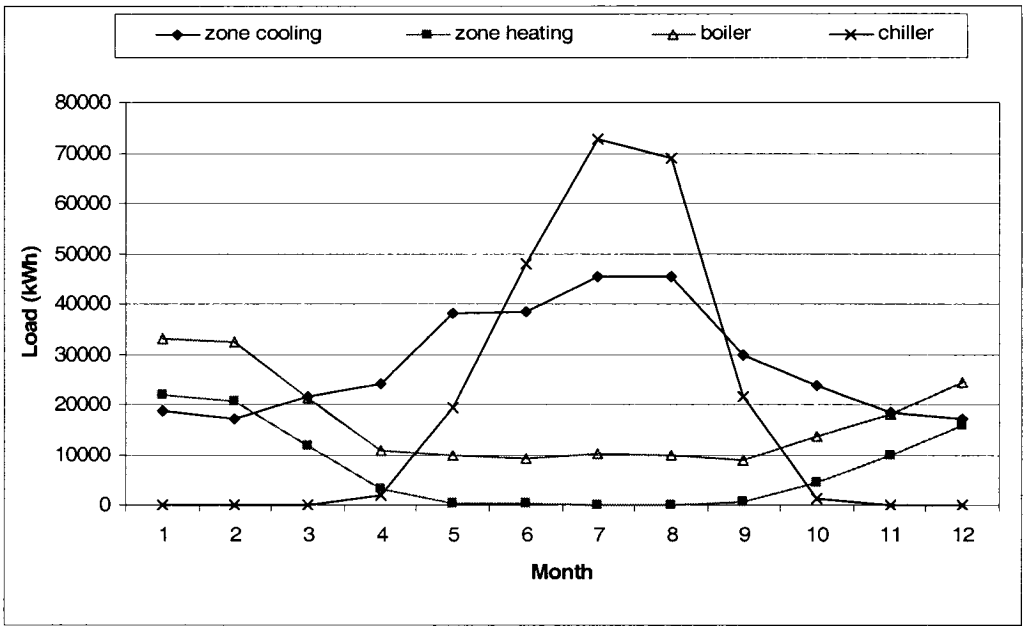

Figure 4-2: Monthly space heating and cooling load vs. boiler and chiller loads for VAV system no. 2

The monthly thermal energy provided by VAV system no. 2 is, by about 30%, less than that of VAV system no. 1 due to the different operation strategies, which cause the different degree of thermal mixing. The thermal energy provided by VAV system no. 2 is lower significantly in the winter and swing months. The maximum monthly reduction of 51% is noticed in October.

Table 4-5 presents the data of each curve in Figures 4-1, 4-2, 4-3, and 4-4.

Table 4-5: Thermal loads of the building, the boiler, the chiller and VAV systems

System		Thermal Loads											
		January	February	March	April	May	June	July	August	September	October	November	December
		[kWh]	[kWh]	[kWh]	[kWh]	[kWh]	[kWh]	[kWh]	[kWh]	[kWh]	[kWh]	[kWh]	[kWh]
Building[1]	heating	21,920	20,757	11,618	3,219	288	184	0	6	521	4,499	9,904	15,962
	cooling	18,752	17,220	21,628	24,215	38,124	38,553	45,462	45,366	29,842	23,726	18,457	17,167
Task[2]	heating	53,965	52,964	35,305	17,116	7,531	2,550	215	669	5,739	18,771	28,272	40,490
	cooling	18,752	17,220	21,628	24,215	38,213	41,664	53,477	52,811	31,329	23,726	18,457	17,167
Boiler	VAV1	46,077	41,273	33,672	22,791	16,527	13,992	12,673	13,994	16,331	27,447	33,375	38,314
	VAV2	33,064	32,242	21,208	10,943	9,838	9,199	10,056	9,776	8,798	13,563	18,073	24,458
Chiller	VAV1	0	0	67	2,897	22,188	52,373	76,716	74,654	27,308	2,573	138	0
	VAV2	0	0	67	2,043	19,248	47,847	72,760	68,770	21,533	1,125	0	0
Central plants	VAV1	46,077	41,273	33,738	25,688	38,715	66,366	89,389	88,648	43,639	30,020	33,513	38,314
	VAV2	33,064	32,242	21,274	12,986	29,086	57,047	82,816	78,547	30,330	14,687	18,073	24,458

1 Building thermal loads refer to the space loads without ventilation loads;
2 Task thermal loads refer to the space thermal loads plus ventilation loads;

Table 4-6 presents the monthly energy consumption of both VAV systems at the system level and at the power plant level, as well as the monthly peak electricity demand. The monthly energy consumption of VAV system no. 2 is less than that of VAV system no. 1. The monthly energy reduction in average is about 22%, with the largest monthly reduction of about 34% in November. The monthly peak electricity demand of VAV system no. 2 is reduced by about 11% in average. The maximum monthly energy consumption of both systems occurs in January, and the reduction of monthly energy consumption in that month is about 21%. In conclusion, the energy performance of VAV system no. 2 is better than that of VAV system no. 1. It is expected that the operation costs of VAV system no. 2 are also reduced.

Table 4-6: Energy consumption of the boiler and the chiller of both VAV systems, energy consumptions of both VAV systems on system level and power generation level, and the hourly peak energy consumptions of both VAV systems – monthly basis

System		Energy consumption												
		January	February	March	April	May	June	July	August	September	October	November	December	Annual
		[MWh]	[MWh]	[MWh]	[MWh]	[MWh]	[MWh]	[MWh]	[MWh]	[MWh]	[MWh]	[MWh]	[MWh]	[MWh]
Boiler	VAV1	64.3	57.3	49.4	36.2	29.6	25.7	24.5	26.5	28.1	42.7	49.2	54.4	487.8
	VAV2	49.2	46.9	34.8	22.0	21.5	19.9	21.4	21.4	19.0	26.1	31.1	38.1	351.2
Chiller	VAV1	0.0	0.0	0.0	1.1	6.7	11.1	15.1	14.9	7.1	1.0	0.1	0.0	57.2
	VAV2	0.0	0.0	0.0	0.7	5.6	10.1	14.5	14.0	5.3	0.4	0.0	0.0	50.8
System level	VAV1	71.1	63.3	56.6	44.8	49.0	50.1	55.2	57.2	46.0	51.8	56.1	60.7	661.9
	VAV2	56.1	53.0	42.0	30.1	39.0	43.0	51.4	51.0	34.2	34.2	37.8	44.5	516.4
Power plant level	VAV1	107.9	96.0	85.8	68.0	74.4	76.0	83.8	86.7	69.7	78.5	85.0	92.1	1003.8
	VAV2	85.1	80.3	63.7	45.6	59.2	65.3	77.9	77.4	51.9	51.8	57.4	67.6	783.2
Peak electric demand [kW]	VAV1	297.70	297.35	262.75	218.60	202.00	209.75	207.20	202.75	202.10	212.15	254.25	330.20	2896.8
	VAV2	282.25	296.10	228.55	160.40	173.95	193.25	205.60	190.00	177.95	170.35	186.80	330.50	2595.7

Table 4-7 and Figure 4-3 show the monthly average Coefficient of Performance (COP) of both VAV systems. The annual average COP of both VAV systems at the system level, estimated at 0.99 and 1.24, respectively, is agreed with the seasonal COP of VAV system applied to office buildings predicted by Dunn et al. (2005), of about 1.19 by using the DOE-2 program, and 0.81-0.91 by using the TAS program.

The average COP of VAV system no. 2 is higher by about 26% compared with that of VAV system no. 1. The system COP improvements are more apparent in winter and swing seasons. In the hottest months, July and August, the rises in system COP are less significant due to the less chances of the use of free cooling in those months.

Table 4-7: Monthly average COP of both VAV systems

Month	Coefficient of Performance (COP)			
	System level		Power generation level	
	VAV1	VAV2	VAV1	VAV2
January	1.05	1.34	0.69	0.88
February	1.16	1.38	0.76	0.91
March	1.08	1.38	0.71	0.91
April	1.03	1.43	0.68	0.94
May	1.03	1.22	0.68	0.81
June	0.93	1.04	0.61	0.69
July	0.99	1.03	0.66	0.68
August	0.97	1.02	0.64	0.67
September	0.88	1.13	0.58	0.74
October	0.89	1.28	0.59	0.84
November	0.87	1.27	0.57	0.83
December	0.98	1.33	0.65	0.88
Average	0.99	1.24	0.65	0.82

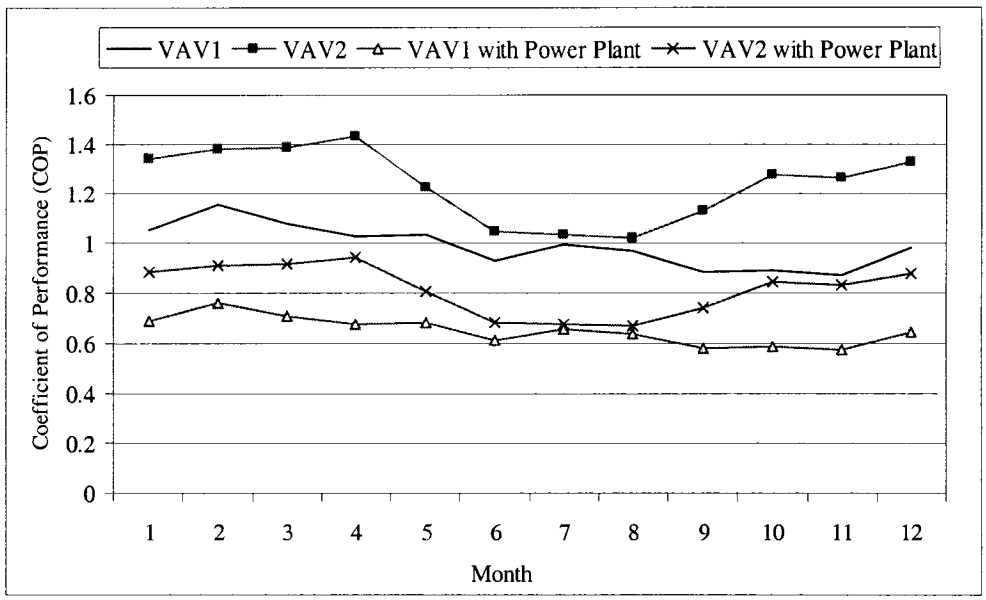

Figure 4-3: Monthly average COP of both VAV systems

When power plants is included, the COP of both systems declines, by about 34%, compared with the COP at the system level, due to the inefficiencies of transmission lines and power generation plants. This could be improved by increasing the efficiency of power generation and delivery aspects, and also, by adopting power cogeneration systems.

Figure 4-6 and Table 4-8 show that the monthly average COP of chillers for both VAV systems is almost equal. The annual average COP of the chiller for VAV system no. 1 is 3.96, and 4.07 for VAV system no. 2.

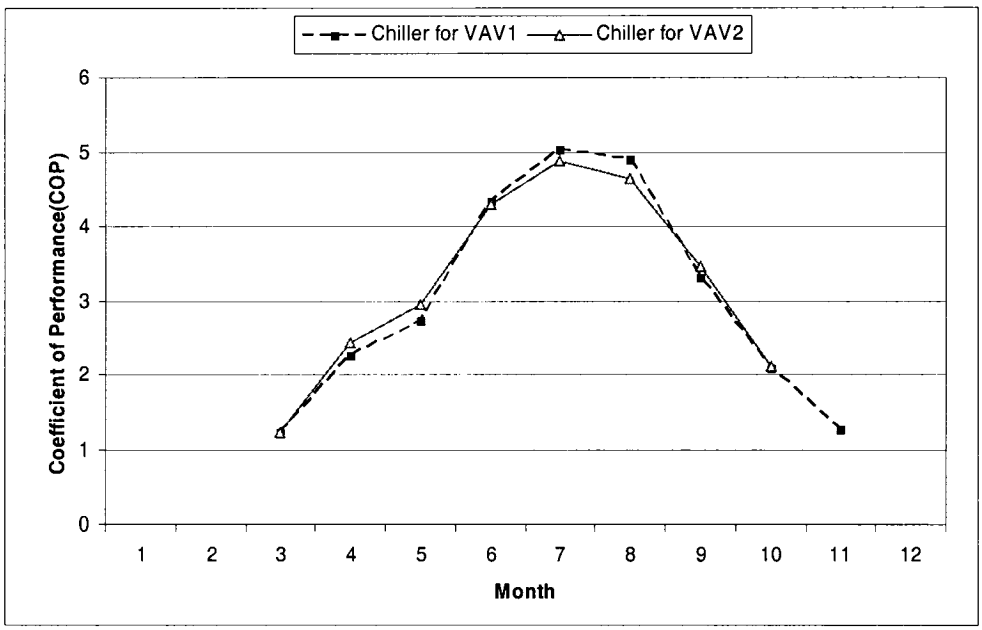

Figure 4-4: COP of chillers for both VAV systems

Table 4-8: COP of chillers of both VAV systems

System	Coefficient of Performance (COP) of Chiller											
	Jan.	Feb.	March	April	May	June	July	Aug.	Sep.	Oct.	Nov.	Dec.
VAV1	--	--	1.22	2.26	2.74	4.34	5.04	4.90	3.30	2.08	1.27	--
VAV2	--	--	1.22	2.44	2.94	4.31	4.89	4.65	3.46	2.10	--	--

Figure 4-5 and Table 4-6 give the comparison of the monthly boiler energy use for the two VAV systems, and Figure 4-6 presents the information about the energy efficiency of boilers for both VAV systems.

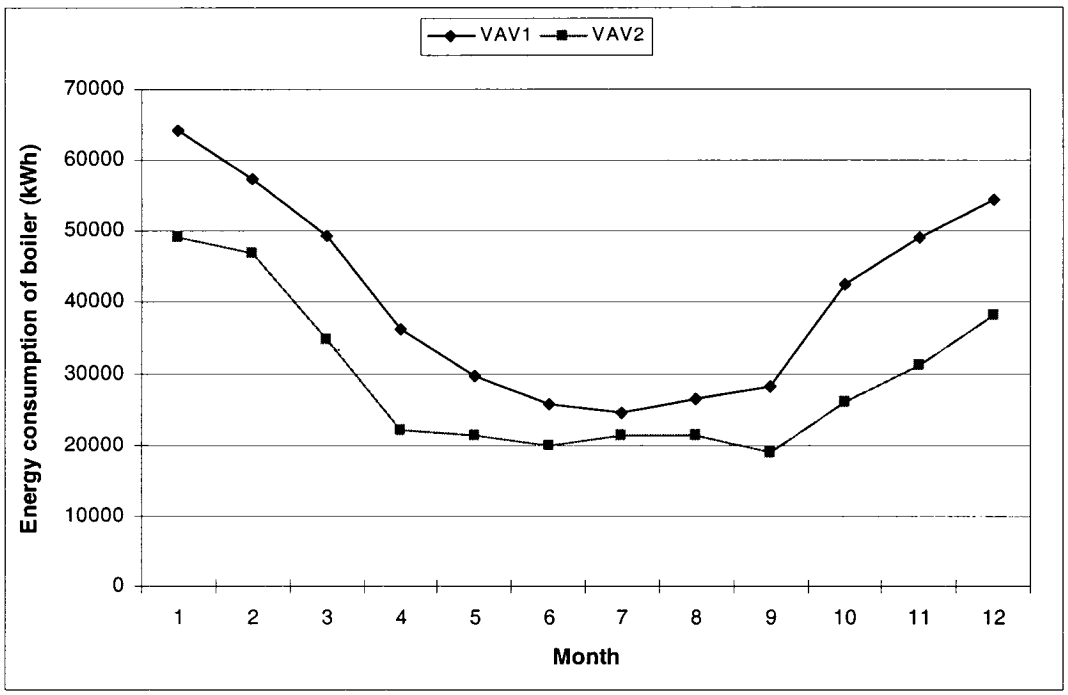

Figure 4-5: Monthly energy consumption of boilers

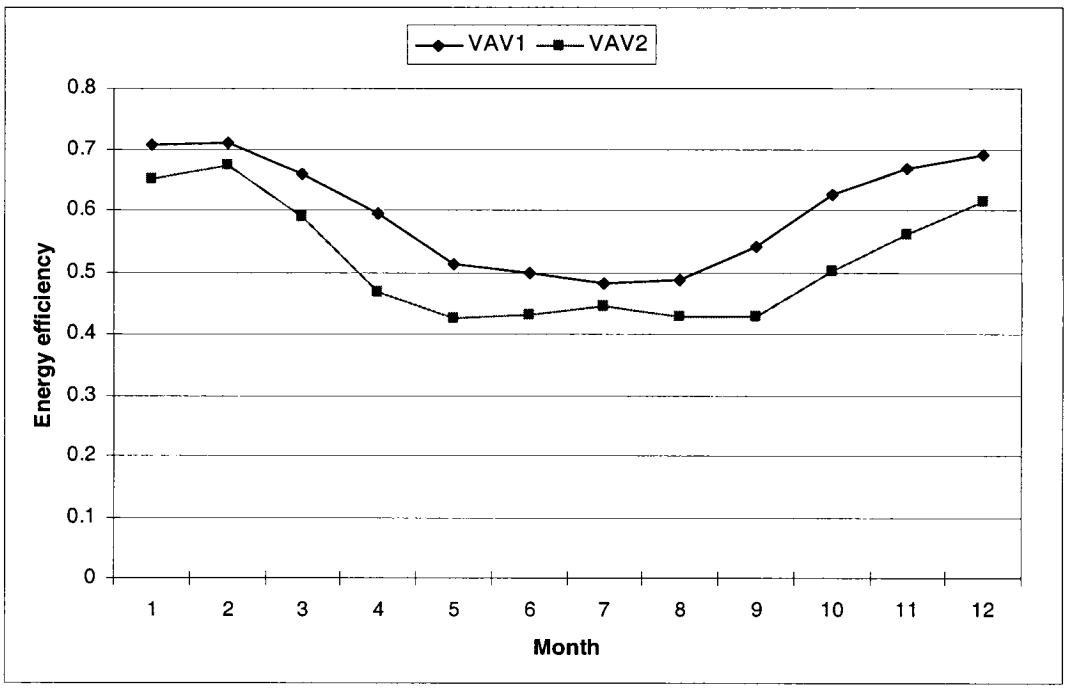

Figure 4-6: Monthly average energy efficiency of boilers

The annual energy consumption of the boiler for VAV system no. 2 is, by 28%, less than that for VAV system no. 1 because of the reduction of reheating coil loads. The maximum energy saving is 39% in April. However, the monthly average energy efficiency of the boiler for VAV system no. 1 is all higher than that for VAV system no. 2 because the boiler of VAV system no. 1 operates at a higher average part-load ratio than the boiler of VAV system no. 2 (Figure 4-6).

According to the energy analysis applied to the boiler and chiller introduced before, it can safely draw a conclusion that the comparisons of the efficiency of components may lead to a limited or even completely wrong result of energy performance of HVAC systems if the efficiency of whole systems is not properly evaluated.

Figure 4-9 and 4-10 show the comparison of daily average energy consumption of boilers for both systems in August and December, which are the hottest and coldest months, respectively. The largest reduction of energy use, of about 50%, is noticed in December.

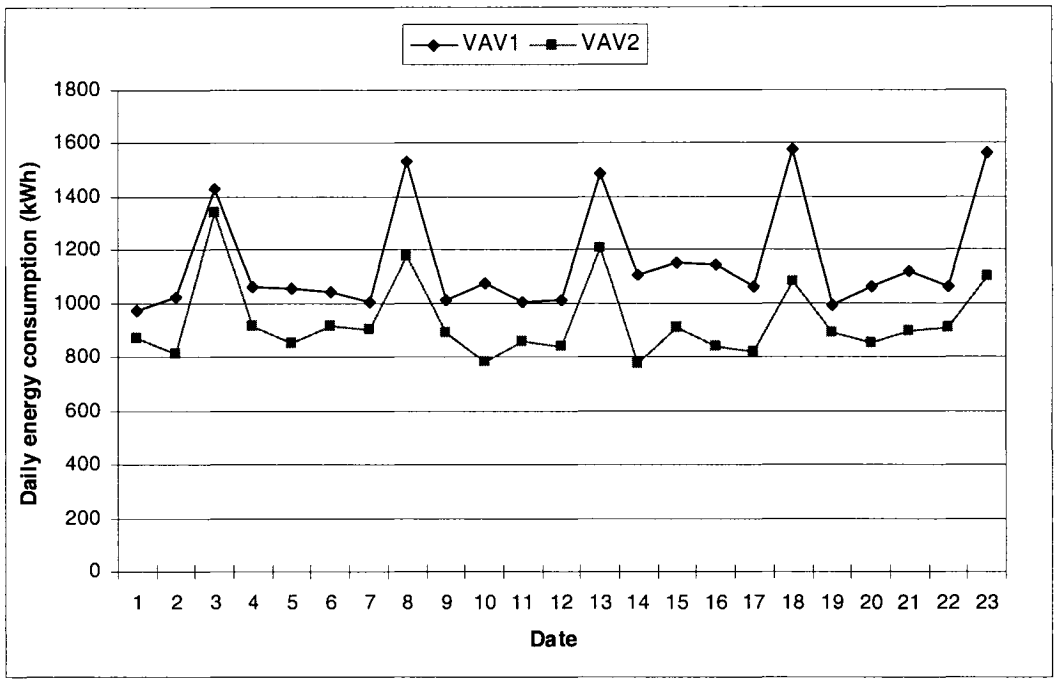

Figure 4-7: Daily energy consumption of boilers in August

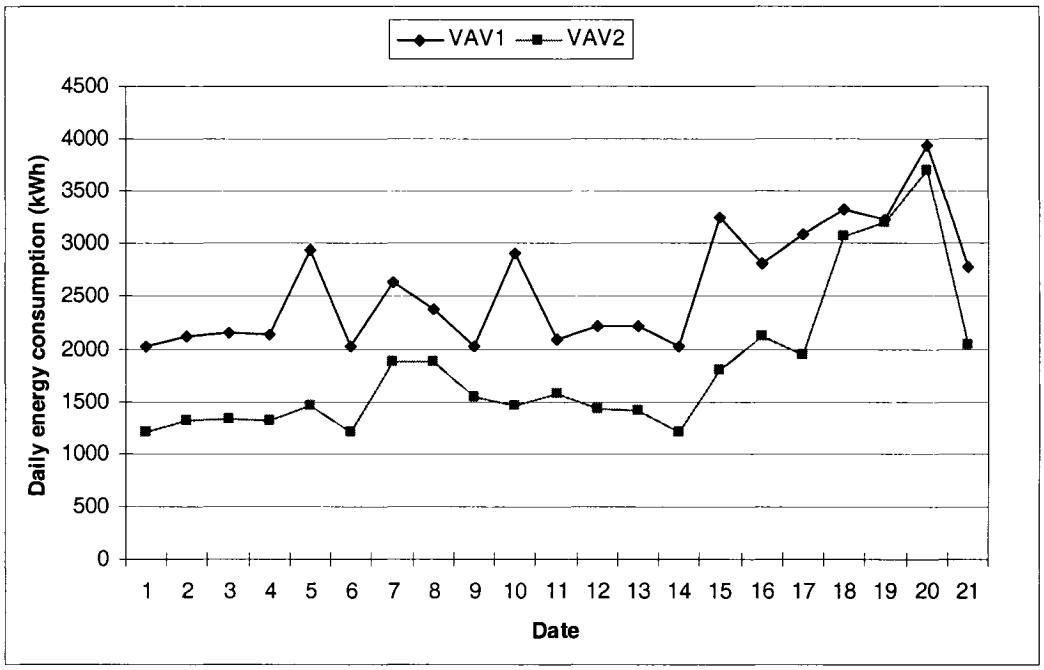

Figure 4-8: Daily energy consumption of boilers in December

Figure 4-9 and Table 4-9 present the comparison of the annual energy consumption of major components for both VAV systems, expressed in kWh/year. Figures 4-10 and 4-11 present the contributions of major components of VAV systems on annual energy use, in percentage of the total annual energy use at the system level. The energy consumption of the boiler has the largest contribution, which annually accounts for 73.7% and 68% of the total annual end-use energy consumption. The energy consumption of fans and pumps has the second large contribution of 17% and 21%, respectively. In addition, the energy consumption of fans is almost four times as large as that of pumps.

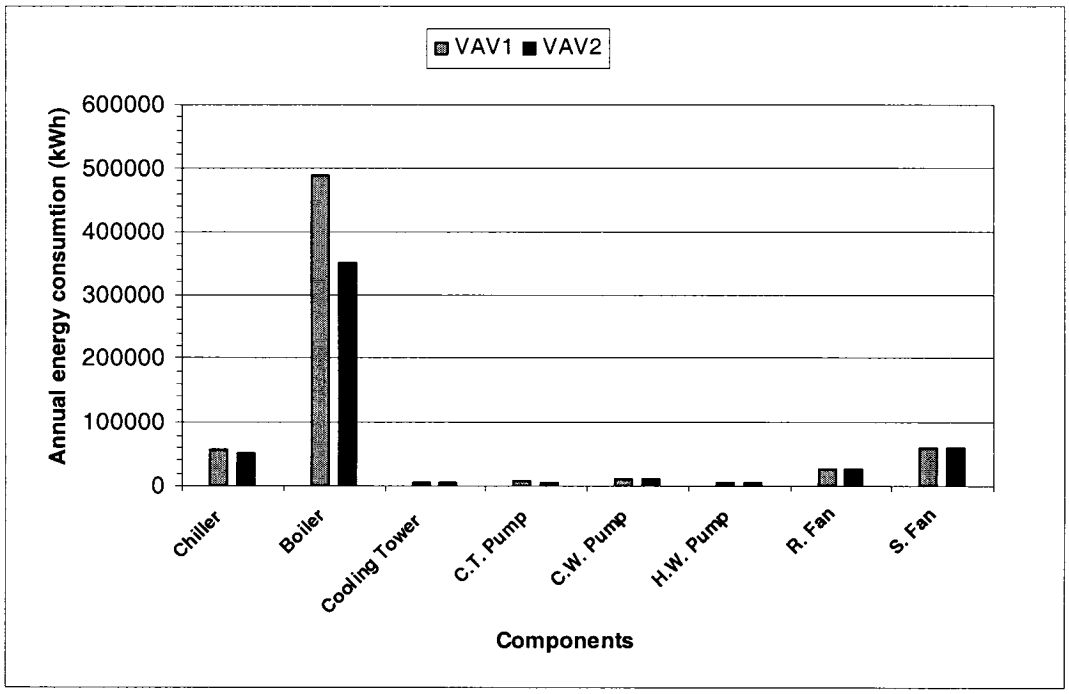

Figure 4-9: Distribution of energy consumption among major components of both VAV systems

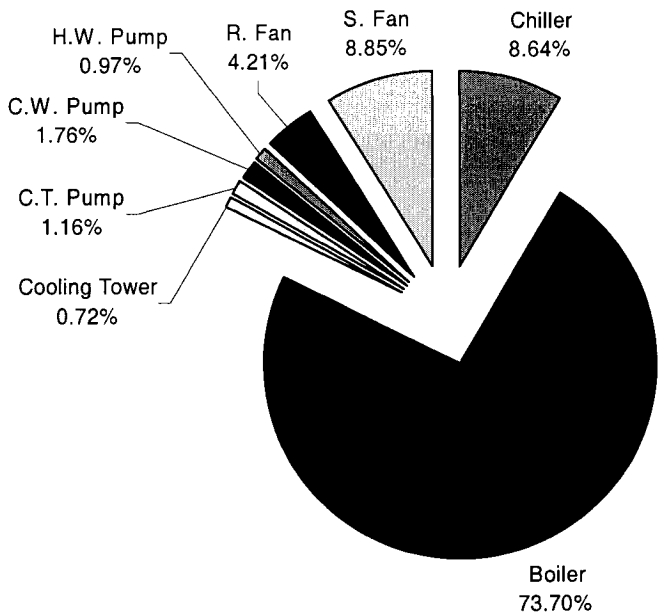

Figure 4-10: Contribution of major components of VAV system no. 1 on annual energy use – at the system level

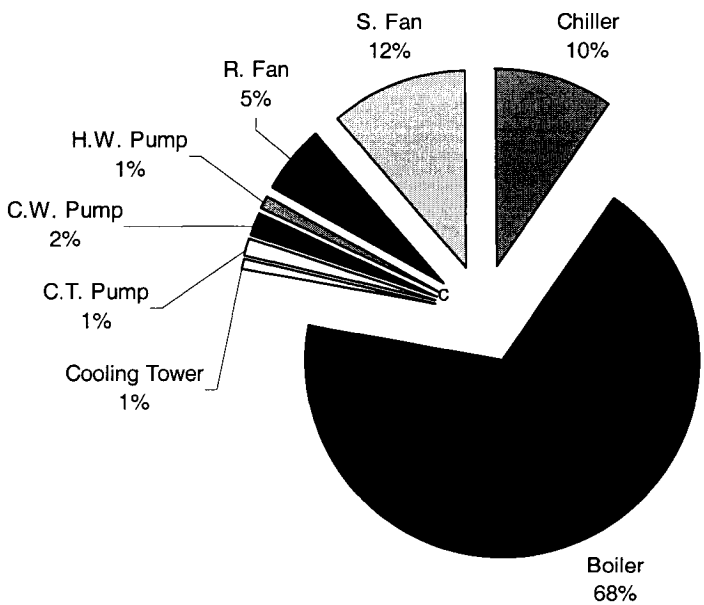

Figure 4-11: Contribution of major components of VAV system no. 2 on annual energy use – at the system level

Table 4-9: Energy consumption of main components of VAV systems

System	Annual Energy Consumption (kWh)							
	Chiller	Boiler	Cooling Tower	C.T. Pump	C.W. Pump	H.W. Pump	R. Fan	S. Fan
VAV1	57,167	487,791	4,741	7,670	11,629	6,419	27,868	58,597
VAV2	50,783	351,233	4,263	6,527	9,896	6,412	27,879	59,433

The major reduction of energy use (136,554 kWh or 94% of the total annual reduction of energy use), from 487,791 kWh for VAV system no. 1 to 351,233 kWh for VAV system no. 2, is noticed for the hot-water boiler, which energy consumption accounts for around 70% of the annual system energy use at the system level. The total reduction of annual energy use by the chilled water system, including the chiller, pumps and the cooling tower, is 9,738kWh (6.7% of the total annual reduction of energy use). The annual energy use by the chilled water system accounts for 12-14% of the total annual system energy use at the system level. The saving of energy use on the hot-water system is about fourteen times that on the chilled water system. Since the energy consumption on the hot-water system account for a major share of the total energy consumption of the system, more savings of energy use are expected from the improvements on the hot-water system.

On the air side, the annual energy consumption of the supply air fan in the case of VAV system no. 2 increases by about 1000 kWh due to the increase of volumetric flow rates of supply air with respect to higher supply air temperatures.

In summary, based on energy analysis, the total annual end-use energy consumption is 661,881 kWh or 132.51kW/m^2·yr for VAV system no. 1 and 516,425 kWh or 103.39kW/m^2·yr for VAV system no. 2. The total annual off-site primary energy

consumption is 1,003,807 kWh for VAV system no. 1 and 783,209 kWh for VAV system no. 2 by taking into consideration the primary energy for the generation of electricity. The annual reduction of energy use is about 22% for the operation of VAV system no 2.

4.4. The second law analysis of VAV systems

Figure 4-12 and Table 4-10 show the comparison of the monthly average efficiency, based on the second law of thermodynamics, of both VAV systems at the system level and the power plant level. The annual average second law efficiency of VAV system no. 1 is of 2.9%, and is 3.8% for VAV system no. 2. The largest improvement of the monthly exergy efficiency occurs in October. When the power plant is considered, the annual average exergy efficiency declines from 2.9% to 2.0% in the case of VAV system no. 1, and from 3.8% to 2.6% in the case of VAV system no. 2. due to the inefficiencies of power generation and transmission lines. The annual exergy efficiency of VAV systems estimated in this research is similar with that of a packaged all-air single zone system with or without dehumidifier, which varies between 2.5% and 6.3% (Guadalpue et al. 2004).

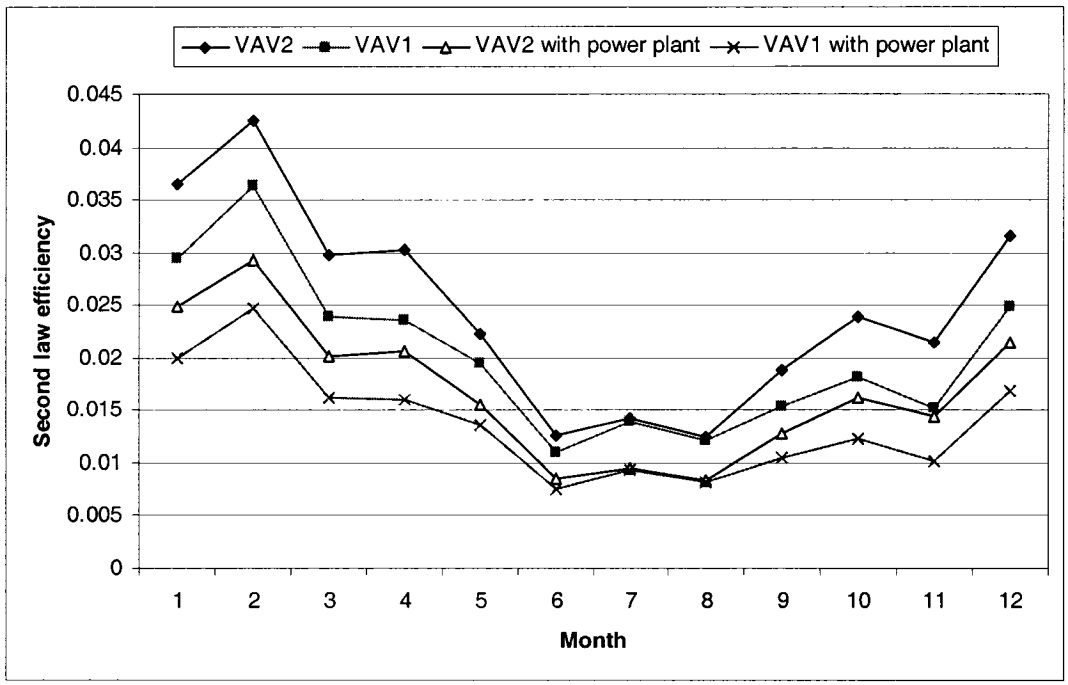

Figure 4-12: Monthly average second law task efficiency of both VAV systems

Table4-10: Monthly second law task efficiency

Month	Overall exergy efficiency (%)			
	System level		Power plant level	
	VAV1	VAV2	VAV1	VAV2
January	4.5	5.6	3.0	3.8
February	5.4	6.5	3.7	4.4
March	3.9	5.2	2.6	3.5
April	3.1	4.7	2.1	3.2
May	2.1	2.6	1.5	1.8
June	1.6	1.9	1.1	1.3
July	1.8	2.0	1.2	1.3
August	1.6	1.8	1.1	1.2
September	1.9	2.5	1.3	1.7
October	2.5	3.7	1.7	2.5
November	2.6	3.8	1.7	2.5
December	3.8	5.2	2.6	3.5
Average	2.9	3.8	2.0	2.6

Figure 4-13 presents the hourly exergy efficiency of VAV systems versus outdoor dry-bulb temperatures. Although the exergy efficiency of the VAV system is a function of both outdoor dry-bulb and wet-bulb temperatures, the representation versus the outdoor

dry-bulb temperature is given for simplification. The trend lines are obtained by using the polynomial curve fitting.

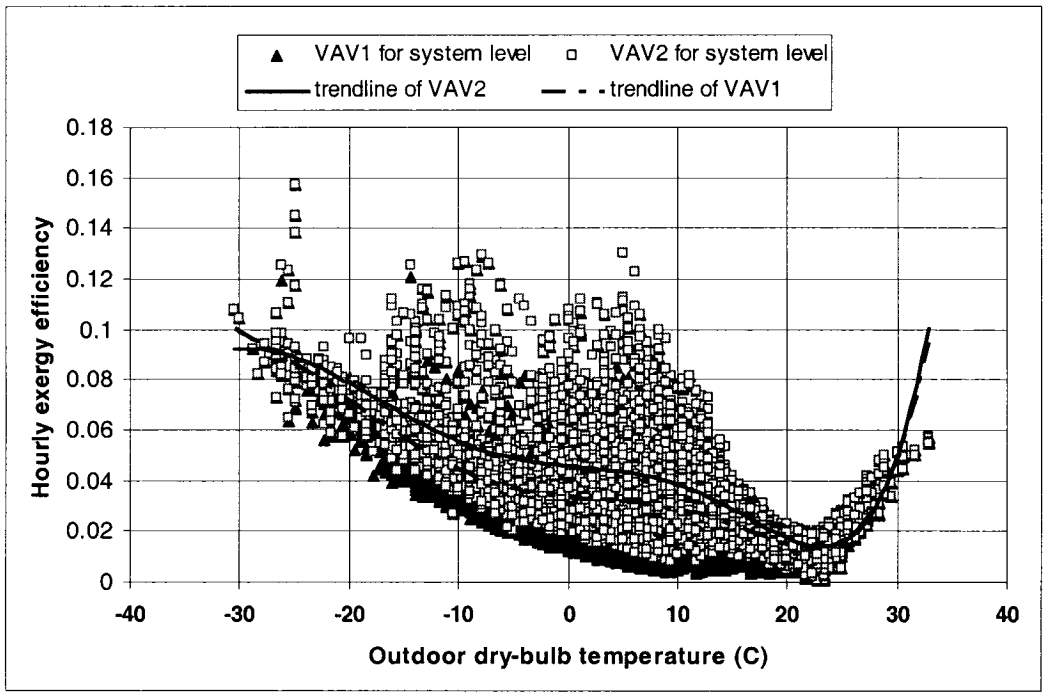

Figure 4-13: Hourly exergy efficiency of VAV systems versus outdoor dry bulb temperatures

The difference of exergy efficiency between the two VAV systems is relatively large when outdoor dry-bulb temperatures are in the range of -20°C to 15°C, corresponding to the operations of the VAV system with 100% outdoor air (air-side economizer). The difference is negligible when outdoor dry-bulb temperatures are higher than 20°C corresponding to the operations with minimum amount of outdoor air (Figure 4-13). The highest hourly exergy efficiency of both VAV systems is less than 16%. The low value of exergy efficiency indicates a large potential for the performance improvement of the VAV systems through a design and operations.

Figure 4-14 presents the annual entropy generation within main components of VAV systems while Figure 4-15 shows the contributions of entropy generation among main components in percentage of total entropy generation. The largest entropy generation is due to the boiler for both VAV systems, which accounts for around 60% or 65% of the total entropy generation in the systems. The annual entropy generation due to the boiler is 1,563kWh/K for VAV system no. 1 and 1,140kWh/K for VAV system no. 2.

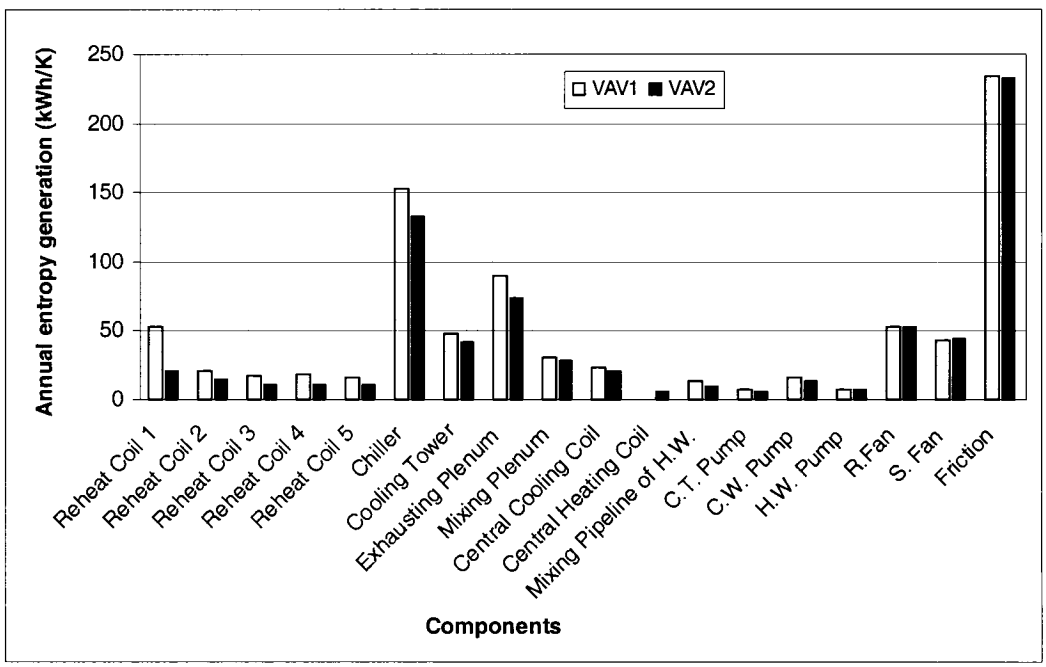

Figure 4-14: Entropy generation of main components of both VAV systems

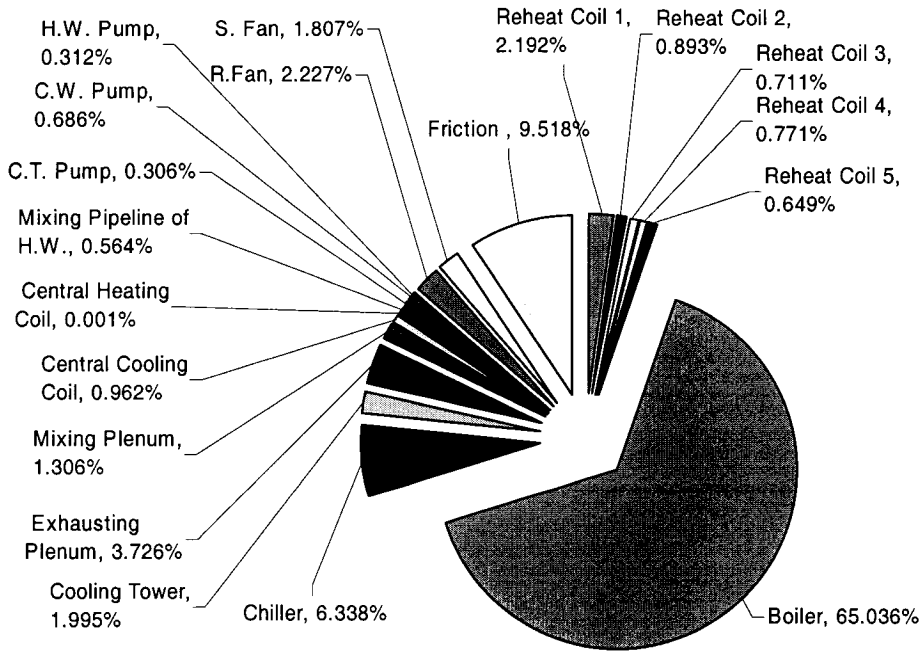

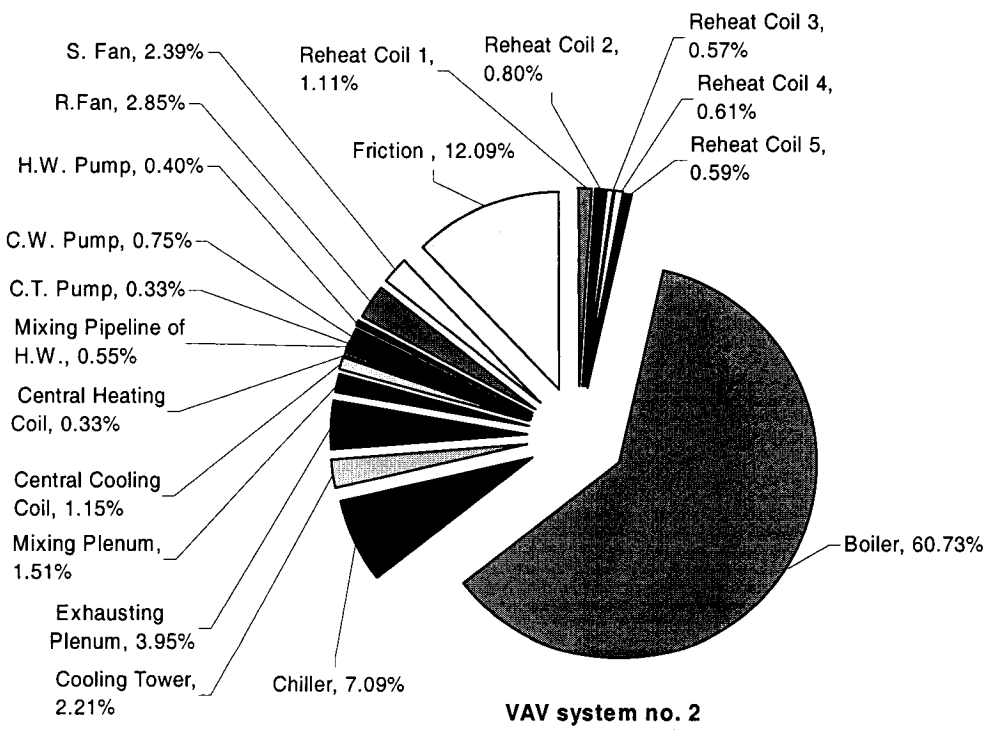

Figure 4-15: Distribution of annual entropy generation among main components of both VAV systems

The total annual entropy generation in VAV system no. 2 is 1,882kWh/K while in VAV system no. 1 is 2,409kWh/K. Compared with VAV system no. 1, the reduction of entropy generation for VAV system no. 2 is around 22%. The annual entropy generation in the boiler accounts for around 65% of the annual entropy generation of systems. Therefore, more attention should be given to an improvement or a more appropriate selection of the heating source. For instance, heat pumps, gas-fired boilers, solar collectors, waste heat from power plants, or geothermal energy can be a better solution than electrical energy for space heating.

Another source of large entropy generation of 10-12% of the total annual generation is the friction losses in all components, ductwork and piping systems. The decrease of the friction losses in the VAV systems can reduce the entropy generation and, thus, decrease the exergy destruction of the VAV systems. However, the negative side of decreasing friction losses is the increase of physical sizes of components, ductwork and piping systems. That can increase the initial cost of HVAC systems as well as the increase of embodied energy. Hence, engineers should consider both sides of this issue in their design. More future work should be done to optimize the index of friction losses to be used in practice.

Entropy generation within the cooling tower, the mixing and exhausting processes of the air distribution system accounts for about 7% of the total annual entropy generation with in the system. The exergy destruction within the cooling tower is due to both irreversibility and the exergy increase of circulating air through the cooling tower, which

is eventually lost to the environment rather than being recovered. Heat recovery equipment can be installed with the cooling tower so that the exergy increase of circulating air could be used for preheating water or air. In addition, the annual entropy generation due to the exhaust air accounts for about 4% of the annual entropy generation in the VAV system and is in respect to 24,750kWh and 20,513kWh of annual exergy destruction in the case of VAV system no. 1 and 2. An extra air-to-air heat exchanger could exploit the portion of exergy contained by the exhaust air. Furthermore, the air-to-air heat exchanger can also bring the temperatures of outdoor air and return air closer, so the performance of the mixing process can also be improved.

Figure 4-16 shows the hourly task exergy needs versus outdoor dry-bulb temperatures. The positive task exergy needs are defined as exergy provided by the system to the conditioned spaces in order to keep the exergy difference between the conditioned spaces and its outdoor environment while the negative task exergy needs are referred to the exergy removed by the system from the conditioned spaces; thus, the conditions when the negative task exergy needs encounter are referred to the removal of heat from the indoor spaces when the indoor temperature set point is higher than the outdoor temperature or the dehumidification of indoor spaces when the indoor humidity ratio is higher than the humidity ratio of the outdoor environment. The same conditions were also discusse by Franconi et al. (1999). Under these conditions, if a heat engine were installed in place of a HVAC system, useful work would have been produced. Even though they cannot produce useful work at any condition, HVAC systems do remove this portion of negative task exergy and maintain the exergy difference between indoor and outdoor. Therefore,

the absolute value of negative exergy is accounted for the calculation of exergy efficiency of both VAV systems. The trend line is based on the use of polynomial curve fitting.

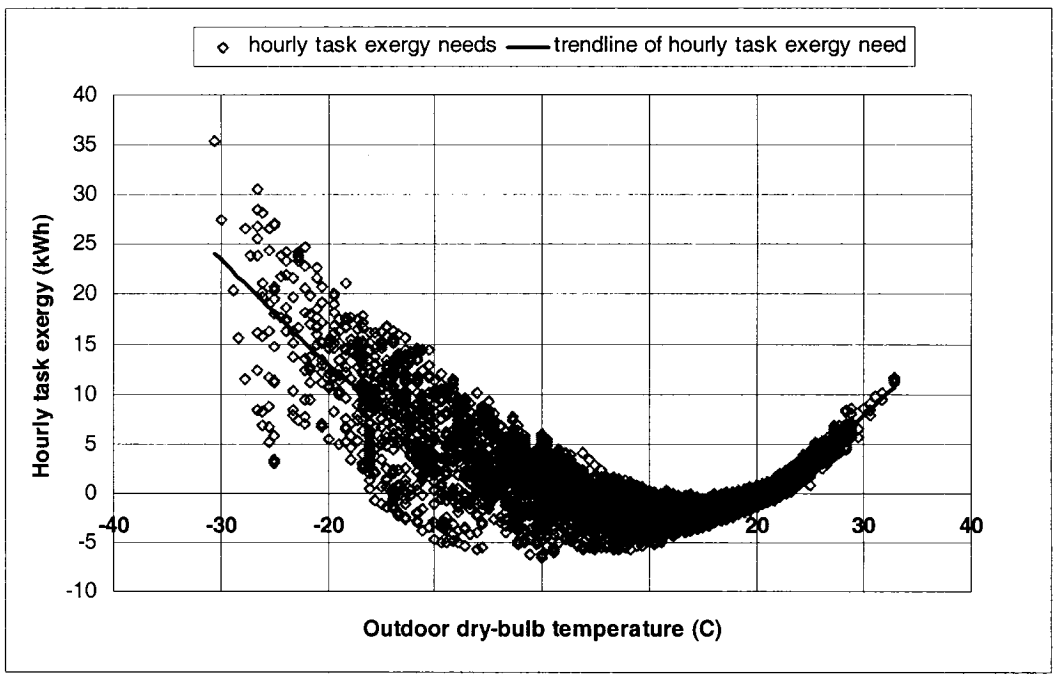

Figure 4-16: Hourly task exergy needs versus outdoor dry-bulb temperatures

The total task exergy demand used to estimate the exergy efficiency of both VAV systems can be calculated as the summation of absolute values of exergy due to the sensible and the latent loads of the spaces and the ventilation requirements. Figure 4-17 presents the trend of the monthly task exergy demand. Figure 4-18 shows the monthly exergy feeding VAV systems versus the monthly task exergy demand. Table 4-11 lists data presented in Figures 4-17 and 4-18.

The target of the optimum design of HVAC systems, with respect to the second law of thermodynamics is to match exergy supply with task exergy demand. Since there is a

large gap between them for both VAV systems (Figure 5-18), a large potential improvement on matching the exergy supply with the exergy demand exists for both VAV systems.

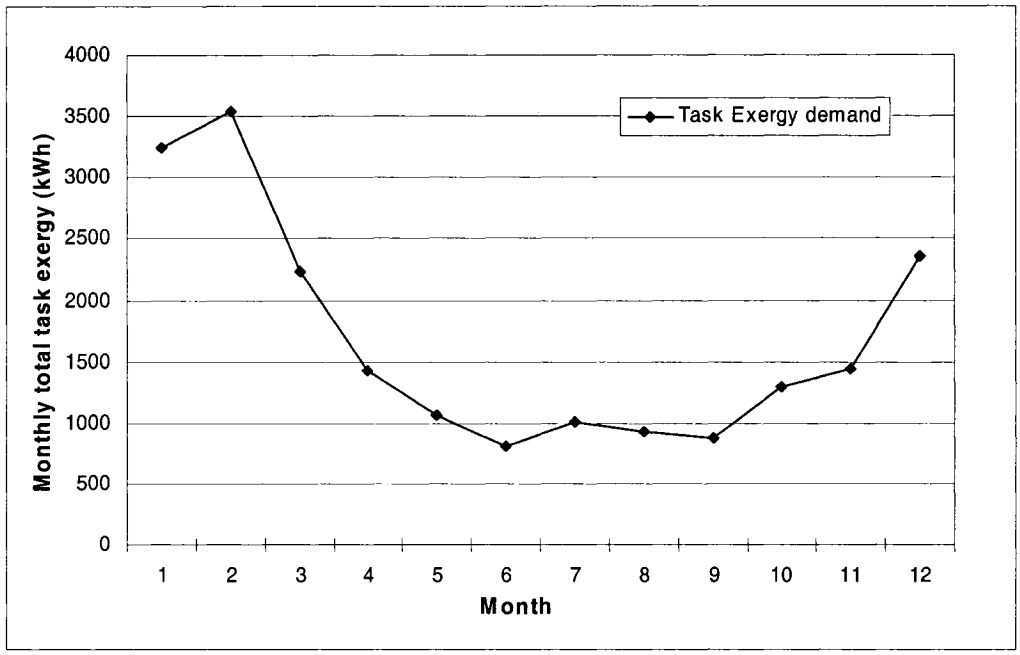

Figure 4-17: Monthly task exergy demands

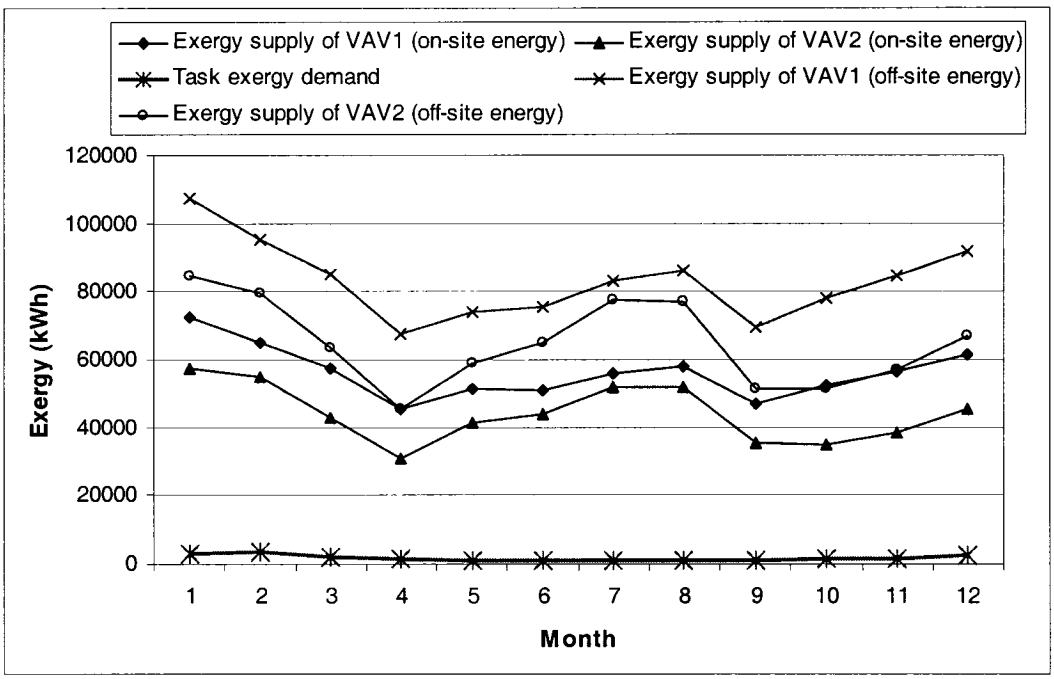

Figure 4-18: Monthly task exergy versus exergy supply to both VAV systems

Table 4-11: Monthly exergy supplied to VAV systems compared with monthly task exergy demand

Month	Exergy supply (kWh)				Task exergy demand (kWh)
	On-site energy		Off-site energy		
	VAV1	VAV2	VAV1	VAV2	
January	72,669	57,674	107,270	84,670	3,242
February	65,102	54,770	95,465	79,888	3,537
March	57,502	42,912	85,343	63,376	2,237
April	45,555	30,699	67,613	45,326	1,431
May	51,475	41,358	73,940	58,819	1,070
June	50,966	43,918	75,516	64,880	811
July	55,935	52,087	83,250	77,414	1,015
August	57,984	51,896	86,192	76,945	929
September	46,811	35,048	69,335	51,631	871
October	52,367	34,711	78,042	51,533	1,298
November	56,477	38,198	84,557	57,058	1,442
December	61,587	45,421	91,549	67,187	2,356
Total	674,431	528,692	998,071	778,726	20,240

Exergy destruction due to the power generation and delivery systems is calculated by subtracting the exergy content of the on-site energy use from that of the off-site primary exergy use. Figure 4-19 presents monthly exergy destruction due to the power generation

and delivery systems for both VAV systems. The annual exergy destruction due to the power generation and delivery systems in the case of VAV system no. 2 is about 31% lower than that in the case of VAV system no. 1. The major reduction of 51% and 53% occur in April and October while the reduction is about 13% in average during the summer period (from June to August).

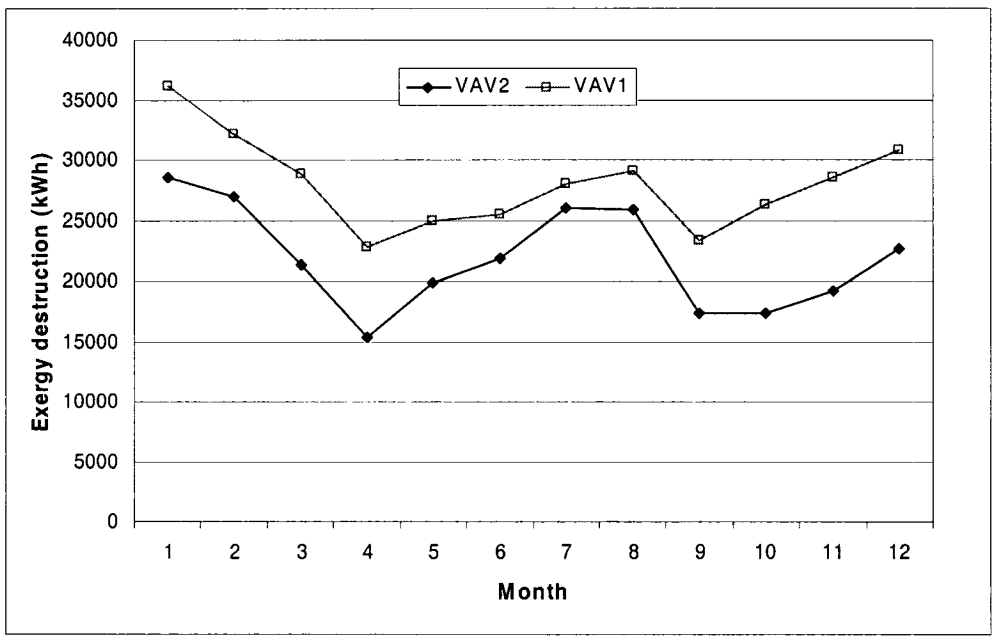

Figure 4-19: Monthly exergy destruction of both VAV systems due to power generation and transmission lines

Figure 4-20 shows the hourly exergy supply to both VAV systems due to the off-site primary energy use versus outdoor dry-bulb temperatures. The two trend lines, which are based on the use of polynomial curve fitting, show that the large reduction in the exergy supply occurs in VAV system no. 2 when outdoor temperatures are in the range of -22°C to 22°C.

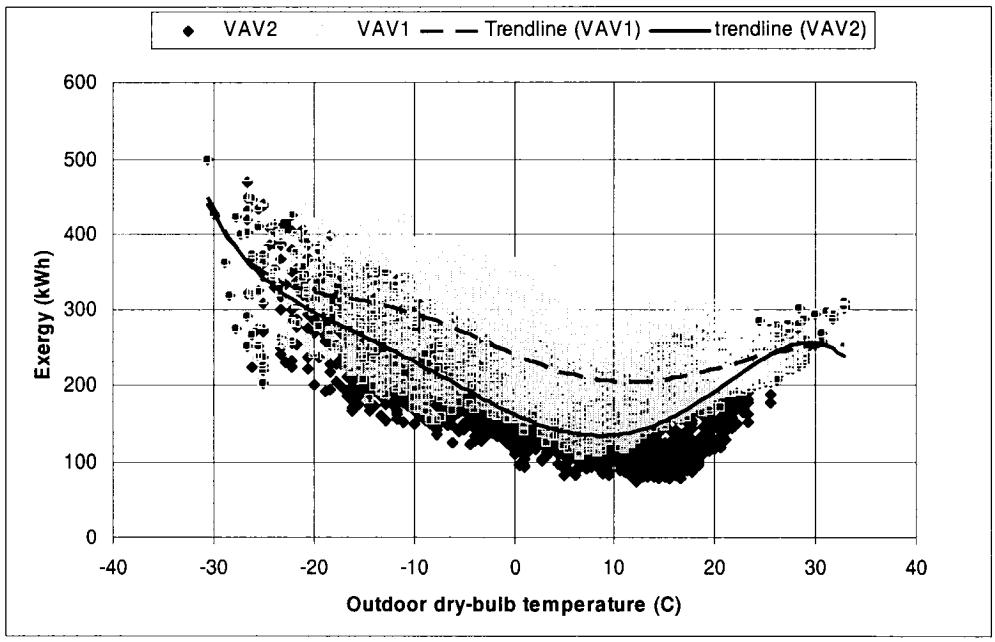

Figure 4-20: Hourly exergy supply due to the primary energy use versus outdoor dry-bulb temperatures

Tables 4-12 and 4-13 list the annual exergy supply, recovery, destruction, and the entropy generation of main components of both VAV systems. The total exergy loss or the entropy generation at the system level is calculated as the sum of the exergy loss or the entropy generation of all components. The exergy supply or recovery of each component does not add up to the total value at system level because the exergy recovery from one component is the exergy supply to the other; for example, the exergy recovery from the chiller feeds the central cooling coil as its exergy supply. The exergy recovery of the system is defined as the summation of the exergy differences between the supply and the return air of each zone. The exergy content of condensation water in both VAV systems is part of the exergy destruction of the central cooling coil.

Table 4-12: Annual exergy and entropy related indices in VAV system no. 1

	VAV system no. 1				
	Exergy supplied	Exergy recovered	Exergy loss	Entropy generation	Percentage of total entropy generation
	kWh	kWh	kWh	kWh/K	%
Reheat coil 1	18,307	3,564	14,743	53	2.19
Reheat coil 2	10,696	4,882	5,814	21	0.89
Reheat coil 3	7,940	3,297	4,643	17	0.71
Reheat coil 4	8,698	3,659	5,039	19	0.77
Reheat coil 5	8,141	3,920	4,221	16	0.65
Boiler	487,791	57,547	430,243	1,563	65.04
Chiller	57,167	12,420	44,747	152	6.34
Cooling tower	14,093	--	14,093	48	2.00
Exhausting air	61,975	37,270	24,705	90	3.73
Mixing box	44,381	36,031	8,350	31	1.31
Central cooling coil	12,420	5,587	6,834	23	0.96
Central heating coil	13	7	6	0	0.00098
Mixing pipeline of hot-water	358,229	354,475	3,753	14	0.56
Cooling tower water pump	7,670	5,521	2,149	7	0.31
Chilled water pump	11,629	6,812	4,817	16	0.69
Hot-water pump	6,419	4,316	2,103	8	0.31
Return air fan	27,868	12,703	15,165	54	2.23
Supply air fan	58,597	46,141	12,456	43	1.81
Friction	--	--	64,405	229	9.52
Condensation water*	--	--	14	--	--
Total in system level	674,431	6,147	668,284	2,403	100.00

* includes in the central cooling coil

Table 4-13: Annual exergy and entropy related indices in VAV system no.2

	VAV System no. 2				
	Exergy supplied	Exergy recovered	Exergy loss	Entropy generation	Percentage of total entropy generation
	kW	kW	kW	kW/K	%
Reheat coil 1	5,897	-118	6,016	21	1.11
Reheat coil 2	8,167	4,140	4,027	15	0.80
Reheat coil 3	5,450	2,565	2,885	11	0.57
Reheat coil 4	5,932	2,846	3,086	11	0.61
Reheat coil 5	6,410	3,412	2,997	11	0.59
Boiler	351,233	37,829	313,404	1,140	60.73
Chiller	50,783	11,582	39,201	133	7.09
Cooling Tower	12,212	--	12,212	41	2.21
Exhausting air	61,376	40,863	20,513	74	3.95
Mixing box	47,690	40,132	7,558	28	1.51
Central cooling coil	11,582	5,208	6,374	22	1.15
Central heating coil	3,127	1,546	1,580	6	0.33
Mixing pipeline of hot-water	376,709	373,863	2,846	10	0.55
Cooling tower water pump	6,527	4,692	1,835	6	0.33
Chilled water pump	9,896	5,784	4,112	14	0.75
Hot-water pump	6,412	4,326	2,086	7	0.40
Return air fan	27,879	12,706	15,173	54	2.85
Supply air fan	59,433	46,593	12,840	45	2.39
Friction	--	--	63,944	227	12.09
Condensation water*	--	--	13	--	--
Total in system level	528,692	6,003	522,690	1,877	100.00

* includes in the central cooling coil

The exergy flow diagrams can give engineers a better understanding of exergy flows through each component of HVAC systems. Figures 4-21 and 4-22 show the exergy flows of both VAV systems at the system level and the power plant level.

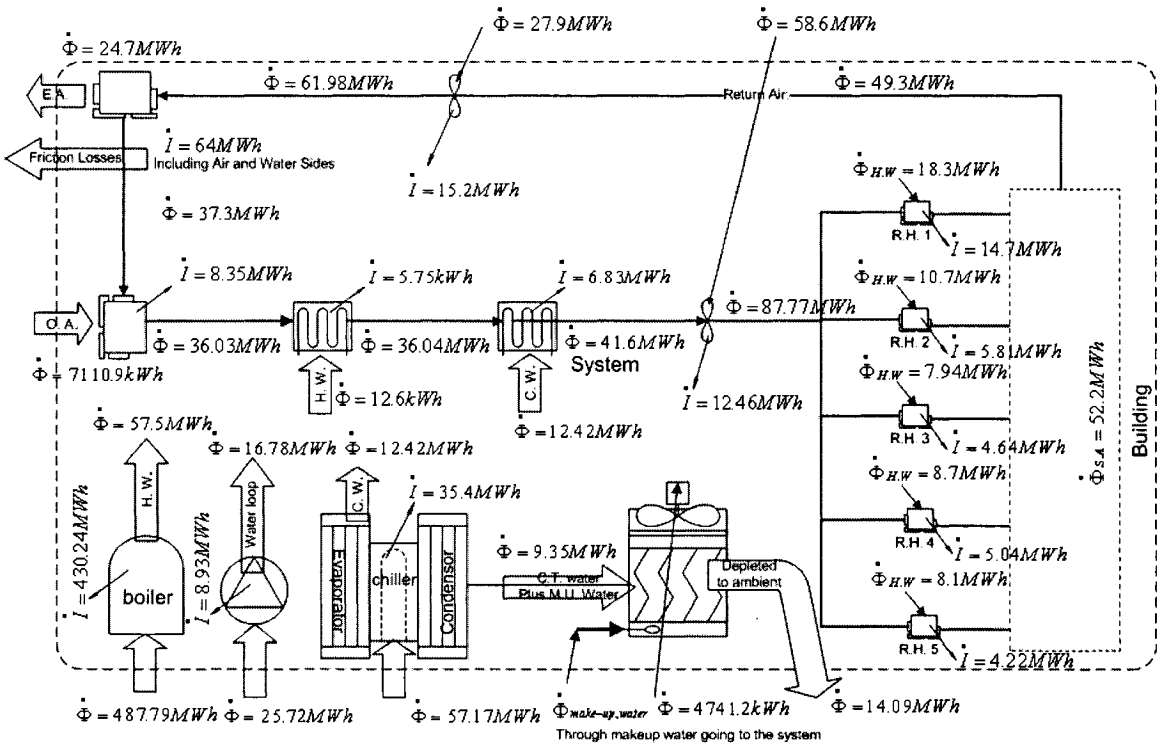

Figure 4-21: Exergy flow diagram of VAV System no. 1 - at the system level

The annual exergy supply at the system level due to the electricity input to each energy conversion component of the VAV system (the chiller, boiler, fans, pumps, and cooling tower) is estimated at about 661.88 MWh, which is the summation of the electric exergy supply to all components (Figure 4-21 or 4-22). The exergy flows carried by air and water streams across each component are presented. For instance, the annual exergy supplied to the chiller is 57.17 MWh, and the exergy destruction in the chiller (35.4Wh) is due to irreversibilities in the chiller. Two exergy flows are leaving the chiller: one corresponds to the chilled water (12.42 MWh), and the other corresponds to the

condenser water loop (9.35 MWh). If an equipment such as a heat pump is used to recover the exergy flow from the chiller to the cooling tower water (9.35 MWh), and use it for heating spaces or domestic water, the exergy performance of the HVAC system will be improved. The analysis of component-level irreversibility shows that the two main places where the exergy destruction occurs are the boiler (430.2 MWh) and the friction losses in the piping and duct systems and inside equipment (64 MWh). The exergy destruction in the cooling plant is significantly smaller because of the use of free cooling. The potential exergy recovery from the cooling tower is not significant when compared with the potential exergy recovery from the exhausting air, boiler, and friction losses in this case.

Exergy inputs to the fans and the pumps are mainly used to circulate the working fluid overcoming the friction losses, which causes 60,000-75,000 kWh of annual exergy destruction. Exergy destruction due to friction can be further divided in two parts – one is occurred in the air distribution system and another is happened in the water loops. The majority of the exergy destruction is occurred in the air distribution system. Therefore, improving the friction losses of the air distribution system is more important than that of water loops. The exergy destruction due to friction losses can be reduced by selecting low velocity of working fluids in pipes and ducts, avoiding sudden area or direction change, and choosing materials with smoother surfaces.

The heating source has the largest contribution to the overall exergy destruction in the VAV system. The annual exergy destruction is estimated at 430.24 MWh or 65% of the

total exergy input as power to VAV system no. 1. The annual average exergy efficiency of the boiler for both systems is less than 20%. By changing the electric boiler with a gas-fired boiler or with other sources, such as solar, geothermal or waste heat, the exergy efficiency can increase.

The exhaust air process is the fourth largest exergy destruction process (24.7 MWh) for VAV system no. 1. The annual average exergy efficiency of this process is only 67% for VAV system no. 2 and 60% for VAV system no. 1. There is still more than 33% energy saving potential for improving the performance of the process. Air-to-air heat exchangers should be used in HVAC systems.

Almost 21% of exergy destruction due to the chiller is rejected through the cooling tower directly to the ambient air. Assuming the use of heat recovery equipment, which can move this portion of thermal energy to heating spaces, this portion of exergy can be used instead of exhausting to the environment, and therefore, the performance of HVAC systems can be further improved.

Since the exergy depleted with the condensation water from cooling coil is negligible (about 14 kWh per year), no efforts are required for using this portion of exergy to improve the energy performance of the HVAC system.

Figure 4-22 details the exergy flows with respect to the following major components: the power generation plants, the power delivery grids, the VAV system and the building. In

the case of VAV system no. 1, the annual exergy supply with the off-site primary energy use is 998.07 MWh, and the major exergy destruction (668.284 MWh) occurs in the VAV system. The annual average exergy efficiency is 0.6% for the VAV system no. 1, and 0.8% for the VAV system no. 2.

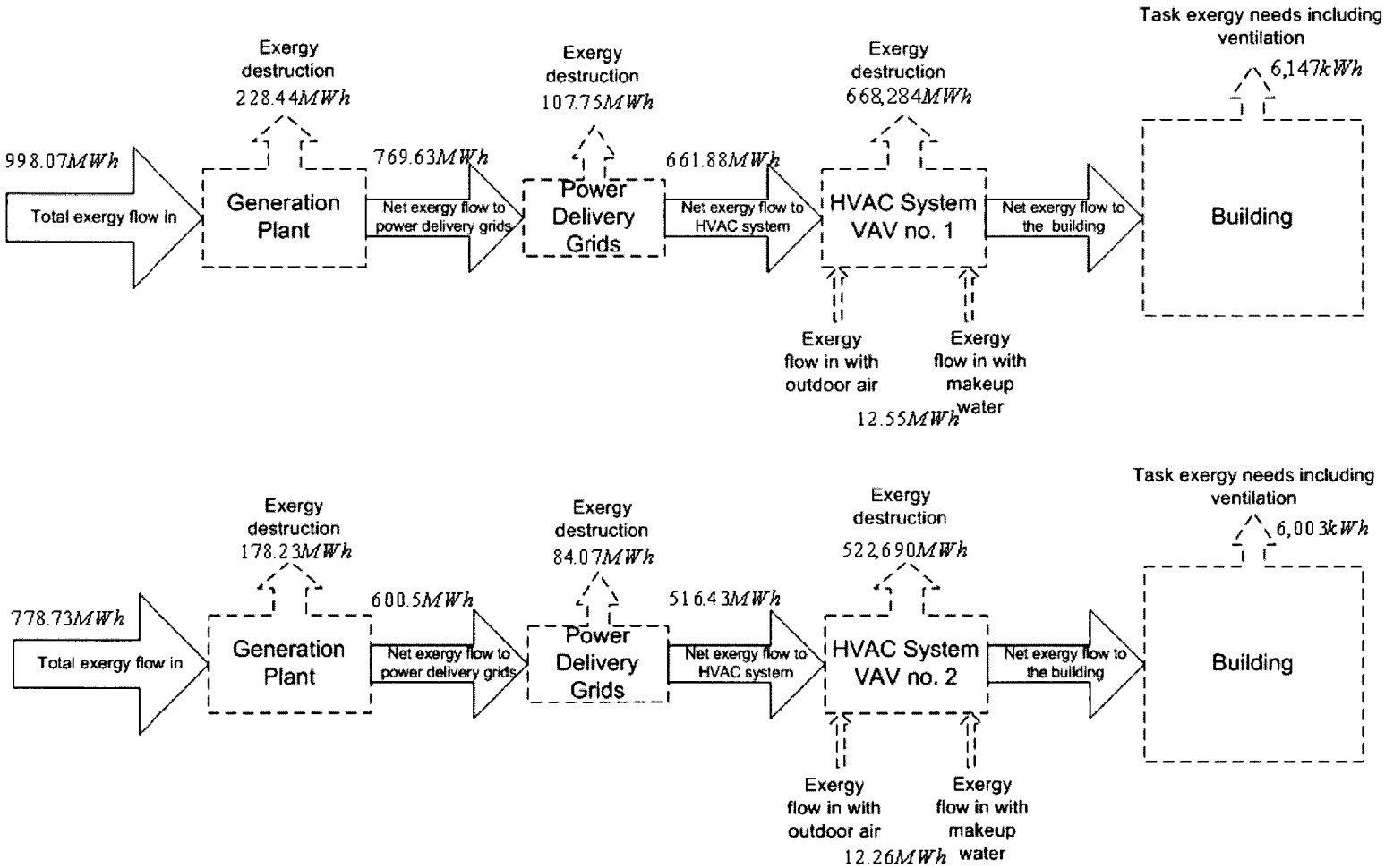

Figure 4-22: Exergy flow diagrams of both VAV systems including the power plant and delivery systems

Chapter 5 Equivalent CO_2 Emissions Corresponding to the Energy Use for HVAC Systems

Global greenhouse gas (GHG) emissions, including carbon dioxide (CO_2), methane, nitrous oxides, and nitrogen dioxide, are increasing and are considered to be the cause of the global warming. Therefore, they attract more and more attention from scientists and governments. Most of GHG emitted are directly related with human energy use, such as the combustion of fossil fuels for heating, power generation, and vehicles. As presented by Gentzis (2000), CO_2 emissions caused by the combustion of fossil fuels accounted for 80% of the gross GHG emissions during the past 50 years in the United States, and 87% for Canada. Although the government of Canada ratified the Kyoto Protocol in 1998 with the target of reducing equivalent CO_2 emissions by 6% of the 1990 level over the years 2008-2012, presently (December 2005), the emissions have increased by 24% since 1990 (NRCan 2005). Therefore, efforts should be made in all aspects of energy use. Analysts should consider the equivalent CO_2 emissions as a necessary index to evaluate the energy performances of HVAC systems. The following section introduces the approach used to calculate the equivalent CO_2 emissions for both VAV systems.

Both VAV systems use electricity as the energy source. The equivalent CO_2 emissions due to on-site energy use and the power generation and delivery systems are estimated as follows (Gagnon et al. 2002):

$$E_{CO_2} = \frac{\left(\alpha_1 E_{hydro} + \alpha_2 E_{nuclear} + \alpha_3 E_{gas} + \alpha_4 E_{oil} + \alpha_5 E_{coal}\right)}{1000} \tag{5-1}$$

where E_{CO_2} is the annual equivalent CO_2 emissions (kg/yr);

E_{hydro}, $E_{nuclear}$, E_{gas}, E_{oil}, and E_{coal} are the annual primary energy (kWh/yr) used by power plants; coal-fired power plants is not included in this research;

α is the specific equivalent CO_2 emissions (kton/TWh) for different types of power generation plants (Gagnon et al. 2002);

α_1 is 15 kton/TWh for hydro power plant with reservoirs; α_2 is 15 kton/TWh for nuclear power plant; α_3 is 443 kton/TWh for gas-fired power plant; α_4 is 778 kton/TWh for heavy oil-fired power plant.

The primary energy use by different types of power plants is calculated as follows, based on the formula 3-212:

$$E_{hydro} = \sum_{t=1}^{4176} \frac{\dot{E}_{total}}{0.86} * \left(\frac{0.967}{0.8} \right) \tag{5-2}$$

$$E_{nuclear} = \sum_{t=1}^{4176} \frac{\dot{E}_{total}}{0.86} * \left(\frac{0.011}{0.3} \right) \tag{5-3}$$

$$E_{gas} = \sum_{t=1}^{4176} \frac{\dot{E}_{total}}{0.86} * \left(\frac{0.011}{0.431} \right) \tag{5-4}$$

$$E_{oil} = \sum_{t=1}^{4176} \frac{\dot{E}_{total}}{0.86} * \left(\frac{0.011}{0.33} \right) \tag{5-5}$$

Based on the on-site energy use of both VAV systems, the off-site primary energy use for different types of power plants is calculated and listed in Table 5-1, along with the annual equivalent CO_2 emissions.

Table 5-1: Annual off-site primary energy use, and annual equivalent CO_2 emissions

systems	The annual primary energy use				CO_2 emission
	Hydro power plant	Nuclear power plant	Gas fired power plant	Oil fired power plant	
	kWh/yr	kWh/yr	kWh/yr	kWh/yr	kg/yr
VAV1	930289	28220	19643	25654	43038.32
VAV2	725848	22018	15326	20016	33580.16

Annual equivalent CO_2 emissions are estimated as 43 tons/yr for VAV system no. 1 (8.61 kg/m^2·year) and 33.5 tons/yr for VAV system no. 2 (6.72 kg/m^2·year). This amount of CO_2 can fill a seven-floor office building that is about 23m high with 1000 m^2 of floor area, and is also equal to the annual emissions from more than 10 energy-efficient cars running about 20,000 km/year. Annual equivalent CO_2 emissions due to energy use in VAV system no. 2 is about 22% less than these in VAV system no. 1.

The annual GHG emissions can be reduced by using renewable energy sources instead of using fossil fuels or electric energy. That will also make future HVAC systems more environmental friendly, and that also satisfy the requirement of the sustainable buildings.

Chapter 6 Conclusions and Future Work

6.1. Conclusions

The detailed first and second law analysis is used to characterize the energy performance of the two VAV systems in an office building, in Montreal. In addition, related GHG emissions due to the primary energy use of both VAV systems are estimated. In summary, the annual energy consumption density of the VAV systems is 132.51kW/m^2·yr and 103.39kW/m^2·yr, for the first and second respectively. The annual system COP of both VAV systems is 0.99 and 1.24, respectively. Considered inefficiencies of the power plant and delivery systems, the annual system COP of both systems is 0.65 and 0.82, corresponding to the primary energy consumption density of 200.76kW/m^2·yr and 156.64kW/m^2·yr, respectively. The annual exergy efficiency of both VAV system 2.0% and 2.5%, respectively, while that of combined systems, including power plant and delivery systems, are all less than 1%. The Annual equivalent CO_2 emissions due to the operations of both VAV systems are 43 tons/yr and 34 tons/yr, respectively. The significant reduction of annual energy use, by about 20%, has been achieved in this research by varying supply air temperatures, diminishing thermal mixing, and utilizing free cooling. Thermodynamic analysis applied to HVAC systems reveals that engineers should pay more attention to the heating system due to their substantial contribution to the total exergy destruction.

The combined analysis should be widely used at the conceptual design stage to integrate HVAC systems. From a green building design point of view, HVAC systems might be

selected from not only the minimum initial costs but also the life-cycle costs and the environmental impacts. Hence, the index of GHG emissions should be included among factors for designing green buildings. The exergy analysis should be involved in design stage due to its merits shown in the study. It gives engineers a detailed picture of the extent of exergy depleted within HVAC systems, informs them of the most potential savings on HVAC systems, and guides them with the most suitable energy sources. In addition, the exergy related indices could be included in design standards. Since the exergy analysis brings a same benchmark between different forms of energy and conducts any practical process with an ideal Carnot cycle, a standard based on exergy is more compact and thermodynamically meaningful. In fact, no specific types of energy are identified, and various baselines are presented in the standard that includes exergy.

It is worth mentioning that the system efficiency is more important than the efficiency of individual components, when the energy performance of HVAC systems is evaluated.

6.2. Future work

The study focuses on two types of VAV systems differing from each other in the control of supply air temperatures. Future studies should be conducted in evaluate the energy performance of HVAC systems using different types of heating and cooling sources, for instance, water-to-water or water-to-air heat pumps.

In addition, further studies should consider the impact of humidity control on the energy performance of HVAC systems.

The simulated results should be further compared with measured data to calibrate the developed mathematical models of the two VAV systems. The presented study should be further extended to other regions of Canada, such as Toronto or Alberta.

Further studies should evaluate the impacts of different selections of the dead-state with the applications of exergy analysis to HVAC systems

References

AIE (Australia Institute of Energy) 1988. Power Station Efficiency. http://www.aie.org.au/melb/material/resource/pwr-eff.htm.

Alpuche, Ma. G., Heard, C., Best, R., and Rojas, J. 2004. Exergy analysis of air cooling systems in buildings in hot humid climates. Applied Thermal Engineering 25 (2005) 507-517.

Ardehali, M. M., and Smith, T. F. 1996. Evaluation of variable volume and temperature HVAC system for commercial and residential buildings. Energy Conversion and Management 37(3), 1469-1479.

Ardehali, M. M., and Smith, T. F. 1997. Evaluation of HVAC System Operational Strategies for Commercial Buildings. Energy Conversion and Management 38 (3), 225-236.

ASHRAE. 1996. HVAC System and Equipment. ASHARE, Atlanta.

ASHRAE. 2002a. HVAC System and Equipment. ASHARE, Atlanta.

ASHRAE. 2002b. Building sustainability. Atalanta, Ga.: ASHARE, Atlanta.

ASHRAE. 2004. HVAC System and Equipment. ASHRAE, Atlanta.

Asada, H., and Takeda, H. 2002. Thermal Environment and Exergy Analysis of a Ceiling Radiant Cooling System. Sustainable Building Conference.

Badescu, V. 2002. First and Second Law Analysis of A Solar Assisted Heat Pump Based Heating System. Energy Conversion and Management 43, 2539-2552.

Baouendi, R. 2003. Development of a Prototype Tool for the Evaluation of the Sustainability of Canadian Houses. M. A. Sc. Thesis, Concordia University.

Bejan, A. 1988. Advanced engineering thermodynamics. New York: John Wiley.

BLAST support office Department of Mechanical and Industrial Engineering. BLAST: the building loads analysis & system thermodynamics program. BLAST User Reference Volume 2.

Brandemuehl, M. J. 2004. ASHRAE research toward sustainable buildings. HVAC&R Research: V10 (No. 1): 1-3.

Bridges, B. D., Harshbarger, D. S., and Bullard, C. W. 2001. Second Law Analysis of Refrigerators and Air Conditioners. ASHRAE Transactions: V 107, part-1: 644-651.

Brzustowski, T. A., and Brena, A. 1986. Second Law Analysis of Energy Processes. Tran. Can. Soc. Mech. Engr. 10(3).

Cengel, Y. A., and Boles, M. 2002. Thermodynamics: An Engineering Approach. New York: McGraw-Hill.

Dunn, G. N., Knight, I. P., and Hitchin, E. R. 2005. Measuring System Efficiencies of Liquid Chiller and Direct Expansion. ASHRAE Journal 47(2), 26-33.

DOE (Department of Energy). 1982. DOE-2 engineers manual version 2.1A, Technical Information Center, United States Department of Energy.

Franconi, E.M., and Brandemuehl, M.J. 1999. Second Law Study of HVAC Distribution System Performance. ASHRAE Transaction, 105 (1), 1237-46.

Franconi, E. M. 1999. Thermodynamic Analysis for Improved HVAC Distribution Performance. Thesis for Ph.D. University of Colorado, U.S.

Gagnon, L., Belanger, C., and Uchiyam, Y. 2002. Life Cycle Assessment of Electricity Generation Options: The Status of Research in Year 2001. Energy Policy, 30, 1267-1278.

Gentzis, T. 2000. Subsurface Sequestration of Carbon Dioxide – An Overview from an Albert (Canada) Perspective International Journal of Coal Geology, 43, 287-305.

Hepbasli, A., and Akdemir, O. 2004. Energy and Exergy Analysis of a Groung Source (Geothermal) Heat Pump System. Energy Conversion and Management, 45, 737-753.

Ileri, A and Gurer, T. 1998. Energy and Exergy Utilization in Turkey During 1995. Energy 23(12) 1099-1106.

Kannan, R., Tso, C. P., Osman, R., and Ho, H. K. 2004. LCA-LCCA of Oil Fired Steam Turbine Power Plant in Singapore. Energy Conversion and Management. v45, n18-19, p3093-3107.

Klein, S. A. 2004. Engineering Equation Solver (EES). F-Chart Software. Madison, U.S.

Krakow, K. I. 1991. Exergy Analysis: Dead-State Definition. ASHRAE Transaction, 1991 (1): 328-336.

NRCan (National Resources Canada). 2005. Energy use handbook tables (Canada): Table 2&3.

http://oee.nrcan.gc.ca/corporate/statistics/neud/dpa/handbook_totalsectors_ca.cfm?attr=0

National Research Council Canada (NRCC) 1998. Performance Compliance for Buildings. Canadian Commission on Building and Fire Codes.

Olsena, E. L., and Chen, Q.Y. 2003. Energy consumption and comfort analysis for different low-energy cooling systems in a mild climate. Energy and Building 35 (6), 560-571.

Ozgener, L., Hepbasli, A., and Dincer, I. 2005. Energy and Exergy Analysis of Geothermal District Heating systems: Application. Building and Environment, 40, 1309-1322.

Reddy, T. A., Kissock, J. K., Katipamula, S., and Claridge, D. E. 1994. An Energy Delivery Efficiency Index to Evaluate Simultaneous Heating and Cooling Effects in Large Commercial Buildings. ASME J. Sol. Energy Eng., 116, 79–87.

Ren, C.Q., Li, N.P., and Tang, G.F. 2002. Principles of exergy analysis in HVAC and evaluation of evaporative cooling schemes. Building and Environment, 37, 1045-55.

Rosen, M. A. 2001. Energy and Exergy Based Comparison of Coal-Fired and Nuclear Steam Power Plants. Exergy - an International Journal, 1(3), 180-192.

Solati, B., Zmeureanu, R., and Haghighat, F. 2003. Correlation based models for the simulation of energy performance of screw chillers. Energy Conversion & Management, 44, 1903-1920.

Tsaros, T.L., Gaggioli, R.A., and Domanski, P.A. 1987. Exergy Analysis of Heat Pumps. ASHRAE Transaction, 93 (2): 1781-97.

Wark, Kenneth Jr. 1995. Advanced Thermodynamics for Engineering. New York: McGraw-Hill.

Wepfer, W.J., Gaggioli, R.A., and Obert, E.F. 1979. Proper Evaluation of Available Energy for HVAC. ASHRAE Transaction, 85 (1), 214-30.

Wu, X.Y. 2004. Second Law Analysis of Residential Heating Systems. M.A.SC. Thesis Department of Building, Civil and Environmental Engineering, Concordia University.

Zhang, M., 1995. Analysis of Energy Conversion System Including Material and Global warming Aspects. Ph. D. Thesis, Oregon State University, Corvallis OR.

Zmeureanu, R., Pasqualetto, L., and Bilas, F. 1995. Comparison of Cost and Energy Saving in an Existing Large Building as Predicted by Three Simulation Programs. Proceedings of the Fourth International Conference Building Simulation '95, Madison, Wisconsin, pp. 485-492.